UNIVERSITY OF CALIFORNIA,
IRVINE

Separation and Detection of Radioactive Materials from Environmental Samples

DISSERTATION

submitted in partial satisfaction of the requirements
for the degree of

DOCTOR OF PHILOSOPHY

in Chemical and Biochemical Engineering

by

Rose C. Pier

Dissertation Committee:
Professor Mikael Nilsson, Chair
Professor Martha Mecartney
Assistant Professor Daniel Knight

2019

DEDICATION

To

my parents, Joel & Ethel,

the love of my life, Jeff,

my siblings and their families, Jonel, Ana, & John

my aunt and uncle, Amado & Ligaya,

and my second family, Soriano family

Thank you for your unconditional love and support

TABLE OF CONTENTS

LIST OF FIGURES

Page

LIST OF TABLES

Page

ACKNOWLEDGMENTS

I would like to express my sincere gratitude and appreciation to my advisor and committee chair, Professor Mikael Nilsson. Thank you for allowing me to participate in your laboratory and introducing me to nuclear science during my time as an undergraduate summer researcher. It truly inspired me to pursue graduate school. Thank you for your support, time, encouragement, patience, and for allowing me to grow as a researcher.

I would like to thank my defense committee members Professors Daniel Knight and Martha Mecartney along with my advancement committee members Professors Diego Rosso and Derek Dunn-Rankin for their time and helpful feedback.

I would like to thank all of my mentors throughout the years. Thank you for your guidance and for your feedback and helpful criticism. Special thanks to Dr. Barbara Cottrell for her mentorship during the early years of my graduate studies as well as Dr. Rebecca Chamberlin at Los Alamos National Laboratory for allowing me to experience researching in a national laboratory setting.

I would like to thank the UC Irvine Reactor Facility personnel: Dr. George Miller, Dr. A.J. Shaka and Mr. Jonathan Wallick for their assistance throughout the years. Thank you for not only helping me at the reactor, but also for providing helpful feedback during lab meetings.

I would like to thank Dr. Dmitry Fishman at the UC Irvine Department of Chemistry Laser Facility for training me and allowing me to use the Jasco 4700 FTIR.

I would like to thank Mr. Larry Gottlieb at ResinTech, Inc. for providing our laboratory with the RSM-25HP resin that was used throughout this project.

I would like to thank my undergraduate students: Betsabe Gaspar-Vargas and Ariana Romero for all their help in the lab.

A very special thanks to the members of the Nilsson Research group, past and present, who have made my graduate studies an enjoyable experience. Thank you for your support inside and outside the lab.

Lastly, I would also like to thank my funding resources: UC Irvine Interdisciplinary Innovation Initiative, UC Irvine Graduate Opportunity Fellowship, Nuclear Science and Security Consortium (NSSC) DE-NA0003180, and the GAANN Fellowship Support from the U.S. Department of Education. This project would not have been possible without the financial support of these sources.

CURRICULUM VITAE

Rose C. Pier

EDUCATION

2015	Chemical Engineering, M.S. University of California, Irvine
2014	Chemical Engineering, B.S. University of California, San Diego

EXPERIENCES

2018	Graduate Research Assistant at Los Alamos National Laboratory Dr. G. Robert Keepin Nonproliferation Science Summer Program
2016-2017	Licensed Reactor Operator University of California, Irvine Reactor Facility
2013-2014	Research Assistant at Space & Naval Warfare Systems Center Pacific San Diego State University Research Foundation
2013	Chemical Engineering Intern San Diego County Water Authority
2013	Research Assistant at Naval Research Laboratory (Washington, D.C) Naval Research Enterprise Internship Program
2012	Undergraduate Research Assistant University of California, Irvine
2011-2014	UC Leadership through Advanced Degrees (UC LEADS) Scholar

FIELD OF STUDY

Environmental Radiochemistry, Separation Sciences, Analytical Chemistry

PUBLICATIONS

Pier, R., Nilsson, M., "Electrodeposition of Uranium and Radium on Stainless Steel from Aqueous Ammonium Acetate Solutions" *Manuscript in preparation for submission to the Journal of Radioanalytical and Nuclear Chemistry*

Pier, R., Gaspar-Vargas, B., Romero, A., Nilsson, M., "Comparative Study Using Ion Exchange Resins to Separate and Reduce NORM from Oil and Gas Flowback Wastewater" *Journal of Radioanalytical and Nuclear Chemistry* (2018) 318: 497-503.

ABSTRACT OF THE DISSERTATION

Separation and Detection of Radioactive Materials from Environmental Samples

By

Rose C. Pier

Doctor of Philosophy in Chemical and Biochemical Engineering

University of California, Irvine, 2019

Professor Mikael Nilsson, Chair

The unconventional production of natural gas from shale resources has increased the total dry natural gas production in the United States. The increasing demand from industrial and electrical power markets will likely cause increase in U.S. natural gas consumption, leading to an increase in the volume of waste. There have been concerns regarding the effective management of the high salinity wastewaters that return to the surface, mainly due to the mobility and local accumulation of naturally occurring radioactive materials (NORMs), such as radium-226. Studies have found radium activity in shale produced wastewater well above federal limits. Current treatment strategies include temporary storage sites and wastewater treatment plants; however, concerns over public and worker exposure and environmental contamination has led to the exploration of other treatment technologies.

This project will explore previously established methods for water treatment and apply them to challenges that emerged due to advancements in oil and gas extraction technologies. Wastewaters from the Eagle Ford Shale formation in Texas were used as a platform for high salinity water samples. Various analytical techniques were explored to accurately determine the amount of radium-226, since the highly saline matrix complicate already established methods. The analysis of radium via electrodeposition and alpha spectrometry is a point of focus in this

project because it allows quantitative determination of small quantities of material. However, separation steps are necessary to ensure the accuracy of this method. Ion exchange and solvent extraction studies coupled with crown ethers were carried out to separate radium and barium from other ions as well as from each other. Results showed high degrees of separation of radium and barium from other ions as well as from each other. The studies done here can help inform the management of environmental samples with high levels of NORM.

INTRODUCTION

Energy Demands and Energy Production

The application of horizontal drilling and high-volume hydraulic fracturing has enabled access to previously unrecoverable natural gas in unconventional reservoirs around the globe. Continued development of this technology has contributed to natural gas having the largest production increase of all fossil fuels as well as resulting in the United States' status as a net energy exporter by 2020[1]. The U.S. natural gas consumption is expected to increase from 28 trillion cubic feet (tcf) to 115 tcf in 2050[1] due to the increasing demand from domestic markets, particularly from the industrial and electric power sectors. This suggests an increase in the volume of waste produced. For example, the total wastewater generated from the Marcellus shale region has increased by approximately 570% since 2004, overwhelming current wastewater disposal infrastructure capacity[2].

Unconventional Gas Extraction

Historically, natural gas was produced from conventional vertical wells drilled into porous hydrocarbon-containing formations[3]. The combination of existing technologies such as horizontal drilling used in 1980s and hydraulic fracturing ("fracking") used in 1950s is an unconventional technique where fluids are pumped into wells under high pressure (e.g. 69,000 kPa[4]) to fracture low permeability geologic formations, resulting in higher oil and gas production.[5] These technological advancements allowed access to vast quantities of natural gas from reservoirs that were previously considered uneconomical. Figure 1 shows the shale plays in the contiguous United States[6]. The Marcellus and Utica shale formations are the major drivers of

total U.S. natural gas production followed by the Eagle Ford and the Haynesville plays in the Gulf Coast region[1].

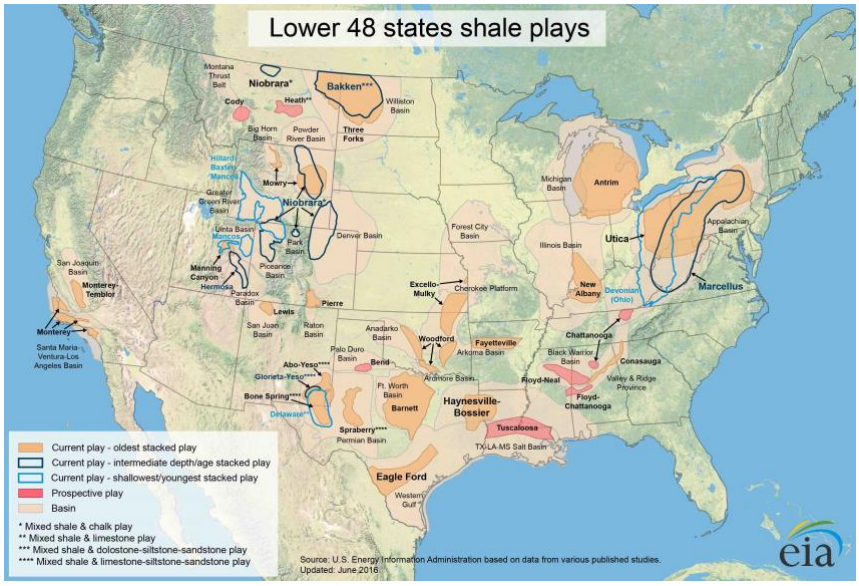

Figure 1: Lower 48 State Shale Plays (U.S. Energy Information Administration, 2016).

During hydraulic fracturing, a 2-5 million-gallon mixture of water and chemicals, known as fracturing fluid, is injected in a well to fracture the formation rock, increase its permeability, and facilitate flow of oil and gas into the well. After the pumping pressure is relieved, some of the fracturing fluid mixed with the formation water returns to the surface along with the gas. This is typically designated as "flowback" water[7] and is collected over a period of 2-3 weeks with a total volume ranging from 10% to 40% of the fracturing fluid volume[8]. "Produced" water continues to be produced throughout the lifetime of the well but at a slower rate than flowback water. Produced water is characterized by the high concentration of total dissolved solids (TDS) and presence of organic compounds[8]. The composition of produced water not only depends on the well location, but it also depends on the time they return to the surface. Water returning to the earth's surface at a later time begin to look more like the formation water, which is water that exists naturally in the rock. Figure 2 provides an overview of the fracking fluid constituents[9]. A

recent assessment indicated that exposure to some chemicals in fracking fluids and wastewater may increase cancer risk, where 2 of the 14 chemicals that were classified as "definitely carcinogenic" are the radium isotopes, radium-226 and radium-228[10]. These types of assessments are justifying concerns regarding the constituents and treatment of the wastewater, prompting additional research on wastewater management.

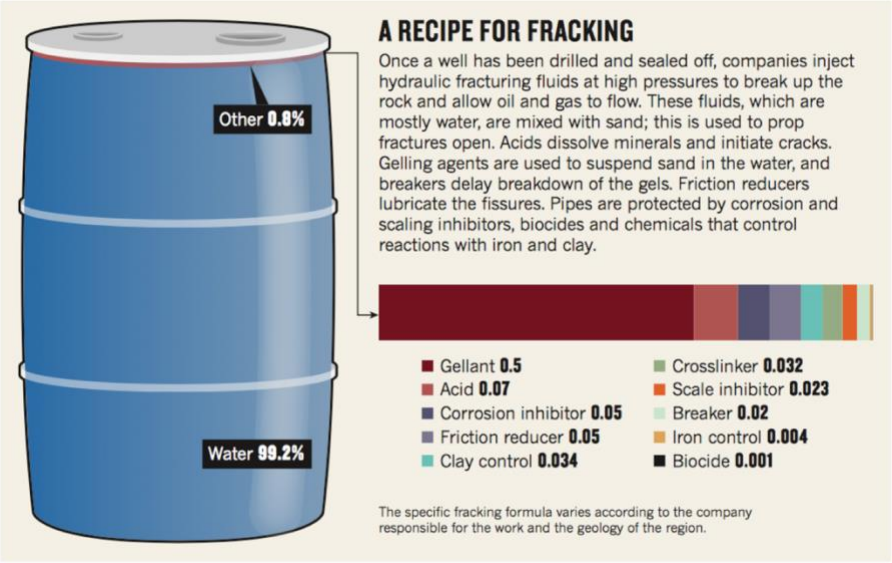

Figure 2: Constituents of fracking fluid (Tollefson, 2013).

Technologically Enhanced Naturally Occurring Radioactive Material (TENORM)

Due to technological advancements that allowed the expansion of unconventional gas extraction, naturally occurring radioactive materials (NORMs), such as uranium-238 (^{238}U, $t_{1/2}$ = 4.5 x 10^9 years) and radium-226 (^{226}Ra, $t_{1/2}$ = 1,600 years) present in the earth's crust at varying levels have been migrating to the earth's surface, and thus increasing the concentration of the NORMs. When the concentration of a radionuclide is enhanced due to industrial activities, it is termed **T**echnologically **E**nhanced **N**aturally **O**ccurring **R**adioactive **M**aterial (TENORM)[11]. Figure 3 shows a theoretical model of how NORM can migrate to the surrounding environment[12].

Most of these radionuclides are members of the radioactive decay chains beginning with ^{238}U, ^{235}U, and ^{232}Th. Elevated amounts of uranium can be found in shale due to reducing conditions, likely favoring insoluble uranium (+VI) and/or uranium sorption onto organic matter. Studies have shown that uranium and radium are positively correlated to total organic carbon[13] and total dissolved solids[14], respectively.

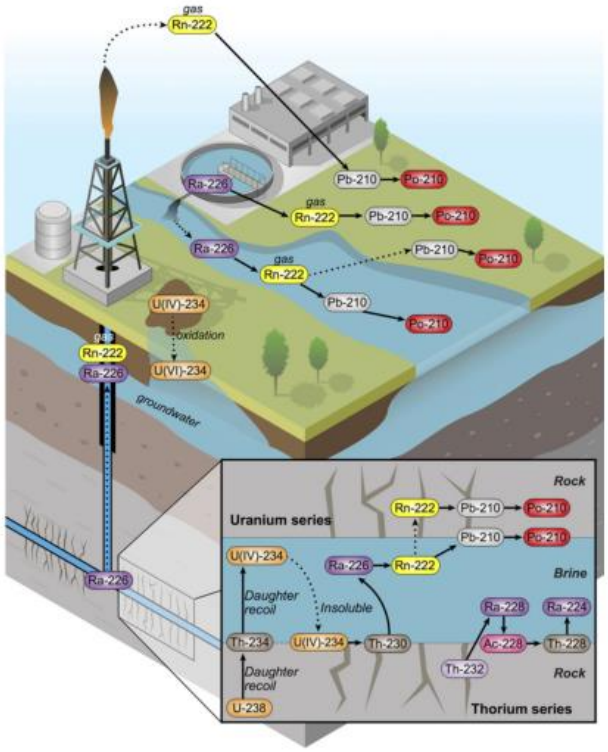

Figure 3: A theoretical model of NORM partitioning. Solid arrows indicate a radioactive decay or series of radioactive decays. Dashed arrows indicate a physical or chemical partitioning process (Nelson et al., 2015).

Rowan (2011) gathered several different literature studies and reported ^{226}Ra and total radium (^{226}Ra + ^{228}Ra) activities from the Marcellus shale and other shale plays. The average values for Marcellus formation and non-Marcellus formation are 2,400 pCi/L and 734 pCi/L, respectively[14]. These values exceed maximum contaminant level (MCL) in drinking water

established by the U.S. Environmental Protection Agency (EPA), which is set at 5 pCi/L for ^{226}Ra and ^{228}Ra combined[15] as well as the U.S. Nuclear Regulatory Commission (NRC) effluent discharge limit of 60 pCi/L[14]. As a result, there have been numerous studies done to effectively determine the ^{226}Ra concentration in a complicated matrix as well as potential treatment of these wastewaters; however, the high salinity of these wastewaters poses challenges.

As reported in Xu et al. (2019), the radium isotopes are classified as carcinogenic and should be prioritized in the exposure assessment process for future fracking-related cancer studies[10]. The U.S. Nuclear Regulatory Commission (NRC) 10 CFR 20.1201 occupational dose limits defined the annual limit for the total effective dose equivalent to be 5 rems (0.05 Sievert)[16]. ^{226}Ra can be a source of internal and external exposure. External exposure may occur as a result of the beta and gamma radiations emitted by radium and its daughters[17]. While the alpha particles do not penetrate skin, the beta and gamma radiation can and therefore contribute to the external exposure hazard[17]. Internal exposure can occur as a result of ingestion of radium-containing substances or dust. Fatal cases have been observed for radium ingested in levels as small as 1 microcurie, which is equivalent to 1 microgram. This is because alpha particles (the main decay mode) have the ability to deposit much of their energy in short distances and potentially cause double DNA strand breaks. In addition, radium is considered a bone tissue seeking element; therefore ingestion of radium may cause accumulation in the bones according to the same pathways as calcium, leading to long residence times in the human body and potentially causing bone cancer[18]. More dangerously, ^{226}Ra decays to noble gas, radon-222 ($t_{1/2}$ = 3.82 days), by emitting alpha particles, which further decays to shorter lived daughter nuclides until it reaches stable lead. Long-term exposure to ^{226}Ra and ^{222}Rn can lead to bone and lung cancer, respectively. The ease in inhaling ^{222}Rn gas, especially if radon accumulates in a poorly

ventilated basement, makes radon the second leading cause of lung cancer in the United States[19]. Scientists estimate about 15,000 to 22,000 lung cancer deaths in the U.S. are linked to radon[19]. In order to prevent these numbers from increasing, additional actions such as increasing ventilation in a house that has a high concentration of NORM under it should be implemented to reduce radon accumulation as well as designing a treatment method to remove TENORM from wastewaters generated by industries such as oil and gas companies.

Treatment Technologies for Oil and Gas Wastewater

Keeping the NORM content at safe or at background levels can be done by carefully managing the treatment of wastewater. While flowback and produced water can be reused if certain water quality conditions are met, most produced water generated is disposed. Disposal is either through deep well injections through Class II wells or using brine treatment facilities. Some of the waste is stored temporarily onsite before their final disposition. However, there are concerns associated with these solutions. The amount of wastewater generated has overwhelmed treatment infrastructure and do not take into consideration the mobility and local accumulation of NORMs.

For example, prior to 2011, most treated effluent from industrial facilities was discharged to rivers in Pennsylvania even though the TDS loads were high. This prompted Pennsylvania legislature to impose strict limits on TDS, resulting in a decline in Marcellus wastewater volumes treated by industrial treatment facilities. This decline lead to a demand for underground injection disposals. Prior to 2010, only 79.8 ± 20.4 million liters (ML) of wastewater from conventional wells was disposed via underground injection disposal per year, but in 2011, this volume surged to 425.7 ML, of which 394.4 ML was from the Marcellus shale[2]. Transportation of this waste has also posed problems for the industry. In addition, there have been studies

investigating if a correlation exists between deep well injections and earthquakes. So far, most of the 30,000 Class II wells that are used for wastewater disposal show no detected seismicity[20]. However, this can be said with confidence only for earthquakes that have magnitudes greater than three; therefore, the propensity of smaller earthquakes are unknown since they are not routinely reported in the central and eastern U.S.[20]. As for temporary storage onsite, there is concern over leakage of these storage pits and potential contamination of groundwater.

Due to the varying composition of the flowback waters, there is a need to establish and validate methods to accurately assay the amount of radium in these wastewaters. One study by Nelson et al. (2014) applied previously established methods as well as the EPA Method 903.0, which is widely used in measuring alpha emitting radioisotopes of radium in drinking water, to flowback wastewater samples from the Marcellus Shale formation[21].

Table 1: Summary of findings on the matrix complications in the determination of radium levels in hydraulic fracturing flowback water from Marcellus Shale (Nelson et al., 2014).

Method	**^{226}Ra Yield (%)**	**Description**
EPA Method 903.0	1%	Sulfuric acid precipitation. Counted on gas flow proportional counter. *Challenge*: excessive precipitates.
RAD disks and 0.5-liter filtrate	Disk: 13% Filtrate: 87%	Disks impregnated with chromatographic extractant. Counted on HPGe.
RAD7	91%	Electronic radon detector. *Challenge*: Excessive foam production, >22 days analysis
Potassium permanganate ($KMNO_4$)	Precipitate: <1% Supernatant: >99%	Pre-concentration using $KMNO_4$. Counted by RAD7, >22 days analysis
High Purity Germanium (HPGe) Gamma Analysis	100%	3-liter sample, 17-hour count, analyzed at 186 keV line.

The results from this study questions the reliability of wet chemical techniques for the accurate determination of radium content in flowback water in Marcellus Shale due to the high salinity. They identified that nondestructive analysis, such as HPGe, are appropriate in assaying radium in a complicated matrix; however, secular equilibrium between ^{226}Ra and ^{222}Ra would need to be achieved (~22 days) and long counting time would be required if the activity is low.

In addition to accurately determining the radium content in a wastewater sample, a previous study considered the impact of shale gas wastewater disposal on water quality near a brine treatment facility[22]. Barium and radium were substantially reduced (>90%) in the treated effluents compared to concentrations in Marcellus Shale produced water; however, the ^{226}Ra concentration (544 – 8,759 Bq/kg) in stream sediments at the point of discharge was ~200 times greater than the upstream and background sediments, which ranged from (22 – 44 Bq/kg)[22]. This was certainly above the radioactive waste disposal threshold regulations. This study has garnered a lot of concern and is prompting investigations near treatment facilities that receive oil and gas wastewater to ensure that TENORM is not accumulating near discharge sites. Therefore, new and advanced treatment technologies should be researched to alleviate stress on current wastewater management but more importantly, to prevent discharge of radioactive contaminants in areas with high hydraulic fracturing activity.

Due to the increasing demand from industrial and power markets, natural gas production from unconventional methods will increase[1] and generate wastewater containing NORMs that will need to be treated to prevent environmental contamination and prevent public exposure. Therefore, the concerns regarding the composition and fate of wastewater that returns to the wells need to be addressed. Different assaying and separation techniques of radium from highly saline samples for remediation of hydraulic fracturing flowback samples will be explored. In

general, the methods and techniques in this research project can be applied to radionuclide detection and separation for different environmental samples.

Research Goals / Dissertation Overview

The current wastewater management strategies do not address the hazards of the technologically enhanced NORMs. In fact, it may make it worse by allowing NORMs to mobilize and locally accumulate in the environment. The overall goal is to investigate the detection and separation of a radionuclide, mainly ^{226}Ra, from highly saline samples using several separation processes. The specific goals are:

1. Characterize and determine the fate of radium and other cations in the environmental samples. Using different analytical techniques, determine the most effective way to assay radium in highly saline samples before and after chemical processing.
2. The presence of radium isotopes in shale gas wastewater poses a unique challenge to common pre-treatment strategies because of its propensity to co-precipitate with scaling minerals (e.g. $BaSO_4$ (s)). This project will investigate various cation exchange resins that can be used to separate ^{226}Ra from other salt constituents and remove ^{226}Ra from high salinity brines. The popular and commonly used resin for radium removal in drinking water, Dowex® 50W-X8 resin, is used as a basis for comparison to ResinTech RSM-25HP, which has very few literature reports regarding ^{226}Ra in highly saline samples. The underlying sorption mechanism of each resin and how they compare to each other will be studied by conducting adsorption equilibrium and kinetic studies.
3. Radionuclides (^{226}Ra and ^{238}U) will be analyzed using previously published electrodeposition methods, followed by alpha spectroscopy. The mechanism of electrodeposition is studied in

detail as well as providing a simpler electrodeposition method for ^{238}U compared to previous techniques.

4. A secondary separation step using crown ethers will be explored to efficiently separate the chemically similar elements, barium and radium, from each other. Separation will capitalize on the size selectivity of crown ethers. Radium has a larger ionic radius compared to barium. This separation will improve low-level radium assay, which is typically encountered in environmental samples.
5. The analytical, separation, and detection methods described in this dissertation will be applied to wastewater samples obtained from the Eagle Ford shale formation to illustrate a lab-scale cradle to grave process.

Chapter 1: Background

1.1 Radium Radiochemistry

Radium was discovered by Marie and Pierre Curie in 1898 in a uraninite (pitchblende) sample[23]. The Curies were able to remove uranium from the mineral; however, they discovered that the material was still radioactive. This eventually led to the discovery of a new element, radium (atomic number 88), which behaved similarly to barium.

Radium is the heaviest element in the alkaline earth metal group, with 34 known isotopes. All isotopes are highly radioactive, with ^{226}Ra being the most stable isotope. Only 4 isotopes are found naturally: ^{226}Ra ($t_{1/2}$ = 1,600 years), ^{228}Ra ($t_{1/2}$ = 5.75 years), ^{223}Ra ($t_{1/2}$ = 11.43 days), and ^{224}Ra ($t_{1/2}$ = 3.66 days). They are part of the naturally occurring ^{238}U, ^{235}U, and ^{232}Th decay series, respectively. Uranium and thorium are abundant in many different rock and mineral types, making radium globally widespread. Radium can be transferred from rocks to water by several mechanisms: diffusion, alpha recoil, leaching, and ion exchange. Ion exchange is the most probable environmental mechanism causing relatively high concentrations of radium. Other sources include uranium mining tailings, and the phosphate mining industry, which is responsible for producing crop fertilizers. Phosphogypsum, a waste by-product from phosphate rock processing contains ~80 - 90% of ^{226}Ra and is disposed of in large land areas without any prior treatment. Studies have found an order of magnitude higher radium levels near phosphate plants compared to outside soil[24].

Separation studies to obtain pure ^{226}Ra can be beneficial, especially for medical applications, because it can capture a neutron and eventually lead to the harvesting of ^{223}Ra. Radium-223 dichloride (Xofigo ®) is the first U.S. Food & Drug Administration (FDA) approved targeted alpha therapy. It significantly improves overall survival (~4 months) in

patients with metastatic castration resistant prostate cancer by delivering alpha particles to bone metastasis sites[25]. However, the supply of ^{223}Ra is limited and expensive. Researchers are currently exploring ways to obtain pure ^{223}Ra. It can be eluted from actinium-227, which can either be produced from a cyclotron or neutron irradiation of ^{226}Ra[26,27].

Analysis of radium is difficult because radium metal is highly electropositive and it reacts readily with water, evolving hydrogen and forming a soluble hydroxide ($Ra(OH)_2$), which adsorbs onto suspended particles, colloids or walls of containers[28]. Similar to other alkaline earth ions, the element only exhibits one oxidation state, +2, in solution. The divalent ion is not easily complexed; hence, most radium compounds are simple ionic salts[28]. The complexation of alkaline earth cations by neutral extractants depend on matching the size of the cation and extractant, where the extractant should be large enough to incorporate Ra^{2+} cations. The table below shows the ionic radii of radium and other group II elements[29].

Table 2: Ionic radii of Group II elements. Ionic radii increases with increasing atomic number[29].

Ion	Ionic Radius (Å)
Ca^{2+}	1.00 - 1.34
Sr^{2+}	1.18 - 1.44
Ba^{2+}	1.35 - 1.61
Ra^{2+}	1.48 - 1.70

Chapter 2: Sample Preparation and Analytical Instruments

2.1 Sample Preparation

2.1.1 Hydraulic Fracturing Flowback Waste Water

Samples obtained from the Eagle Ford Shale formation in South Texas were delivered in two 4 Liter bottles. Prior to experimentation, these samples were mixed thoroughly. They were either used as is (wet samples) or were dried at 100 °C overnight and weighed to desired weight. Dried samples were digested using a mixture of acids and heat. All water discussed herein was purified with a resistivity of >18 MΩ/cm. Nitric acid (HNO_3, Macron Fine Chemicals) was used for majority of digestion and dilution efforts. Hydrochloric acid (HCl, 36.5-38%, EMD Millipore GR ACS grade) and 30% hydrogen peroxide (H_2O_2, Fisher Scientific Certified ACS) were also used for acid digestion experiments.

2.1.2 Surrogate Samples

Surrogate samples were created to first understand the experimental system and to aid in the creation of protocols prior to using unknown samples. Chloride salts of different ions were weighed then diluted to 50 mL to yield desired concentrations. The salts used were: barium nitrate ($Ba(NO_3)_2$, Fisher Science, Reagent grade), sodium chloride (NaCl, Macron Fine chemicals, ACS grade), calcium chloride dihydrate ($CaCl_2 \cdot 2H_2O$, Macron Fine Chemicals, ACS grade), iron (III) chloride hexahydrate ($FeCl_3 \cdot 6H_2O$, Acros Organics, 99+% for analysis), strontium chloride hexahydrate ($SrCl_2 \cdot 6H_2O$, Acros Organics, 99+% ACS grade), barium chloride dihydrate ($BaCl_2 \cdot 2H_2O$, Acros Organics, 99+%, ACS grade), potassium chloride (KCl, Fisher Scientific, ACS grade), and magnesium chloride hexahydrate ($MgCl_2 \cdot 6H_2O$, Acros Organics, 99+%, ACS grade). Table 3 details the constituents of the surrogate samples, expressed

in parts per million (ppm). Samples S1-S4 were made to mimic the high ionic strength of environmental samples. In samples S0F-S4F, barium concentrations were kept constant across four different samples while other ions (mainly group II metals) were varied to study the effect of sample matrices on the quantitative determination of barium.

Table 3: Constituents of surrogate samples and their theoretical concentrations in parts per million (ppm, mg/L).

Ions	S1	S2	S3	S4	S0F	S1F	S2F	S3F	S4F
Ba^{2+}	1,090	2,188	4,522	6,429	2,150	2,162	2,133	2,133	2,229
Sr^{2+}	814	1,513	3,319	4,906	-	522	1,016	5,040	9,070
Ca^{2+}	3,485	7,139	13,925	20,882	-	540	1,017	5,057	10,361
Na^{+1}	11,608	23,983	46,633	69,790	-	496	979	5,033	9,776
Mg^{+2}	-	-	-	-	-	507	981	5,107	9,985
Fe^{3+}	-	-	-	-	-	499	966	4,626	9,868
K^{+1}	-	-	-	-	-	552	1,033	4,415	10,426

2.1.3 Calibration Standards Preparation

Concentrations of unknown solutions were quantified via Inductively Coupled Plasma – Mass Spectrometry (ICP-MS) using proper dilutions of various standard stock solutions: 10 ppm tuning solution containing cerium, cobalt, lithium, thulium, and yttrium in 2% HNO_3 (Agilent Technologies), 1,005 ± 4 ppm sodium in 0.1% v/v HNO_3 (Inorganic Ventures), 1,005 ± 4 ppm magnesium in 0.1% v/v HNO_3 (Inorganic Ventures), 1,000 ± 4 ppm potassium in 0.1% v/v HNO_3 (Inorganic Ventures), 998 ± 2 ppm calcium in 0.1% v/v HNO_3 (Inorganic Ventures), 10,000 ± 50 ppm iron in 5% HNO_3 (Ricca Chemical), 1,005 ± 5 ppm strontium in 0.1% v/v HNO_3 (Inorganic Ventures), 1,003 ± 2 yttrium in 2% v/v HNO_3 (Inorganic Ventures), 10,000

ppm indium in 5% HNO_3 (Ricca Chemical), and 1,000 ± 3 ppm barium in 2% HNO_3 (Ricca Chemical). Single and multi-element element standards were created. All standards were diluted to appropriate values using 2% HNO_3.

2.1.4 Radionuclide Solutions

The ^{226}Ra solution was purchased from Eckert & Ziegler Isotope Products with an original activity of 74.26 kBq/mL (2.0069 μCi/mL) and a 10 mg/L barium carrier in a 1 M nitric acid solution. A secondary stock solution was created by taking 200 μL of the primary stock solution then diluting to 2 mL using >18 MΩ/cm water to yield a final activity of 7.43 kBq/mL (0.2 μCi/mL). The pH was adjusted to 6 using small nitric acid additions to keep radium in solution and prevent adsorption on walls of the container. This secondary stock solution was further diluted for experiments, which will be described in their respective experimental sections.

The ^{238}U solution was purchased from Inorganic Ventures with a concentration of 10,000 ppm (42 mM) in 2% nitric acid (v/v). This solution was diluted ten times to yield concentration of 4.2 mM, of which 50 μL of this solution was added to the electrodeposition samples.

2.2 Analytical Instruments

2.2.1 Inductively Coupled Plasma – Mass Spectrometry (ICP-MS)

Samples were analyzed on an Agilent 7500 cx ICP-MS instrument, which is equipped with a vacuum, heat exchanger, automatic sample changer, and collision gas capabilities. Prior to analysis, the instrument warmed up for at least 20 minutes. The plasma is sustained using ultra-high purity argon gas (AirGas) flowing at 15 mL/min. Once warm, the instrument was tuned for sensitivity using a 1 ppb tuning solution in “no gas” (argon gas only) and “helium gas” mode.

Once complete, the instrument was rinsed with 2% HNO_3 for 15-20 minutes before sample analysis.

Single and multi-element calibration standards were prepared to quantify unknown concentration of samples. The abundance of ions present in the samples may inflate or deflate certain ion counts. As a result, several analyses were done in "no gas mode" where only the carrier gas, argon, is present as well as in "helium gas mode" where high purity helium gas (AirGas) is introduced as a collision gas to reduce the kinetic energy of interfering ions and not allowing them to reach the detector. Unless otherwise stated, all samples were run in helium mode, utilizing helium as the collision gas flowing at 4 mL/min.

2.2.2 High Purity Germanium (HPGe) Gamma Analysis

The HPGE, equipped with a Genie-2000 analysis software and cooled using liquid nitrogen (AirGas) was previously calibrated using known sources (Canberra U.S.A). It was used to analyze samples that decay through gamma emission. Figure 1 shows a spectrum of ^{226}Ra and its daughters, following secular equilibrium with radon-222 (>22 days).

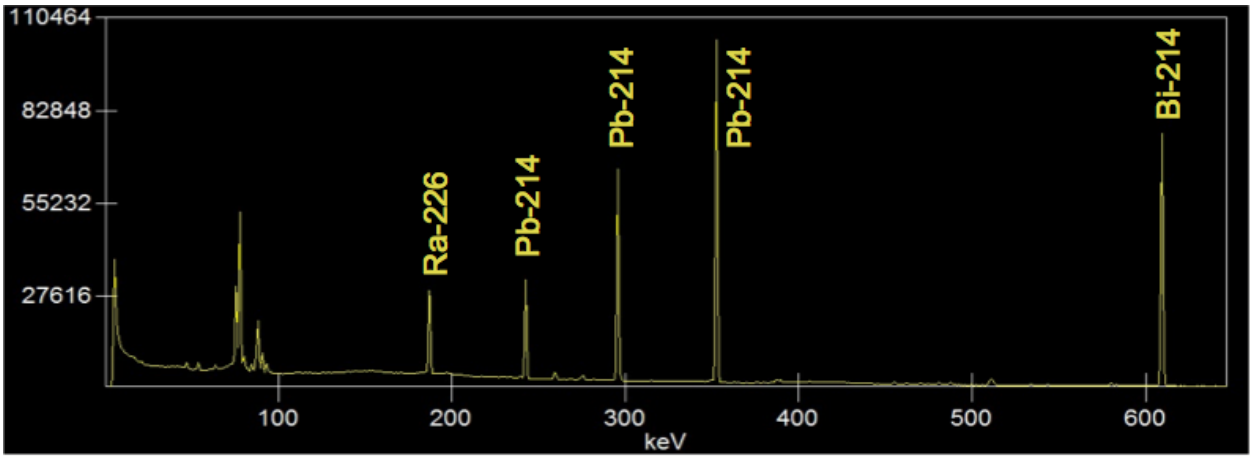

Figure 4: HPGe spectra of ^{226}Ra with short-lived daughter nuclides, counted after >22 days. (^{214}Pb $t_{1/2}$ = 26.8 min; ^{214}Bi $t_{1/2}$ = 19.9 min).

2.2.3 Alpha Spectroscopy

A calibrated alpha spectrometer (Model 7200-12 with eight passivated implanted planar silicon (PIPS) detector and Genie-2000 alpha spectroscopy software, Canberra U.S.A.) was used to analyze samples that were electrodeposited on stainless steel disks. The alpha spectrometer was calibrated with a source containing ^{238}U, ^{234}U, ^{239}Pu, and ^{241}Am, with a total activity of 6.143 Bq (Eckert & Ziegler, Jan 21, 2011, 12:00 PM EST). The efficiency of all detectors for all energy levels ranged from 4.8% to 5.0%.

The chambers were operated at 60 V and pressures between 0.13 - 2.67 kPa (1 - 20 torr). Samples were placed 1.9 cm away from the detector with the air thickness (adjusted by the vacuum pump via the detector software) set at 12.00 g/cm^2 to limit recoil contamination of the detector[30]. Analysis time varied depending on the activity of the samples. The area under the peak was divided by the counting time and corrected for the efficiency of the detectors at the specific energy level. This experimental activity was compared to the reference activity to determine the yield and in the case for the separation studies, activities of the initial and final were compared to determine the distribution values and uptake percentage.

A background count was performed on all eight detectors for 84 hours and all were very low. The activities ranged from 2.8 x 10^{-4} to 9.5 x 10^{-4} Bq for the ^{226}Ra region (4.7 MeV); 3.2 x 10^{-3} to 3.6 x 10^{-2} Bq for the ^{222}Rn region (5.5 MeV); and 2.0 x 10^{-3} to 2.3 x 10^{-2} Bq for the ^{218}Po region (6.0 MeV).

Chapter 3: Characterization of Oil and Gas Wastewater

3.1 Introduction

FracFocus (www.fracfocus.org), the national hydraulic fracturing chemical registry, managed by the Ground Water Protection Council and Interstate Oil and Gas Compact Commission, provides public access to reported chemicals used for hydraulic fracturing in their area. The purpose is to provide factual information concerning hydraulic fracturing and groundwater in one place since the nature of the water is formation and location dependent. However, this site does not report any naturally occurring radioactive materials (NORMs) concentrations. Therefore, there is a need to characterize the specific sample and determine the extent of which radium is enhanced by this specific technology.

Experiments to perform these characterizations include determining the amount of total dissolved solids and using different analytical techniques to determine the concentration of metals and radionuclides. Prior to metal analysis, chemical digestions were performed in order to destroy the organic compounds present in the samples.

Table 4 provides a summary of studies conducted on different shale formations. This is by no means an exhaustive list, but it illustrates the different constituents present in flowback or produced water as well as the fact that the constituents will vary based on the type of formation and the location of the well.

Table 4: A summary of studies conducted on different shale formations. Ionic concentrations and TDS are reported in ppm (mg/L) and ^{226}Ra is in pCi/L (1 Ci = 3.7 x 10^{10} Bq)

Location & Type[a]	**pH**[b]	**TDS**	**[Ba]**	**[Ca]**	**[Na]**	**[Sr]**	**^{226}Ra**[c]
Marcellus: 5 day[d] FBW[31] (19 wells)	4.9-6.8	38,500-238,000	21.4-13,900	1,440-23,500	10,700-65,100	345-4,830	N/A
Colorado: FBW[32]	6.8	22,500	8.542	524.1	6,943.90	60.25	N/A
Marcellus: FBW[33]	N/A	278,000	9,000 ± 400	13,000 ± 1,000	29,000 ± 1,000	36,000 ± 2,000	18,108
Marcellus: FBW[34] (9 wells)	N/A	44,000-415,000	740-7,660	2,280-25,300	11,800-156,000	381-10,350	1,580-21,550[e]

[a] Flowback = FBW, Produced = PW

[b] pH values with N/A indicate that it was not measured in the study.

[c] ^{226}Ra with values N/A indicate that it was not measured in the study.

[d] Samples were collected 5 days after the hydraulic fracturing event

[e] ^{226}Ra concentrations were measured for 24-72 hours.

3.2 Neutron Activation Analysis (NAA)

3.2.1 Introduction

Neutron Activation Analysis (NAA) is an extremely sensitive and precise method, which yields a wealth of elemental information even for small sample quantities that can be analyzed "as is" without prior chemical treatment. NAA has become a powerful analytical tool with the advancement of nuclear reactors and semiconductor detectors[35]. The process requires a source of neutrons, which can be obtained from a nuclear reactor. The sample is bombarded with neutrons, causing the elements to form radioactive isotopes, which will decay through alpha, beta, or gamma emissions. These decay paths are well known and can be used to determine the constituents of the unknown sample or quantify the amount of material in the sample.

3.2.2 Experimental Setup

Raw fracking samples as well as dried samples (100 mg) were sealed into a 1.4 mL NAA polytube followed by a secondary containment (8 mL NAA polytube). The samples were irradiated with a neutron flux of 8×10^{11} neutrons cm^{-2} s^{-1} for one hour at a power level of 250 kW. Following irradiation, samples were cooled and removed from the reactor core until they were safe for transportation. The gamma emissions were analyzed via HPGe.

3.2.3 Results

Due to the high concentration of chloride and sodium ions present in the sample, the irradiated sample was allowed to decay up to a week to decrease the detector dead time to a reasonable amount. Table 5 lists information of the isotopes produced upon irradiation of raw fracking samples.

Table 5: The table lists information regarding analytes of interest (gray highlight) in the irradiated samples as well as the main contributors to the high background activity. Natural abundance refers to the abundance of isotopes that are naturally found (e.g. if 1,000 chlorine atoms were analyzed, one would expect to find 242.4 ^{37}Cl atoms and 757.6 ^{35}Cl atoms.)

Reaction	Natural Abundance	Half-life	Decay Mode	Daughter Nuclide
^{23}Na (n,γ) ^{24m}Na	100%	20.2 ms	IT[1]	Na-24 ($t_{1/2}$ = 14.97h)
^{37}Cl (n,γ) ^{38}Cl	24.24%	37.2 m	γ	Ar-38 (stable)
^{86}Sr (n,γ) ^{87m}Sr	9.86%	2.8 h	IT	Sr-87 (stable)
^{88}Sr (n,γ) ^{89}Sr	82.58%	50.61 d	γ	Y-89 (stable)
^{138}Ba (n,γ) ^{139}Ba	71.70%	1.4 h	γ	La-139 (stable)

The abundance and half-lives of chlorine and sodium made the sample too radioactive so samples could not be analyzed immediately due to high detector dead time and background. By the time all chloride and sodium isotopes have decayed to background levels, the isotopes of interest, which are present at much lower concentrations, have either decayed or their signals were lost in the high background. Though this technique is very sensitive and requires no additional chemical modifications, the issues with high background activity in the sample complicate elemental analysis of the current environmental samples. This technique can be utilized once samples have undergone separation.

[1] IT (isomeric transition): When a nucleus has excess energy, it will undergo an isomeric transition by emitting energy and dropping to the ground state. Isomers have the same atomic and mass numbers.

3.3 Total Dissolved Solids (TDS) Analysis

In order to dispose and handle flowback and produced waters, it is necessary to understand the origin and characteristics of these waters. The amount of total dissolved solids (TDS) is an indicator of general water quality and can dictate the type of treatment and purification a water sample will receive. The dissolved solids comprises of inorganic salts and some small amounts of organic matter that are dissolved in water[36]. It is known that for Marcellus shale, the concentration of dissolved salts in flowback and produced waters increase dramatically with time[14,31,37]. In addition, Rowan et al. (2011) shows a positive correlation between amount of TDS and radium concentration[14,38]. Typically, in a highly saline sample, there are numerous positive ions that compete with radium for adsorption types; therefore, there is a greater percentage of radium remaining in the solution and not adsorbing. In a low saline sample, there is less competition; therefore, radium would be preferentially adsorbed compared to univalent ions. This explains why current treatment technologies for ordinary drinking water is not sufficient for oil and gas produced wastewater treatment[39].

3.3.1 Experimental Setup

In order to determine the TDS, four well-mixed samples were filtered through a standard glass fiber filter (Whatman grade 934AH, 1.5 μm pore size) and the filtrate was evaporated to dryness in a weighed dish and dried to constant weight at 180 °C. The total dissolved solids (in mg/L) can be calculated by subtracting the weight of the empty dish from the weight of dried residue in the weighing dish then dividing by the sample volume[40,41]. Depending on the amount of TDS, water can be designated as either freshwater with TDS less than 3,000 mg/L; brackish

with TDS values between 3,000 and 10,000 mg/L, saline with TDS values greater than 10,000 mg/L, or brine, which generally have TDS greater than seawater, >35,000 mg/L[42].

The original fracking samples (Figure 5) were first counted on the HPGe for 24 hours to determine if there were any naturally occurring radionuclides; however, the counts registered background activity, inferring that there is no NORM present in the samples. These samples will instead serve as a platform for highly saline environmental samples.

Figure 5: Raw fracking samples (left) compared to ultrapure (>18 MΩ/cm) water (right).

To determine the fate of ^{226}Ra in these samples, a 6.7 g of sample was spiked with 0.01 μCi (372 Bq) ^{226}Ra solution. Four samples were vacuum filtered then washed using 6.6 g of >18 MΩ/cm water. The filters and the filtrates were collected, allowed to sit for 22 days or more in a sealed container to reach secular equilibrium then counted on an HPGe for 24 hours.

3.3.2 Results

Due to the lack of information of the exact composition of the flowback samples, experiments were conducted to determine characteristics pertaining to the current sample. The total dissolved solids were calculated to be 16,000 ± 3,000 mg/L. This TDS amount places it in the "saline" category[42]. The fate of radium experiment, verified by HPGe, indicated that most of the radium concentrated in the solids that could not pass through the filter. Several background counts were collected, and no daughter peaks were observed in the background counts. The presence of the daughter peaks in the samples indicates that the peak at 186 keV is not only due

to the background radiation, but due to the presence of radium in the samples. The background counts at 186 keV were subtracted from the samples to determine the radium activity relative to the background. The average activity of the filters was 1.5 ± 0.2 counts per minute (CPM) compared to the filtrate activity of 0.4 ± 0.2 CPM, which is three times less. The results show that ^{226}Ra concentrated in the filters, therefore, digestion of solid samples is necessary to assay and perform separation studies.

3.4 Chemical Digestions

The goal of the digestion process is the complete dissolution of the analytes and the complete decomposition of the solids while avoiding loss or contamination of the analyte. The digestion procedures in open systems (e.g. hot plate digestions) have longer time requirements and lower digestion quality. This is due to their operation under atmospheric pressure and temperature limitations by the boiling point of the acid solution, compared to digestions in closed systems (e.g. microwave digestion), where higher temperature and pressures can be achieved and can be carried out in a few hours[43].

3.4.1 Theory

3.4.1.1 Nitric Acid and Hydrogen Peroxide (HNO_3 + H_2O_2)

The addition of an oxidizing acid, nitric acid, gives the chemical reaction:

$$(CH_2)_n + 2\ HNO_3 \rightarrow CO_2 + 2NO + 2H_2O$$

These form soluble nitrates with many elements. Adding hydrogen peroxide will increase the oxidation potential due to the reaction:

$$2H_2O_2 \rightarrow 2H_2O + O_2$$

This will re-oxidize nitrogen oxides, NO_x, into nitrate, NO_3^-, and thus suppressing the formation of yellow nitrous oxides, which is typical of nitric acid[43].

3.4.1.2 Nitric Acid, Hydrogen Peroxide, and Hydrochloric Acid ($HNO_3 + H_2O_2 + HCl$)

Hydrochloric acid, which is a non-oxidizing acid, forms soluble chlorides with many elements. It is capable of dissolving salts of weaker acids (carbonates, phosphates) and digesting iron alloys. The addition of hydrochloric acid will form nitrosyl chloride, *NOCl*, which itself will form *NO* and Cl_2,

$$2NOCl \rightarrow 2NO + Cl_2$$

which is a yellow gas that is encountered as a decomposition product of aqua regia (3:1 hydrochloric acid and nitric acid). It is an oxidizing agent and is most commonly used in the digestion of precious metals and sulfides[43].

3.4.2 Experimental Setup

Four different digestion methods were explored using EPA Method 3050B for sediments, sludges, and soils[44]. Digestion tubes were cleaned after usage by soaking overnight in 20% nitric acid, rinsed with water, and air-dried. All samples were diluted by a factor of 10,000 prior to ICP-MS analysis. Digestion #1 - #4 were analyzed in standard (no gas) mode and #3 and #4 were analyzed using helium collision mode.

3.4.2.1 Digestion #1: $HNO_3 + H_2O_2$

The first digestion method required addition of ten mL of 50% (v/v) nitric acid to one gram of sample and refluxed for ten minutes. Then, five mL concentrated nitric acid was added

and refluxed for 30 minutes. This step was repeated until digestion was complete and sample was evaporated down to 5 mL. Two mL of water was then added to the sample followed by 3 mL of 30% hydrogen peroxide addition. Hydrogen peroxide was added in 1 mL aliquots (not more than 10 mL) until bubbling subsided. The sample volume was reduced down to 5 mL then filtered using a Whatman No. 41 filter paper. This sample was diluted to a final volume of 100 mL to yield a sample in a 5% (v/v) nitric acid matrix.

3.4.2.2 Digestion #2: HNO_3 + H_2O_2 + HCl

The second digestion method was similar to the Digestion #1 method. However, following the hydrogen peroxide addition and the volume reduction to 5 mL, an additional 10 mL of concentrated hydrochloric acid was added to the digest and refluxed for 15 minutes. The sample was filtered and diluted to a final volume of 100 mL.

3.4.2.3 Digestion #3: HNO_3 + HCl + 2 Filter Papers

The third digestion method was also the EPA Method 3050B but modified specifically to improve the solubility and recovery of barium. It is possible that the barium was not able to pass through the filter; therefore, digesting the filter would encourage more recovery. One gram of dried sample was weighed then 2.5 mL of concentrated nitric acid and 10 mL of concentrated hydrochloric acid was added to the sample. Samples were refluxed for 15 minutes then filtered using a Whatman No. 41 paper filter. The filter was washed with 5 mL of 90 °C concentrated HCl and 20 mL of 90 °C >18 MΩ/cm water. The filtrate was collected and set aside while the filter paper was placed in the digestion vessel with 5 mL of concentrated HCl to be digested a second time. Following this second digestion, the filter paper was washed with concentrated HCl

and water as described previously. Filtrates were collected and added to the previously set aside filtrate. The sample was diluted to 100 mL and then analyzed using ICP-MS.

3.4.2.4 Digestion #4: HNO_3 + HCl + 3 Filter Papers

The fourth digestion method was the same process as Digestion #3, but the filter was digested a third time. The filter paper was washed with hot concentrated HCl and water then the filtrate was collected and added to the previous filtrates. Sample was diluted to 100 mL and then analyzed using ICP-MS.

3.4.2.5 Blank Digestions

To determine potential leaching of metals, all the glassware used for the digestions were used in two blank digestion processes performed on random days in between digestion methods. Digestion method #1 was performed on the cleaned glassware. Blank digestions (2% HNO3) were also performed on known amounts of samples to determine percent recovery of analytes. Sample 4 (S4, see Table 3) was evaporated to dryness and 1-2 grams of known sample was weighed and placed in the digestion vessel. Duplicate digestions using digestion method #4 were performed on Sample 4 while varying the dried sample amount: 2.0 and 1.5 g. Following digestions, samples were diluted accordingly and analyzed via ICP-MS.

3.4.3 Results

Results from the fate of NORM study showed that ^{226}Ra concentrated mainly in the filter. Chemical digestions of these samples were necessary to decompose the matrix and to free the metals for ICP-MS analyses. Prior to digesting actual flowback samples, a known sample

(Sample 4) was digested using Digestion Procedure #4. The percent yield for sodium, calcium, strontium, and barium were 121 ± 5%, 96 ± 9%, 99 ± 4%, and 95 ± 10%, respectively. The high recoveries in these digestion samples suggest that procedure #4 is an acceptable method for digesting unknown environmental samples because of minimal sample loss; however, because sodium is prevalent in the natural environment, >100% recoveries were seen.

Table 6 shows the ICP-MS calculated concentrations of each ion in the actual flowback water for each digestion method. All samples were spiked with an internal standard, 10,000-ppm indium, in order to determine if there were losses of analyte throughout the digestion process. Digest 1 - 4 was analyzed in standard mode and the highlighted rows in the table were analyzed using helium collision mode. The reported ion concentration for samples analyzed using collision mode decreased due to polyatomic interferences not being able to make it to the detector. The > 90% indium yields here and in Digestion #3 indicate that the digestion procedure is acceptable since there was no significant loss in analyte during the process.

Table 6: Metal ion concentrations in digested samples using ICP-MS analysis. The errors represent one sigma uncertainty based on triplicate digestion samples.

Digest	Na	Ca	Sr	Ba	In
#1	43,627 ± 129	32,684 ± 1,368	1,355 ± 4	131 ± 21	N/A
#2	46,849 ± 5,753	36,381 ± 2,312	1,399 ± 23	124 ± 23	N/A
#3	44,383 ± 6,538	34,208 ± 2,441	1,519 ± 91	344 ± 15	N/A
#4	52,913 ± 6,161	38,456 ± 2,118	1,583 ± 64	623 ± 53	N/A
#3 (He)	31,048 ± 3,401	9,922 ± 424	1,337 ± 33	219 ± 37	9,383 ± 146
#4 (He)	65,140 ± 4,238	13,426 ± 3,493	1,437 ± 156	526 ± 34	9,435 ± 617

3.5 Summary

The characterization of oil and gas wastewater is very important because the wastewater content will vary based on location, shale formation, and the time it takes for the wastewater to emerge to the surface. For example, wastewater from the Marcellus shale tend to be more orange due to the amount of iron as compared to the samples we have, which has an oily residue because oil and gas were extracted from the Eagle Ford formation.

The wastewater was analyzed for its TDS and ionic content. They were used as a platform for highly saline sample matrices, though they did not originally contain any ^{226}Ra. However, by spiking the samples with ^{226}Ra and through filtration, we found that the ^{226}Ra exhibited preference for accumulating in the solids; therefore, digestion procedures for barium were developed in order to recover as much barium for separation studies. Barium was used as an analog for ^{226}Ra due to their chemical similarities.

As seen from Table 6, it is apparent that the chemical recovery of barium was much higher in digestion #4 for both analysis methods. This is due to the increased solubility of barium in hydrochloric acid. The solubility of $BaCl_2$ in water is 385 g/L (20 °C), which is much more compared to $Ba(NO_3)_2$ at 105 g/L (25 °C). This is also true for $RaCl_2$, with solubility in water of 245 g/L (20 °C)[44]. Modifying digestion #3 by adding another filter dissolution step increased the barium recovery because the barium stuck in the filter was brought into solution. Since barium and radium have similar chemical properties, to maximize radium recovery, procedure #4 will be used as the main digestion method to maximize radium recovery.

Chapter 4: Radioactive Source Preparation and Detection

4.1 Introduction

The analyses of radionuclides in various matrices are in great demand. A cost-effective technique for separation and recovery of analytes is an ongoing requirement in nuclear forensics and in general, the nuclear industry. This chapter focuses on the analysis of low-level radium and uranium using electrodeposition and alpha spectrometry for applications in nuclear forensics and environmental radiochemistry.

Current analysis methods of radium include measuring radon emanation by collecting ^{222}Rn (daughter nuclide); however, large sample volumes are required when low level samples are analyzed and radon ingrowth necessitates long waiting period to achieve secular equilibrium (approximately 22 days)[45]. Researchers have since moved to electrodeposition due to its capabilities of depositing low-level alpha-emitting radioactive material and can be counted using an alpha spectrometer immediately. Electrodeposition is a technique used to prepare thin solid films of the radioactive material of interest, even if they are present in small quantities. The thin films created are very strong, reducing detector contamination. In addition, for radium analyses, there is no need to wait for secular equilibrium (~22 days) and therefore, analysis can be performed immediately after deposition.

However, there have been very few attempts to electrodeposit radium for routine determinations due to its very soluble oxide, $Ra(OH)_2$[46]. For radium analysis, co-precipitation with barium sulfate has generally given satisfactory results for radium determination by alpha spectrometry; however it lead to poor energy resolution due to the thickness of the layers deposited[47]. In addition, the existence of interfering ions causes thicker layers and can drastically decrease ^{226}Ra yields[47,48]. The most cited literature study of the electrodeposition of radium was

written by Roman in 1984, where they used aqueous ammonium acetate at lower voltages[49]. Similar studies done by Garcia-Tenorio and Garcia-Leon in 1986[50] and Short in 1986[51] were performed. They varied parameters such as the amount of ^{226}Ra and initial pH, as well as successfully using the method on samples like acid extracts of pure clays and even on dry ashed kangaroo/sheep meats and organs. Orlandini et al. (1991) used 0.17 M ammonium oxalate and 0.14 M HCl with addition of platinum in microgram amounts and they got ^{226}Ra recoveries ranging from 90-100%[52]. Alvarado adapted Orlandi et al. method for the determination of low levels of ^{226}Ra and ^{224}Ra in environmental samples (e.g. drinking water, well water, and dissolved bones)[53]. Roman (1984) claimed a 100% deposition efficiency, which was attainable; however, due to the difficulty in plating radium, this method alone was inconsistent and produced large error margins. This project adapted the method described by Roman (1984) and added ^{238}U as a carrier. Previous studies have shown that addition of ^{238}U carrier gave quantitative reproducible electrodeposition of microgram quantities of the actinides[54]. In addition, to our knowledge, there lacks a thorough investigation of the electrodeposition of uranium in aqueous ammonium acetate mixtures and its role as a carrier for reproducible and quantitative radium electrodeposition, ranging from 60-90%, which is consistent with other literature values[50,55].

The most widespread methods for electrodeposition of actinides is described by Talvitie (1972) and modified by Hallstadius (1984)[56]. The Hallstadius method is now the most extensively used method of source preparation for alpha-particle spectrometry, which can deposit 90-100% of the actinides (99% for U). However, this method is not sufficient for radium as it can only deposit 1% radium. The use of sulfuric acid electrolyte to prevent the adsorption of the low mass concentration of most actinides onto the wall of the electrodeposition cell can also be

detrimental to quantitative radium recovery. In addition, this method required a pH adjustment to 2 by blowing gaseous ammonia over the surface while swirling the solution. The solution was then poured into the electroplating cell and the beaker was washed with 1% sulfuric acid and the pH was adjusted again to 2.0 - 2.3. Then, the sample was electrolyzed at 1.1 - 1.2 amperes for 120 minutes[57]. Torrico et al (2015) plated samarium as an analog for actinides using an ammonium acetate matrix to study the surface characterization of this method[58] but currently, a thorough investigation of plating ^{238}U in an ammonium acetate matrix does not exist.

In this chapter, ^{238}U and ^{226}Ra with activities as low as 0.6 Bq (counts per seconds) is plated on stainless steel disks using ammonium acetate solutions. The addition of 50 μg of ^{238}U to samples encourages the reproducibility of ^{226}Ra electrodeposition. The method described here was found to be a simpler version of methods found in the literature[56,57,59–61]. Our method consists of the addition of sample into the 0.35 M ammonium acetate solution with a starting pH of 5 and allowed to run for several hours (2 hours for ^{238}U, 4 hours for ^{226}Ra) undisturbed except for the addition of 2.7 mL electrolyte to account for evaporative losses. After four hours, the pH reached a value of 9 due to the reduction of water to hydrogen gas and hydroxyl ions, allowing the formation of the hydroxyl layer[46,62] and allowing the precipitation of radium hydroxide on the cathode surface.

4.2 Electrodeposition Mechanism

During the electrodeposition process, a thin film is deposited on the surface of the stainless-steel cathode. The thin film is believed to involve either the hydroxide of the element plating out, or initially a hydroxide precipitate forming near the cathode before being reduced to

the metal and subsequently deposited on the cathode[63]. The standard reduction potential for radium is[64]:

$$Ra^{2+}(aq) + 2e^{-} \rightarrow Ra\ (s) \qquad E^{0} = -2.80\ V$$

The standard reduction potential for barium is similar to radium, E^{0} = -2.90 V[28,64]. A high concentration of hydroxyl ions adjacent to the cathode surface is required to precipitate hydroxides on the "hydroxyl layer." Hansen (1959)[62] explored the formation of hydroxide precipitates at the cathode. His theory of electrodeposition of lanthanides and actinides hydroxides at low current densities provides a starting point to explain the mechanism of the electrodeposition process. A high concentration of hydroxyl ions forming a "hydroxyl layer" near the cathode surface is needed in order for radionuclides in the electrolyte to form hydroxide precipitates. To produce the "hydroxyl layer" on the cathode, hydrogen ions supplied by the electrolyte or the dissociation of water must occur according to the reaction,

$$2H_3O^{+}(aq) \rightarrow 2\ H_2\ (g) + 2OH^{-}\ (aq)$$

Hansen's theory describes equations and conditions that control the electrodeposition of insoluble hydroxides at the cathode surface. However, in order to apply his theory, the following assumptions must be met: (1) steady state diffusion conditions, (2) obtain good control of diffusion layer, (3) obtain hydroxyl layer thickness, and (4) maintain a well stirred bulk electrolyte with uniform composition. This is possible when a rotating disk electrode (RDE) is used; however, it is not possible to develop simple equations to explain the mechanism of conventional electrodeposition[62], which is the method employed in these experiments. In conventional electrodeposition, the thickness of the cathodic layer cannot be controlled because the arrangement usually consists of a cylindrical cell with a metallic cathode and platinum anode

wire, which are both in contact with a stagnant electrolyte that is usually not equipped with mechanical stirring or forced flow (see Figure 6).

Using the Hallstadius method, Beesley et al. (2009) confirmed through optical microscopy that there is slow dissolution of the platinum anode. They found through SEM-EDX that there were small amounts of platinum on the surface of the source, which resembled mossy aggregates[59]. These platinum aggregates contributed to the thickness of the deposits, which lead to the deterioration of the energy resolution of the alpha spectra. However, uranium deposition still occurred without platinum interference, indicating the important role of platinum in the electrodeposition of the hydroxides. The high specific surface of the platinum deposits increased the surface hydroxyl concentration, providing nucleation sites for preferential uranium precipitation, which is in line with Hansen's theory that a hydroxyl layer was necessary. Mendez et al. (2010) also found that uranium precipitation seems to occur preferentially at points in the surface containing precipitated platinum dissolved from the anode[60] suggesting that platinum acts a carrier for electrodeposition of analyte atoms[61]. Nørskov et al. (2005) found that platinum is a better electrocatalysts than other metals for hydrogen evolution[65], which is helpful in understanding the need for a hydroxyl layer in order to accelerate the precipitation reaction on the cathode. These findings validate the addition of microgram amounts of platinum in the electrolyte[52,53,66,67].

Most routine methods use aqueous electrolytes since electrodeposition from organic media requires high voltages (>50 V)[46]. Ammonium acetate was chosen because it did not require high voltages and therefore did not require a cooling system to maintain a lower operating temperature. Instead, it requires low voltage (~10 - 20 V) to achieve quantitative depositions[57,58]. Torrico et al. (2015) attempted a surface characterization of the stainless-steel

disk with lanthanides deposited in an ammonium acetate electrolyte. They tested various ammonium acetate concentrations of 0.175 M, 0.35 M, and 0.7 M with a constant voltage and 4 hour electrolysis time and they found that increasing the electrolyte concentration resulted in increased gas production accompanied by splattering of the solution[58]. They observed that lower ammonium acetate concentrations resulted in a more uniform thickness due to decreased gas production, resulting in fewer disturbances in the solution. These findings are consistent with a well-studied example of an electrolytic reaction involving the acetate ion, the Kolbe reaction. It involves the oxidation of carboxylate at the anode, followed by decarboxylation and dimerization of the alkyl radical[68,69]:

$$RCOO^- \rightarrow RCOO^+ + e^-$$

$$RCOO^* \rightarrow R^* + CO_2$$

$$2R^* \rightarrow R_2$$

The Kolbe product, R_2, is assumed to be a recombination of the intermediate radical. Further analysis is needed to differentiate between the gases released in the reaction (e.g. H_2, CH_4, and C_2H_6). These gases can lead to the generation of bubbles at the cathode, which can lead to brief voltage instabilities by restricting conduction and preventing deposition.

4.3 Experimental Setup

4.3.1 Electrodeposition Setup

The electrodeposition apparatus (Model: EP-4, Phoenix Scientific Sales) has 4 stations, a power supply between 13-15 V with a current capacity of at least 2 Amperes per station. The plating stations are electrically in parallel and each station is wired to supply a positive voltage starting from the binding post at the top, connected to a platinum electrode (99.5%, ~10 cm,

diameter = 1.3 mm, SurePure ChemMetals), which is immersed in the plating cell as a single formed wire with a ~90° bend. A 3⁄4-inch polished stainless steel planchet (d=0.75", 0.032"-0.036" thick, AF Murphy Die & Machine Co. Inc.) is inserted into the cap with the polished side toward the inside of the vial and acts as the surface for which the deposition occurs. It contacts the cathode stud that is connected to a meter, fuse holder (3A), and the rheostat that allows for current adjustment in the cell. The solutions are assumed to be well mixed and uniformly deposited due to bubbling action caused by the electrolysis of the solution. Figure 6 shows the electrodeposition instrument used throughout this project, which is similar to that of Talvitie (1972).

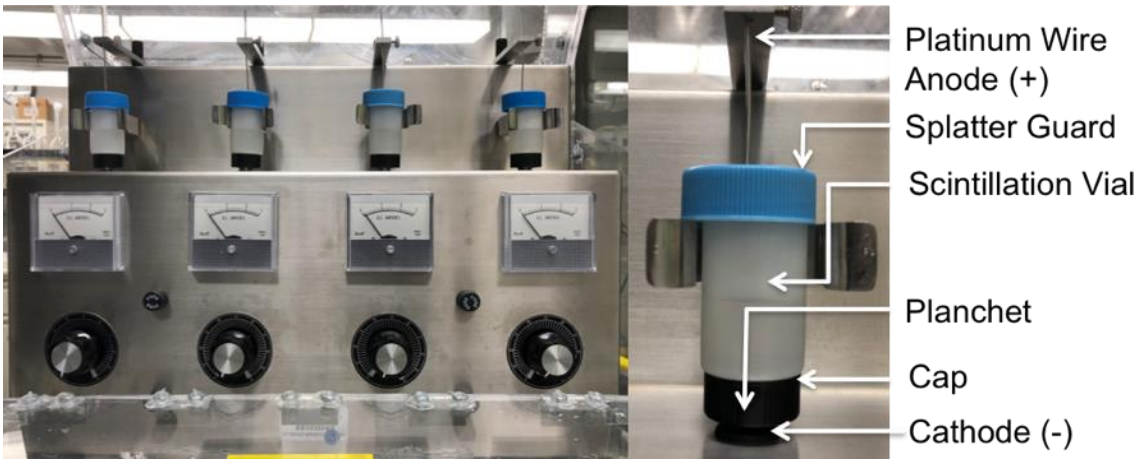

Figure 6: The electrodeposition apparatus in our laboratory. A maximum of four cells can be assembled at once. The current can be adjusted using knobs.

4.3.2 Material Preparation

Planchets were prepared by first marking the non-polished surface, degreasing using warm, soapy water, then rinsing with acetone. They were immersed in warm 2% sodium dichromate - 4 M nitric acid for 10 minutes and rinsed with water until cell assembly. The cells were cleaned by immersing in chromerge® for 3-4 hours, then rinsed and immersed in 4 M nitric acid for 1 hour to remove any traces of chromium. Cells were stored in water until ready for

assembly. After each electrodeposition, a brown deposit was observed on the anodes, which is likely the electrolyte solution. The brown deposits were removed by immersing the anode in boiling 1% sulfuric acid and rinsed with water. This encourages radium sulfate precipitation and ensures no ^{226}Ra carryover in the platinum wire.

4.3.3 Preparation of Electrolyte and Radioactive Solutions

The electrolyte was prepared by weighing 13.5 g of ammonium acetate ($C_2H_7NO_2$, NH_4Ac, Fisher Chemical, HPLC grade) and diluting to 500 mL with 0.1 M HNO_3. The pH of the electrolyte was about 5 and after electrodeposition, the pH increased to 9, which is due to the cathodic reduction of the water evolving hydrogen gas and producing hydroxyl ions[64].

The secondary ^{226}Ra stock solution described in Section 2.1.4 was diluted further to yield a solution containing 2 Bq/mL. Aliquots of this solution was added to the cells to deposit 0.6 Bq. Similarly, 0.6 Bq ^{238}U was added to the cells by taking 50 μL of the secondary ^{238}U solution.

4.3.4 Electrodeposition Procedure

After cleaning and assembling cells, 300 μL of 2 Bq/mL ^{226}Ra and/or 50 μL of 4.2 mM ^{238}U solution was added to 10 mL of 0.35 M ammonium acetate. For the time and cell dependence study, the pH of each sample was measured before pouring into the cells and after each time point (1, 2, 3, 4 hours). The experiment was allowed to run with the addition of electrolyte at the second hour to account for evaporative losses. Upon completion of the study, the electrolyte was discarded, the stainless steel planchets were washed with water twice followed by an ethanol rinse. They were transferred to an oven (182 ± 2 °C) and allowed to dry

for 10 minutes. Samples were counted on a previously calibrated alpha spectrometer for 24 hours (see previous chapter).

Blank samples (electrolyte only) were run periodically using similar conditions to ensure that the platinum anodes were not retaining or leaching any metals as well as to ensure that the cleaning procedure is satisfactory.

4.3.5 Analysis of Radium-226 and Uranium-238 via Alpha Spectroscopy

The electrodeposited samples were analyzed for 24 hours. The activity (Bq) was calculated using the equation:

$$A = \frac{Area}{t_{count} I_\alpha \psi_{eff}}$$

The area is the number of counts per second (CPS) in a specified region of interest, t_{count} is the count time in seconds, I_α is the branching ratio of the alpha particle at the specified energy, and ψ_{eff} is the detector efficiency at the region of interest. The percent recovery was calculated by:

$$\% \ Recovery = (A / A_{ref}) \times 100\%$$

where A_{ref} is the activity of the initial or reference samples.

When ^{238}U is electrodeposited independently and analyzed using alpha spectroscopy, there is a small peak at 4.7746 MeV (71.37%). This peak is ^{234}U, which is a decay product of ^{238}U and is present in all ^{238}U electrodeposited samples. The addition of uranium when analyzing radium samples helps stabilizes the electrodeposition; however, when analyzing the activity of ^{226}Ra, the ^{234}U and ^{226}Ra overlap at 4.77 MeV, causing an inflation in the observed ^{226}Ra activity.

As a result, 0.6 Bq of ^{238}U was independently deposited ($n > 24$) in order to determine the ratio of ^{238}U and ^{234}U ($R_{238/234}$). This ratio was used to calculate the ^{234}U contribution based on the count rate of ^{238}U.

$$R_{238/234} = \frac{^{238}U}{^{234}U}$$

When ^{238}U and ^{226}Ra are co-deposited, the contribution of ^{234}U can be calculated by taking into account the ^{238}U count rate during co-deposition and the count ratio of the uranium isotopes,

$$^{234}U = \frac{^{238}U_{+^{226}Ra}}{R_{238/234}}$$

The ^{234}U contribution can be subtracted by the overall counts present in the 4.77 MeV range to get the count rate of ^{226}Ra:

$$^{226}Ra = {}^{226}Ra_{+^{234}U} - {}^{234}U$$

$$^{226}Ra = {}^{226}Ra_{+^{234}U} - \frac{^{238}U_{+^{226}Ra}}{R_{238/234}}$$

4.4 Results

4.4.1 Electrodeposition as a Function of Time

As can be seen in Figure 7, a 98.1 ± 12.8% deposition was observed after 2 hours for ^{238}U (*n = 3*), which is comparable to the results found using the Hallstadius method but a more simpler electrodeposition process. However, for ^{226}Ra, only a 71.2 ± 10.8% deposition efficiency was observed when co-deposited with ^{238}U (*n = 8*) for 4 hours, which does not match results from Roman's (1984) studies but matches well with other literature values[50,55].

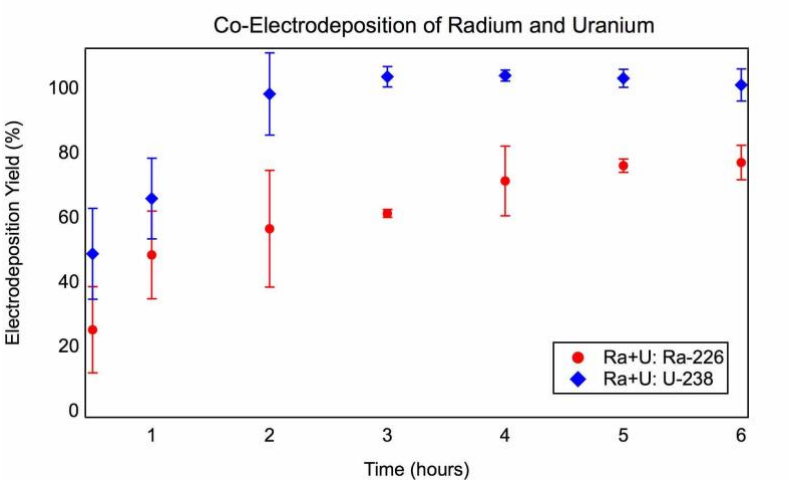

Figure 7: Electrodeposition yield as a function of time when 0.6 Bq of ^{238}U and 0.6 Bq of ^{226}Ra are co-electroplated in 0.35 M ammonium acetate electrolyte with a starting pH of 5.

4.4.2 Effect of Uranium-238 spike on Radium-226 Recovery

When ^{226}Ra is electrodeposited individually, sometimes a >90% electrodeposition is observed; however, it is widely inconsistent. As seen from the cell dependence study in Figure 8, independent deposition of radium (black squares) had error values greater than 30% (*n = 8)*; however, co-depositing with uranium (red circle) decreases the error on the radium yield to less than 11% *(n = 8)* but is only capable of 60%-80% efficiency. This recovery value is consistent with the time dependence study.

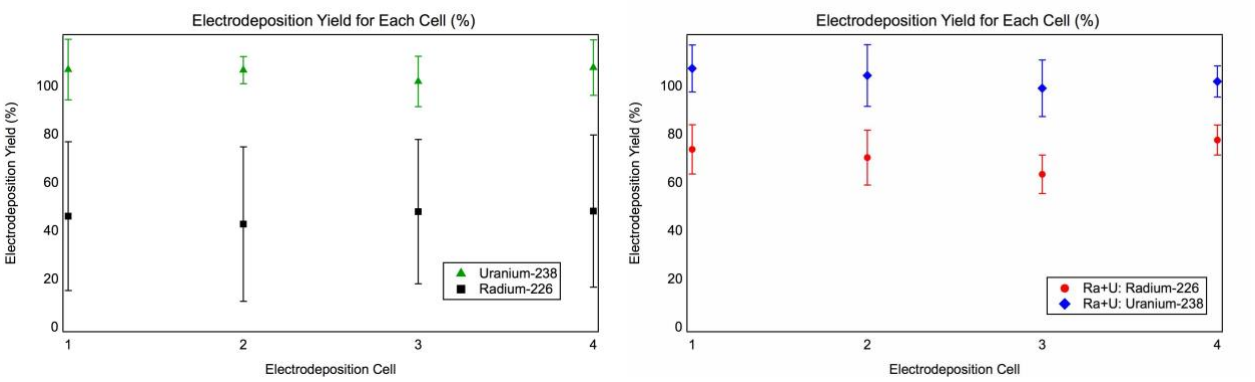

Figure 8: Electrodeposition yield for each cell. ^{226}Ra and ^{238}U are plated individually (left) as well as ^{226}Ra and ^{238}U co-plated in the same cells (right).

As seen from Figure 8, the recovery of ^{238}U whether deposited independently or with ^{226}Ra is reproducible and is not affected by the addition of ^{226}Ra. However, the independent deposition of ^{226}Ra generated large error values, whereas co-deposition of ^{226}Ra with ^{238}U decreased the errors. As mentioned earlier, radium is highly electropositive and has very soluble oxides; therefore, it is difficult to electroplate radium[28,46]. The addition of 50 µg of ^{238}U to samples encourages the reproducibility of radium electrodeposition. Similar to the addition of platinum to increase the surface hydroxyl concentration[59–62], it is possible that uranium behaves similarly to platinum where it acts as a carrier to deposit small quantities of material. Previous studies have shown that addition of ^{238}U carrier gave quantitative reproducible electrodeposition of microgram quantities of the actinides[54]. A one-time addition of ^{238}U carrier increased average recovery of 98.3 ± 0.77% and incremental addition of ^{238}U increased the average recovery of 99.8 ± 0.2%[70]. Natural uranium (^{238}U) is highly suitable as a carrier because of its low specific activity (1.5 dpm/µg)[70]. Donnan and Dukes (1964) found that the rate of deposition increased as the concentration of carrier and/or radionuclide increased; therefore, it was possible to take full advantage of the concentration effect to increase the deposition rate by the addition of a carrier[70].

4.4.3 Effect of Other Group II Metals on Radium-226 and Uranium-238 Recovery

The effect of interfering ions such as barium ($n = 2$) and strontium ($n = 2$) on uranium and radium deposition were also investigated. In Figure 9, despite the increasing amount of barium and strontium, ^{238}U still attained near 100% deposition. This has not been documented in literature previously. Meanwhile, the deposition of radium suffered with an addition of barium as low as 10 μg. The addition of strontium does not seem to affect the radium deposition as drastically as the addition of barium. From the images of the stainless-steel planchets, it appears that an opaque layer has been deposited when barium is added to the solution. This layer prevents the alpha particles from reaching the detector, contributing to the decrease in ^{226}Ra yield. The drastic effect of barium on the radium electrodeposition is consistent with literature findings[47,48,67]. To avoid a reduction on the yield, separation of ^{226}Ra from barium must be done prior to electrodepostion[47].

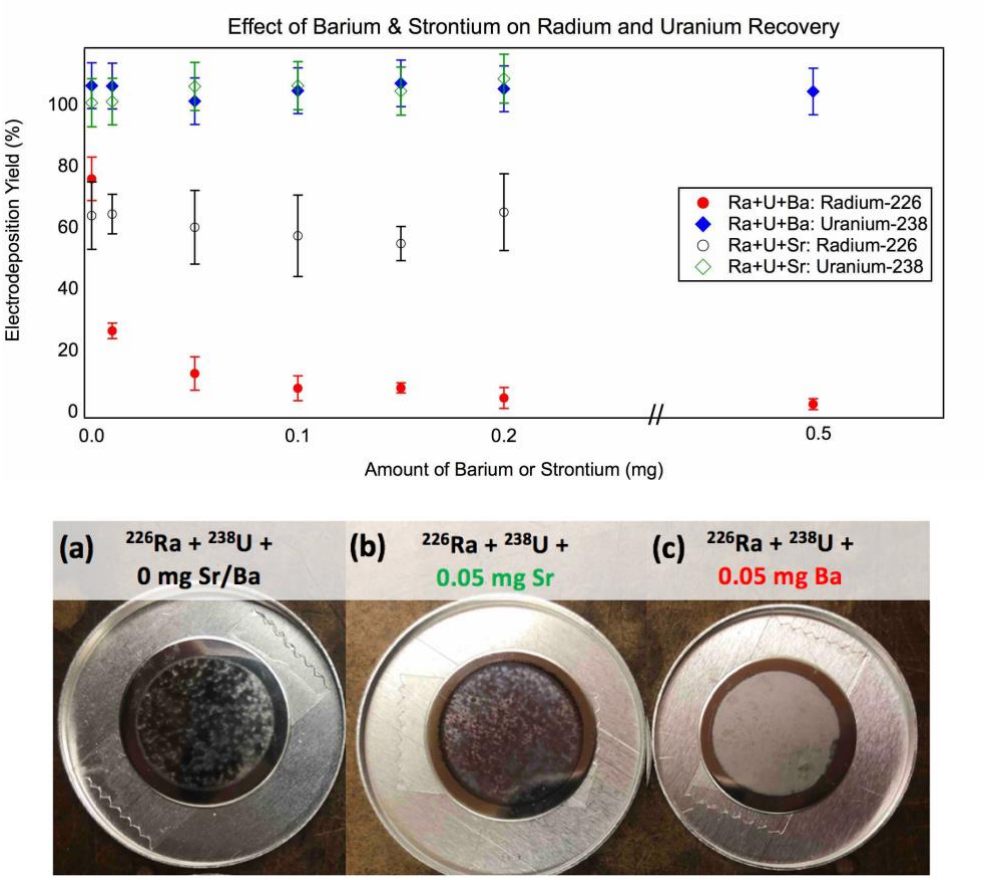

Figure 9: The graph shows the effect on yield of barium and strontium addition on ^{226}Ra and ^{238}U recovery. The stainless-steel disks show deposits of ^{226}Ra and ^{238}U with (a) 0 mg strontium (Sr) or barium (Ba) (b) 0.05 mg Sr, and (c) 0.05 mg Ba.

4.4.4 Analysis of the Integrity of Deposited Sample

The electrodeposition method described in this chapter produced a thin film that was very strong and provided good energy resolution. The radium daughters grow into full equilibrium activity in the film and are retained quantitatively for at least 3 months at ambient temperatures, which is consistent with literature findings[49,71]. The figure below shows the alpha spectra and percent yield after analysis of one sample on the same detector. This figure shows the integrity of the electrodeposition process and shows that the daughter nuclides are growing in and not

escaping, which is important as to not contaminate the detector.

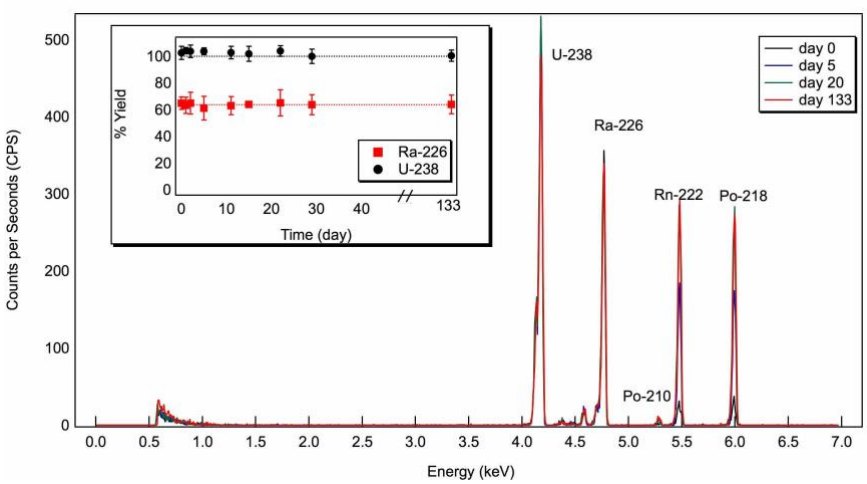

Figure 10: Alpha spectra of ^{238}U and ^{226}Ra and its daughters. The sample was electrodeposited using the procedure outlined here and analyzed using the same detector on the given number of days. The inset shows the ^{238}U and ^{226}Ra activity being stable during the 133 days of analysis.

4.5 Summary

Electrodeposition is a useful technique for radiochemical assay work, especially to prepare sources for alpha spectrometry for quantitative and accurate determinations of low-level radionuclides. Our laboratory has demonstrated that the procedure outlined by Roman (1984) for ^{226}Ra analysis can also be applied to reproducibly prepare ^{238}U sources on stainless steel disks using aqueous ammonium acetate solutions in 2 hours, which is an improvement from previously published methods. This method is robust as it allowed a 100% electrodeposition of ^{238}U even with the addition of 0.5 mg interfering ions such as barium and strontium. We also identified that the addition of microgram amounts of uranium increases the reproducibility of ^{226}Ra electrodeposition, similar to the effect of adding platinum in the electrolyte to encourage the deposition of ^{226}Ra by way of the concentration effect as well as the increase of the hydroxyl layer on the cathode to facilitate precipitation.

Chapter 5: Separation of Radium & Barium from Group II Metals

5.1 Introduction

In a highly saline sample mixture, additional ions (e.g. group II ions) present in the sample complicate analysis of analyte ions (barium and ^{226}Ra). Therefore, standard separation techniques for ordinary drinking water are not sufficient for highly saline sample mixtures such as flowback wastewater generated by oil and gas companies. In this chapter, a new ion exchange cation resin, RSM-25HP, developed by ResinTech, is compared to the well-researched, Dowex® 50W-X8, for its ability to separate ^{226}Ra from group II ions using batch and column experiments. The separation of ions reduces matrix interferences, allowing more accurate metal concentration assay. Aside from studies published in our laboratory[48], no other literature data exists on RSM-25HP.

5.2 Theory

5.2.1 Ion Exchange Technology

An ion-exchange reaction is defined as the reversible stoichiometric exchange of ions between a solid phase (ion exchanger) and a solution phase. Ion exchangers capable of exchanging cations are known as cation exchangers, whereas those with replaceable anions are known as anion exchangers. The ion exchanger is, ideally, insoluble in the medium in which the exchange is carried out. Ion exchange technology is used to purify solutions by the exchange of counter ions, $A^{z_A}$and B^{z_B}, with general valences, z_A and z_B, respectively:

$$z_B A^{z_A} + z_A \bar{B}^{z_B} \rightleftharpoons z_B \bar{A}^{z_A} + z_A B^{z_B}$$

where the top bar distinguishes the solid phase[72].

The mechanism of ion exchange is dictated by various parameters related to the ion exchange materials such as the nature and type of fixed functional groups, the physical forms, and the origin of the ion exchange material[72]. The resins described in this chapter are strong cation exchangers containing sulfonate $(-SO_3^-)$ groups, macroporous gel beads, with polystyrene divinylbenze backbone. Divalent ions are more tightly held by the resin than monovalent ions and even when ions have the same valency, the resin still has preferences. For 50W-X8 resins, the selectivity decreases according to the order: $Ba^{2+} > Sr^{2+} > Mg^{2+} > K^+ > Na^+ > H^+$[73].

The stability (chemical, physical, and mechanical) and the behavior of the ion exchange resins depend primarily on the structure, degree of cross-linking of the resin matrix, and the nature of the number of fixed ionic groups. The structure and degree of cross-linking determines the porosity of the matrix, the degree of swelling of the resin, and the mobility of the counter ions through it, which in turn controls the rates of ion exchange in the resin. Cross-linking of the resins is essential in order to ensure that the resins are tough and insoluble. The level of cross-linking plays an important role in the physical and chemical properties such as moisture content and particle size. Generally, low degree of cross-linking in gel resins allow absorption of large amounts of water, resulting in resin swelling, which leads to the variation in volume[72]. On the other hand, resins with high degree of cross-linking tend to be more resistant to mechanical breakdown and less swelling; however, it limits counter ion accessibility[72]. Macroporous resins, such as the ones used in this project, usually have high effective surface area, which leads to higher solute ion diffusion, increasing the interaction with fixed ionic sites, and leading to faster reaction rates.

In addition, resin particle sizes have impact on performance. Smaller particles will improve kinetics of the ion exchange reaction but cause an increase in the pressure drop, leading

to a decrease of the flow rate. The performance of ion exchange resins in terms of kinetics and sorption equilibrium depends on the physical and chemical properties of the resin.

The selectivity coefficient can also be used to describe ion exchange equilibria. This applies if the ion exchange reaction obeys the mass action law because the ion exchange process can be regarded as a physical redistribution of ions without chemical reaction. The molar selectivity coefficient, k_B^A, is given as:

$$k_B^A = \frac{\bar{C}_A^{\,z_B} C_B^{\,z_A}}{\bar{C}_B^{\,z_A} C_A^{\,z_B}}$$

In this expression, C_A and C_B represent the corresponding molarities. These parameters strongly depend on the operation conditions; as a result, when trying to compare over a range of conditions, care must be taken to ensure that the speciation and ionic strength effects are taken into account.

5.2.2 Calculation of Distribution Values and Resin Uptake

Distribution ratios, *D* (mL/g), generally give an idea of the extractability of a compound from one phase to another. Generally, high distribution values indicate high affinity for the resin to take up the ion; however, too high distribution values could be problematic because it will be difficult to strip the resin and recover the ion for reuse. The equilibrium distribution ratio is defined as:

$$D = [(A_0 - A_f) / A_f] \times (V/m)$$

where A_o and A_f are the activities or concentration of the initial (pre-contact with resin) and final (post-contact with resin) aliquots, respectively. *V* is the volume of solution (mL) and *m* is the mass of the resin (g). The percent uptake is similar to the distribution value,

$$\% \text{ Uptake} = [(A_0 - A_f) / A_0] \times 100\%$$

5.2.3 Adsorption Capacity

Adsorption is the process of adhering atoms, ions, or molecules in a liquid or gas onto a surface. It is widely used in wastewater treatment processes to remove pollutants due to its simplicity, efficiency, and economic viability[74]. The three different sorption types are (1) physisorption, which is reversible and is a rapid process that is based on van der Waals forces, dipole forces, and dispersion forces and the energy of reaction is usually below 50 kJ/mol; (2) chemisorption relates to the chemical bonding between the adsorbate and adsorbent and the interactions are generally much higher (60 - 450 kJ/mol); and (3) ionosorption is when ion transfer occurs[75].

The adsorption capacity is the amount of adsorbate (ions) taken up by the adsorbent (resin) per unit mass of the adsorbent. The adsorption capacity, q_e (mg/g), is defined as:

$$q_e = (A_0 - A_f) \times (V/m)$$

where A_0 and A_f are the initial and equilibrium (final) concentrations of solute (in our case radium) in solution (Bq/mL), respectively. The difference between the initial and the equilibrium ion concentrations determines the amount of ion adsorbed on the resins.

5.2.4 Adsorption Kinetics

The three steps in an adsorption process are (1) external mass transfer of the adsorbate (ions) from the bulk solution to the external surface of the adsorbent (resin), (2) internal diffusion of the adsorbate to the sorption sites, and (3) transport into the pores of the adsorbent. Studying the adsorption kinetics is necessary because it elucidates the adsorption mechanism and helps

determine the rate limiting step of the process[74]. It's important to predict the rate at which the contaminant is removed from the aqueous solution in order to properly design treatment plants. The kinetic parameters of the 50W-X8 resin is well studied; however, few papers identify radium as the metal of interest. In addition, to date, there is no adsorption kinetic parameters available for RSM-25HP due to its novelty. There are several models to obtain the adsorption kinetics. This section will focus on the pseudo-first-order and the pseudo-second order models.

5.2.4.1 Pseudo-first-order Model

The pseudo-first-order model introduced by Lagergren (1898)[76] is generally used in the form proposed by Ho and Mckay (1999)[77],

$$\ln\big(q_e - q(t)\big) = \ln(q_e) - k_1 t$$

where k_1 is the pseudo-first order rate constant (1/min), $q(t)$ is the amount of ion removed at time t (mg/g), q_e is the adsorption capacity at equilibrium (mg/g), and t is the contact time (min). A plot of $ln\ (q_e - q(t))$ versus t can be used to determine the adsorption capacity and the rate constant.

5.2.4.2 Pseudo-second-order Model

The linearized pseudo-second-order model equation is given in the form proposed by Ho and Mckay (1999)[77],

$$\frac{t}{q(t)} = \frac{t}{q_e} + \frac{1}{k_2 q_e^2}$$

where k_2 is the pseudo-second order rate constant (g mg^{-1} min^{-1}). A plot of $t/q(t)$ versus t can determine the adsorption capacity and the rate constant.

5.3 Experimental Procedures

5.3.1 Ion Exchange Resin Preparation

The cation resins used for the column exchange experiments were Dowex® 50W-X8 and a new resin, Radium Selective Media 25 High Purity (RSM-25HP). There are few literature data on RSM-25HP; therefore, experiments will be done to assess the potential of RSM-25HP compared to the very well researched Dowex 50W-X8 resin. Table 7 shows a side-by-side comparison of the two different resins that will be used.

Table 7: A side-by-side comparison of the resins used.

	Dowex ® 50W-X8	ResinTech RSM-25HP
Polymer Type	Styrene/Divinylbenzene	Styrene/Divinylbenzene
Resin Type	Macroporous	Macroporous
Functional Group	Sulfonic Acid	Sulfonic Acid
Mesh Size[1]	50-100	16-50
Ionic Form	H^+	Na^+
% Cross Linking	8%	Not specified
Total Exchange Capacity (meq/L)	1.7	1.8
Water Retention Capacity	50-56%	45-55%

[1] Mesh size corresponds to the number of openings per linear inch in the sieve. For example, a resin described as 50 mesh (equivalent to 0.0117 in) indicates that 90% of the resin will be retained by a 50-mesh sieve (particles larger than 0.0117 in) and any particles smaller than 0.0117 inch will pass through. The smaller the mesh size, the larger the particle. In our case, RSM-25HP resins are larger than 50W-X8 resins because they can be retained by 0.132 in (16-mesh) openings, whereas the 50W-X8 resins will just pass through.

Prior to conditioning, both resins were purified. Fifty grams of resin was weighed then a 1:1 ratio of 50% sodium hydroxide (NaOH, Fisher Chemical) and 30% hydrogen peroxide (H_2O_2, Fisher Chemical) was added. The addition of NaOH transformed the resin from hydrogen to sodium form and the hydrogen peroxide oxidized any residual organics. The resin and solution were stirred using a glass rod for five minutes then 50 mL of water was added. The resin solution was stirred using a magnetic stir bar for an additional five minutes then filtered through a vacuum filtration unit and washed with copious amounts of water. Following filtration, the resin was placed in a new beaker with excess water and stirred for an hour to remove any traces of NaOH and H_2O_2. The resins were filtered again and stored in water prior to conditioning to a cation exchange resin.

The resin and column conditioning step was adapted from Zhang *et al.* (2015)[34]. The polypropylene columns (Eichrom Technologies, internal diameter, ID: 0.8 cm) were cleaned by soaking in 2% HNO_3 prior to loading with 2.7 g of cation exchange resin. The resin was conditioned with three bed volumes (9 mL) of 6 M HNO_3 to ensure that it is in the protonated form. Prior to sample introduction, the resins were washed with five bed volumes (15 mL) of water and five bed volumes of 2% HNO_3.

5.3.2 Batch Experiments

All batch experiments were performed using 7.5 mL borosilicate glass vials. A 3-4 mL solution of standardized hydrochloric acid (HCl) or standardized nitric acid (HNO_3) was mixed with 100 mg resin (either RSM-25HP or 50W-X8). Samples were loaded on a Scilogex MX-RD Pro Digital Tube Rotator. The rotation speed was set at 45 rev/min for a specified amount of time. Aliquots were taken prior to resin contact and after pre-determined times. Non-radioactive

metals (e.g. group II metals) were diluted accordingly and analyzed via ICP-MS and ^{226}Ra was electrodeposited then analyzed via alpha spectrometry. Electrodeposition samples were performed in duplicate. All experiments were carried out in room temperature.

5.3.2.1 Blank Experiments

Blank experiments (no resin) were performed first to ensure that no metals were either sticking to or leaching out of the glass vials. Known amounts of metal were prepared in 2% HNO_3. The metals used in the experiment were barium, calcium, sodium, iron, magnesium, potassium, and strontium. These solutions were evaporated to dryness and re-suspended in 3 mL of 0.001 M HCl. Each sample was sonicated for 30 minutes to ensure complete dissolution of metals in solution. Vials were loaded on the rotary wheel for 24 hours. Samples were filtered using glass wool or frits to ensure that the filtering process was not contributing any additional metals.

In addition to these experiments, another set of blank experiments were run to identify possible contaminants in the resin and acid mixtures. The procedure is similar to the previous experiment sans metal, with 100 mg resin, and using either HNO_3 or HCl acid with concentrations ranging from 0.001, 0.01, 0.1, 1.0 to 10 M. Vials were loaded on the rotary wheel for 24 hours.

5.3.2.2 Acid Dependence Studies

Acid dependence studies were conducted to determine the influence of the acid concentration on metal uptake by the resins. Known amounts of metal (barium, sodium, strontium, calcium, magnesium, iron, and potassium) were prepared in 2% HNO_3. These

solutions were evaporated to dryness and re-suspended in 4 mL of either HNO_3 or HCl acid with concentrations varying from 0.001, 0.01, 0.1, 1.0, to 10.0 M. These solutions were added to 100 mg of resin then loaded in the rotary wheel for 24 hours.

5.3.2.3 Adsorption Kinetic Studies

Samples containing 5 Bq/mL ^{226}Ra in 3 mL 0.01 M HCl was prepared and contacted with 100 mg of resin and loaded in the rotary wheel. Samples were unloaded at specific times (5, 10, 30 min, 1, 3, 6, 8, and 9.5 hours). Aliquots were taken prior to resin contact and after pre-determined times and analyzed via electrodeposition followed by alpha spectrometry.

5.3.3 Column Experiments

To study the resins' ability to separate ions, column experiments were performed. Separation studies via cation exchange resins were performed similarly to Zhang (2015)[34] with few modifications. A 2 mL aliquot of a sample was taken and evaporated to dryness. Samples were re-suspended in 2 mL standardized 0.01 M HCl acid matrix, which was loaded in a 2 mL column (ID: 0.8 cm) with a 25 mL extension funnel. The column was loaded with 2.7 gram of wet resin in the H^+ form. The inner diameter of the column is 8 mm and when the column was filled with resin, the bed height was 60 mm. This resin amount is equivalent to a 3 mL bed volume. The loaded resin was first washed with 6 mL of 2% HNO_3, followed by the 2 mL sample, then using 100 – 150 mL 1.75 ± 0.02 M HCl, followed by 25 mL 6.12 M HNO_3, and 25 mL of >18 MΩ/cm water. Eluents were collected every 10 mL at flow rates ranging from 0.3 – 0.6 g/min (volumetric flow rate: 0.1 – 0.2 cm^3/min). The amount of 1.7 M HCl wash was also varied to determine the optimum amount for separation. Surrogate samples with known ion

content (Table 3) were performed to assess the validity of the methods prior to conducting experiments with the actual environmental samples (digested samples). Error bars were generated based on three different column experiments from the digested samples. Non-radioactive ions in the eluent were analyzed via ICP-MS and ^{226}Ra was electrodeposited in duplicate and analyzed via alpha spectrometry.

5.4 Preliminary Results and Method Validation

Batch resin uptake experiments were performed to determine the optimum acid, acid concentrations, and contact time needed for the resins to take up 100% of the ions. These results inform the conditions for column experiments (e.g. what acid matrix the samples should be in and how long to wait prior to starting the washing process).

5.4.1 Batch Experiments

5.4.1.1 Blank Experiments

To ensure that no metals were either sticking to or leaching out of the 7.5 mL borosilicate glass vials, known amounts of metal were prepared in 2% HNO_3. An analysis of the counts measured by the ICP-MS showed that for calcium and iron, the percent increase of the final aliquot was 8.7% relative to the initial aliquot; however, for all other metals, the percent increase was less than 2.5%. This analysis confirms that no metals were lost during the procedure. The slight increase in iron and calcium can be attributed to the elements occurring naturally in the environment, causing an increase in the ICP-MS counts.

Another set of blank experiments was run to identify possible contaminants in the resin and acid mixtures. An analysis of the varying acid concentration before adding the resin shows

elevated signal as high as 30 times the background for elements such as sodium, magnesium, and strontium. This indicates small impurities in the acid; however, since samples are prepared well above the background level, it is not enough to interfere with quantitative analysis, unless the analyte in question occurs in trace levels (<1 ppb).

Additionally, experiments with 10 M acid effectively strips the ions off the resins, indicating that the resins are introducing additional contaminants. For example, for the 50W-X8 resins, the ICP-MS signal for the final aliquot of the 10 M HNO_3 acid compared to the initial aliquot increased from 10 to 33 times relative to background signals. Similarly, for the RSM-25 resins, the results worsened, going from 12 to 224 times relative to background signals. The sample that has a signal 224 times the background level corresponded to a concentration of less than 7 ppb. As a result, samples were prepared at concentrations ranging from 100-200 ppb. These blank experiments emphasize the importance of the protonation step described previously to replace existing ions with hydrogen ions.

5.4.1.2 Acid Dependence Studies

Metal uptake experiments as a function of the acid concentrations are shown in Figure 11. Based on these experiments, the majority of the ions experience 100% uptake by both resins when the concentration of the acid is 0.01 M. As a result, the concentration and acid of interest that will be used for future experiments is 0.01 M HCl due to the near 100% metal uptake by the resin and to mimic the high chloride concentration of the environmental samples. The 0% uptake of 10 M acid concentrations for most ions indicates a way to strip the ions off and regenerate the resin back to H^+ form.

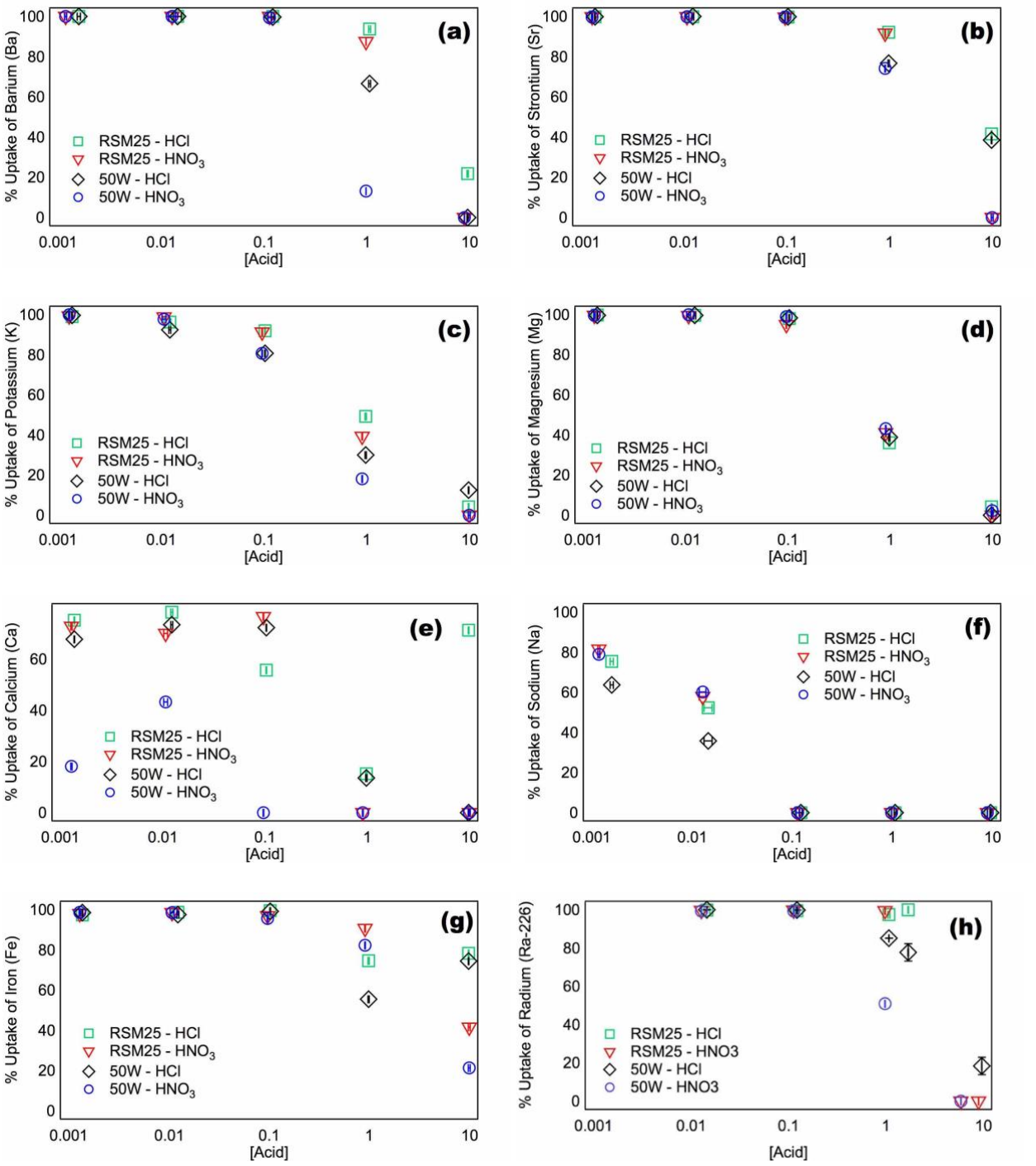

Figure 11: Figures show resin uptake experiments using 100 mg resin and varying hydrochloric acid (HCl) and nitric acid (HNO_3) concentrations for different metal ions: a) barium, b) strontium, c) potassium, d) magnesium, e) calcium, f) sodium, g) iron, and h) ^{226}Ra.

5.4.1.3 Adsorption Kinetic Studies

Primary investigations about the sorption rate of radium ions by both 50W-X8 and RSM-25HP indicated that the sorption process is rapid, as shown in the figure below, where 95% - 99% of the equilibrium sorption for radium occurred within 5 minutes of contact. These results are consistent with findings in the literature describing sorption kinetics for strontium ions using 50W-X8[78]. This information can be applied to the column experiment process. When performing column experiments, it is possible to begin the washing steps five minutes after loading the column with the sample since the uptake occurs rapidly.

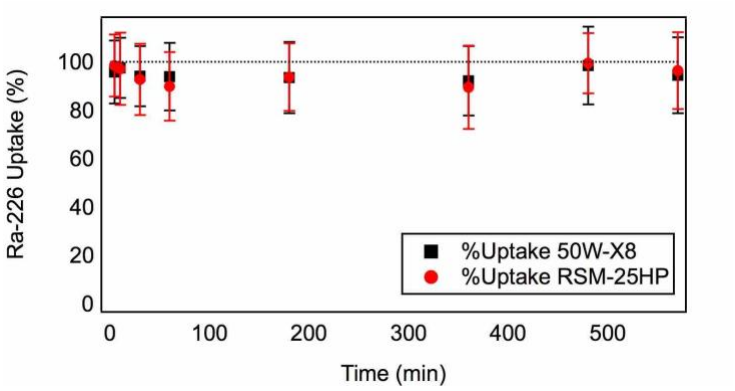

Figure 12: ^{226}Ra percent uptake as a function of time. 15 Bq of ^{226}Ra in 0.01 M HCl was contacted with 100 mg resin.

While the percent uptake gives good insight on the behavior of the resins, it is necessary to gain more information regarding the sorption mechanism of the process. This can be done by modeling the kinetics of ^{226}Ra using the pseudo-first-order and pseudo-second-order models. The plots based on the kinetic models and the fitted parameters for both resins are shown in Figure 13 and Table 8. The applicability of the kinetic models was judged by the correlation coefficient (R^2) and the agreement between the experimental and calculated equilibrium adsorption capacity, q_e. However, it is important to note that q_e is an apparent adsorption capacity because the amount of

^{226}Ra used were trace amounts (nanogram levels), whereas the total exchange capacity of the resins are 1.7 – 1.8 meq/L, which is much higher than the experimental concentrations. The correlation coefficient for the pseudo-first-order model is low (R^2 < 0.53) compared to the pseudo-second-order model (R^2 > 0.98) for both resins. The experimental equilibrium adsorption capacity for the pseudo-second-order model is in better agreement with the calculated adsorption capacity than the pseudo-first-order model, indicating that the pseudo-second-order kinetic model best fits the data. This model assumes that the rate limiting step may be chemisorption involving valence forces through sharing and exchange of electrons[79].

Table 8: Parameters of kinetic models of radium-sorbent system

Parameters	**50W-X8**	**RSM-25HP**
Pseudo-first-order		
k_1 (1/min)	4.02 x 10^{-4}	4.27 x 10^{-4}
q_{e1} (ng/g)	2.45	2.44
R^2	0.5268	0.4447
q_e (calculated, ng/g)	2.03	2.10
Pseudo-second-order		
k_2 (ng mg^{-1} min^{-1})	4.87 x 10^{-4}	4.96 x 10^{-4}
q_{e2} (ng/g)	2.05	2.01
R^2	0.9983	0.9898
q_e (calculated, ng/g)	2.03	2.10

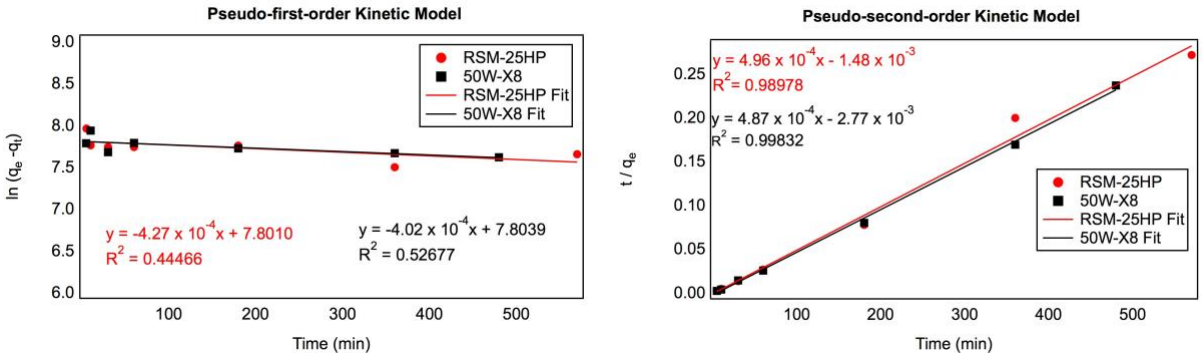

Figure 13: Plots show the pseudo-first-order (left) and pseudo-second-order (right) kinetics models for RSM-25HP and 50W-X8 resins.

5.4.2 Column Experiments

Ion exchange technology is very well researched to separate ions, especially for drinking water contamination; however, few studies have been done for their use in highly saline samples such as the samples we have. The goal for this study is to use the information gathered from the batch experiments to investigate the separation efficiency of radium and barium from sodium, potassium, magnesium, calcium, and strontium.

5.4.2.1 Barium and Radium Elution Profiles

To study the individual elution profiles, four different columns were loaded: (1) barium in 50W-X8, (2) ^{226}Ra in 50W-X8, (3) barium in RSM-25HP, and (4) ^{226}Ra in RSM-25HP under the same experimental conditions. The elution profiles for barium and ^{226}Ra in 50W-X8 resin matched literature profiles very well, where most of the ^{226}Ra is eluted using 6 M HNO_3[34]. The resin uptake studies presented in an earlier chapter (Figure 11) provide some explanations for the phenomena observed in the column studies.

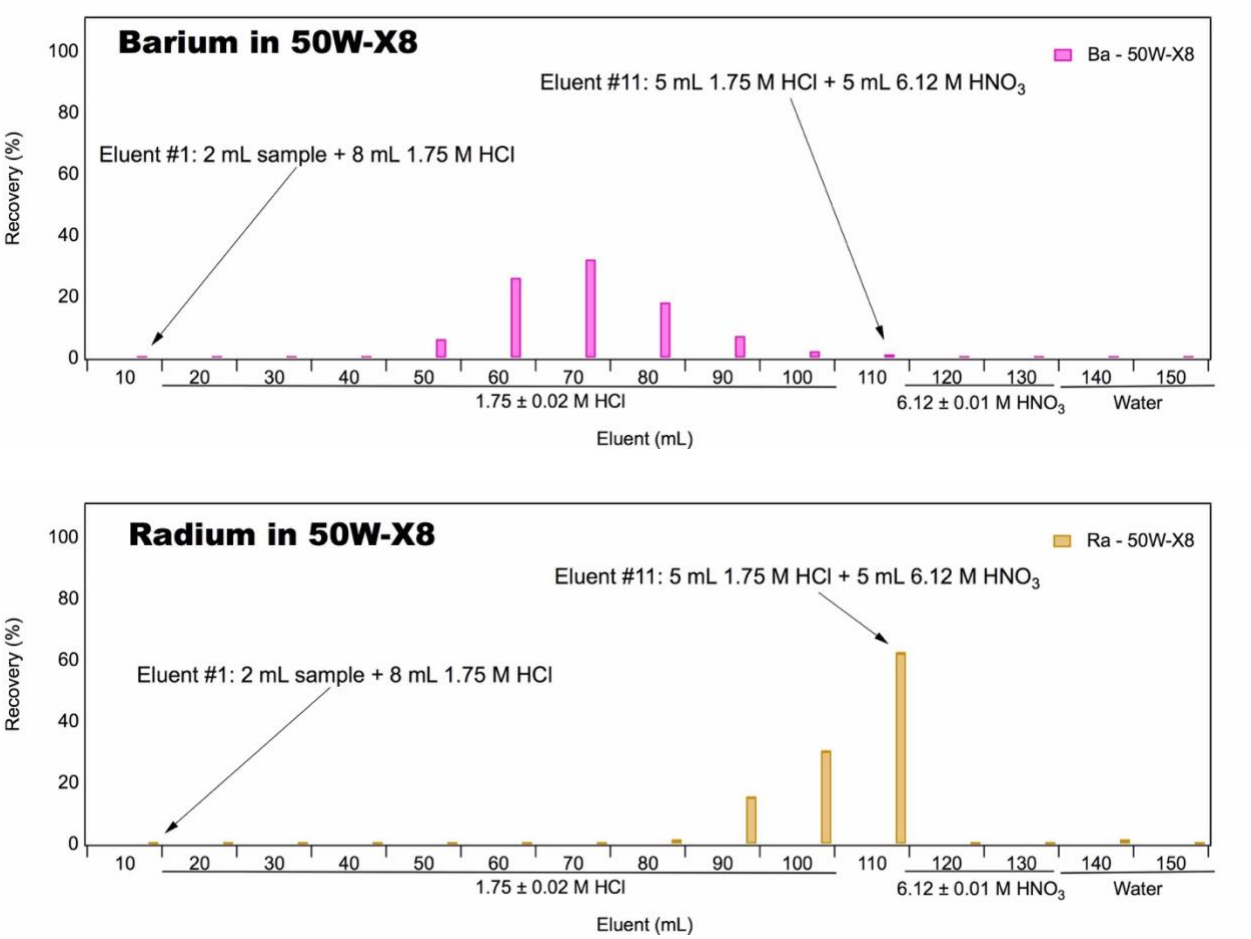

Figure 14: Elution profiles of barium (top) and ^{226}Ra (bottom) using 50W-X8 resin.

The elution profiles for ^{226}Ra and barium using 50W-X8 resin show that most of the ions will elute out after a 1.6 M HCl wash, where barium elutes out much earlier than ^{226}Ra. From the resin uptake studies, the percent uptake for 1M HCl using 50W-X8 resin is 69% whereas the percent uptake for ^{226}Ra is 86%. This indicates that the 50W-X8 has a stronger preference for ^{226}Ra at 1M HCl compared to barium; hence, why barium elutes out in the earlier stages of washing.

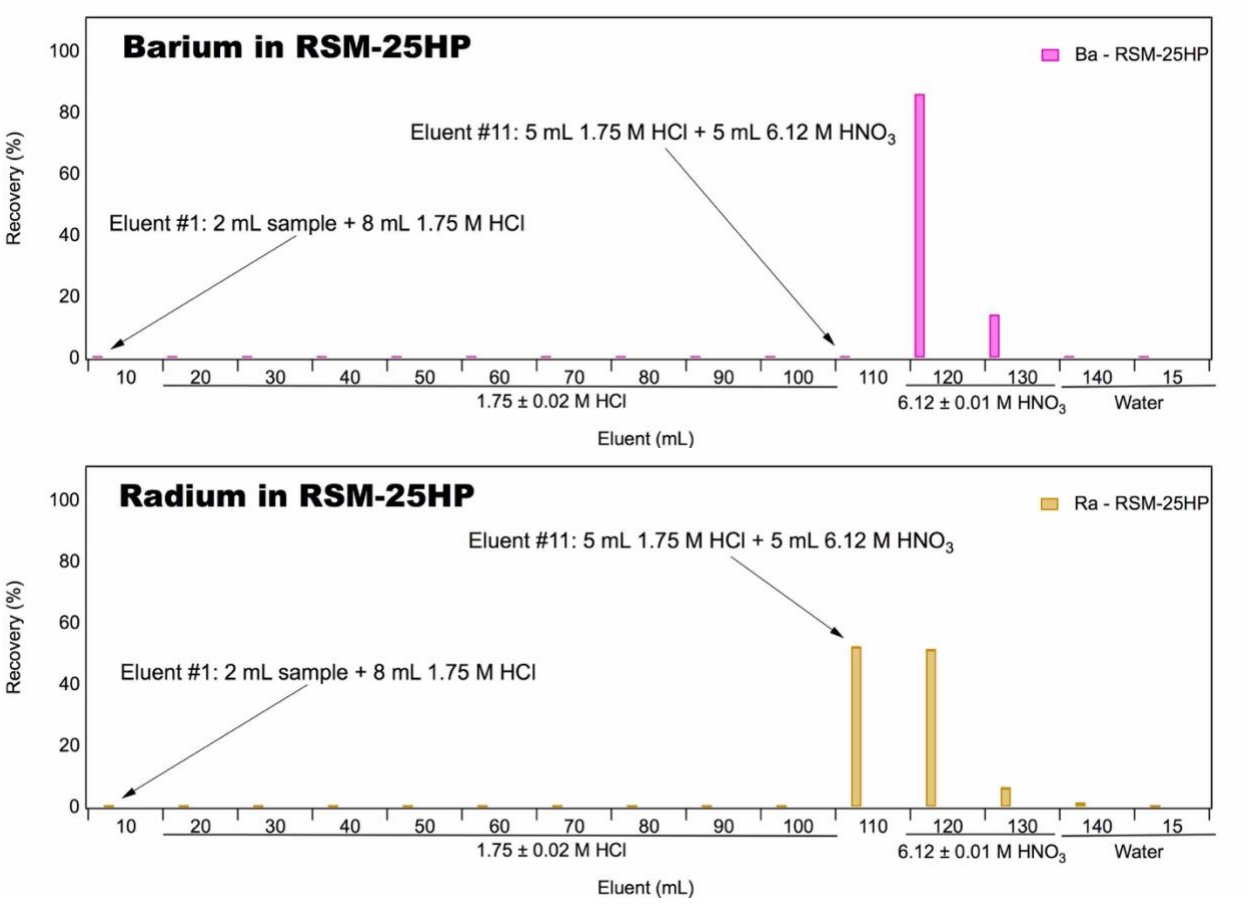

Figure 15: Elution profiles of barium (top) and ^{226}Ra (bottom) using RSM-25HP resin.

The elution profile for barium and ^{226}Ra using RSM-25HP resin look very similar, where elution only occurs when a strong acid, in this case, ~6 M HNO_3, is introduced. Compared to the 50W-X8 resin, it is obvious that the RSM-25HP resin has a stronger preference for these ions. A closer look at the resin uptake studies show that at 1 M acid concentrations, the percent uptake for barium using RSM-25HP resin is 90% and the percent uptake for ^{226}Ra is 99%. RSM-25HP exhibits a small preference for ^{226}Ra compared to barium at 1 M nitric acid. Resin uptake studies on ^{226}Ra on both resins using 6 M HNO_3, show that the percent uptake drops down to nearly 0% and this explains why 100% of the ions are eluted out after the introduction of the 6 M acid. Barium is expected to behave similarly. As mentioned previously in the electrodeposition

studies, the presence of barium (in excess of 10 μg) could drastically reduce ^{226}Ra yields; therefore, it is necessary to perform additional separation experiments since ^{226}Ra and barium are expected to elute out at the same time using RSM-25HP.

5.4.2.2 Surrogate Sample Elution Profiles

The elution profile for Sample 1F (see Table 3 for constituents) containing various other ions sans ^{226}Ra was studied on both resins, using similar conditions as the single cation experiments in the previous section. A comparison between Sample 1F elution profiles of both resins are shown in Figure 16. As seen from both elution profiles, under the same conditions, the 50W-X8 resins do a much better job separating all other ions (*Ca, Fe, K, Mg, Na, Sr*) from barium; however, the eluate volume is much higher compared to the eluate volume coming off the RSM-25HP resin.

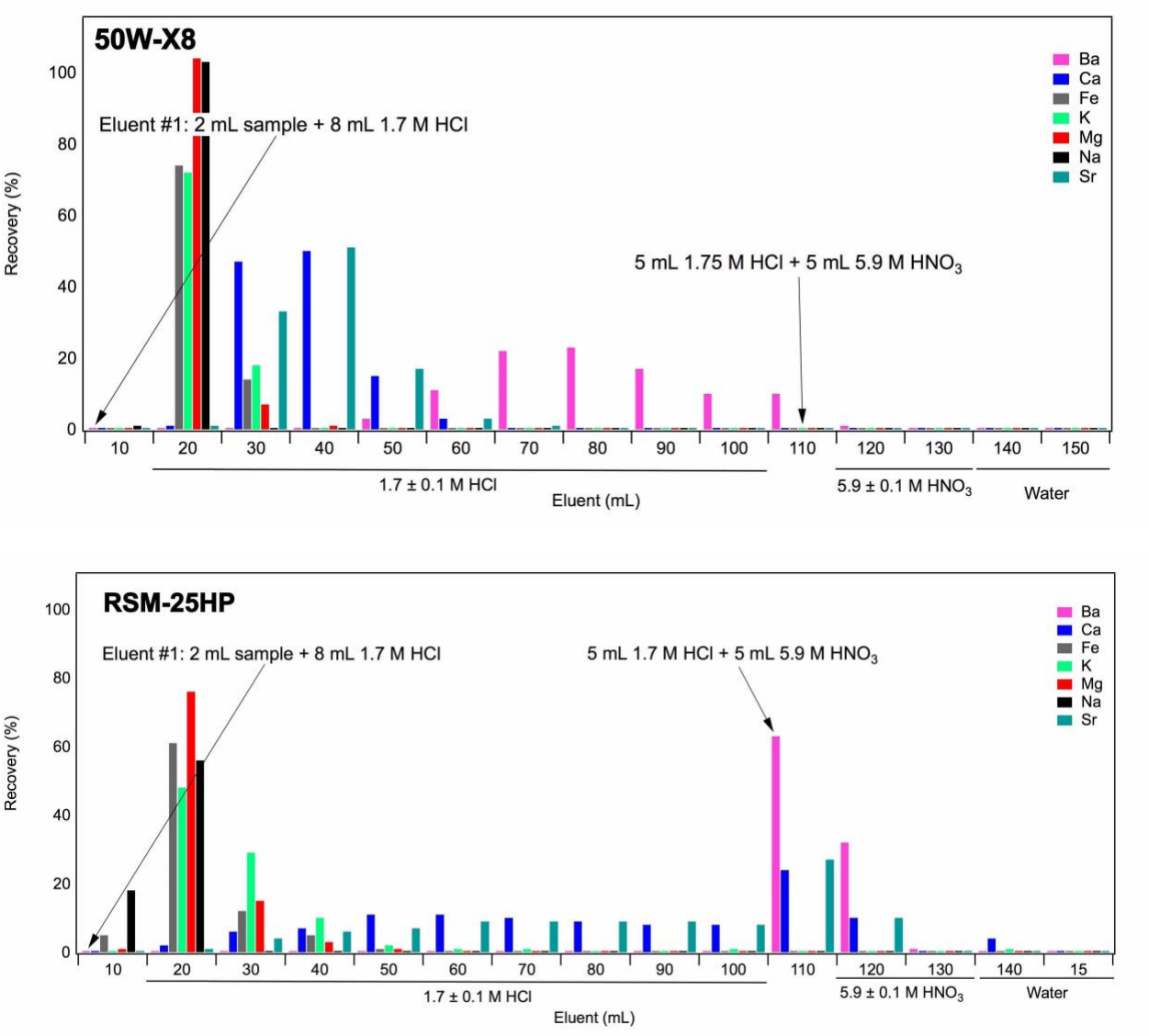

Figure 16: Elution profile of Sample 1F on (a) 50W-X8 and (b) RSM-25HP resin using a total wash volume of 150 mL.

Results from the 50W-X8 resin column study matches the results reported by Zhang (2015)[34]. From Figure 16, barium started eluting out using 1.75 M HCl, after most of the cations have been eluted out. Sodium eluted out almost immediately due to the low selectivity coefficient of sodium (K_{Na} = 52) compared to strontium (K_{Sr} = 4,700), calcium (K_{Ca} = 3,200), and barium (K_{Ba} = >10^4)[34]. The selectivity of RSM-25HP in 0.1 M HCl is similar to that of 50W-X8

but should theoretically be much higher because barium does not elute out until after introduction of strong acid, at which time all ions except Ca and Sr are stripped from the resin. The additional ions eluting in the RSM-25HP study might introduce complications to the analysis of ^{226}Ra. As seen from the single ion elution profiles, ^{226}Ra is expected to elute out in the same area.

To study the separation efficiency of RSM-25HP resin, the total wash volume was increased from 150 mL to 180 mL using the RSM-25HP resin. The increase in 1.7 M HCl washes decreased the interfering ions coming off during the 6 M HNO_3 wash. However, this elution profile cannot be compared to Figure 16 because the experimental conditions have been altered. At a total wash volume of 110 mL (Figure 16), a mixture of HCl and HNO_3 were used to elute out ions whereas at a total wash volume of 160 mL (Figure 17), the acid wash only contained 6 M HNO_3. Though they cannot be compared, this shows that 6 M HNO_3 can elute all barium ions (100%) in less than 30 mLs, far fewer than the 50W-X8 resin (>80 mLs).

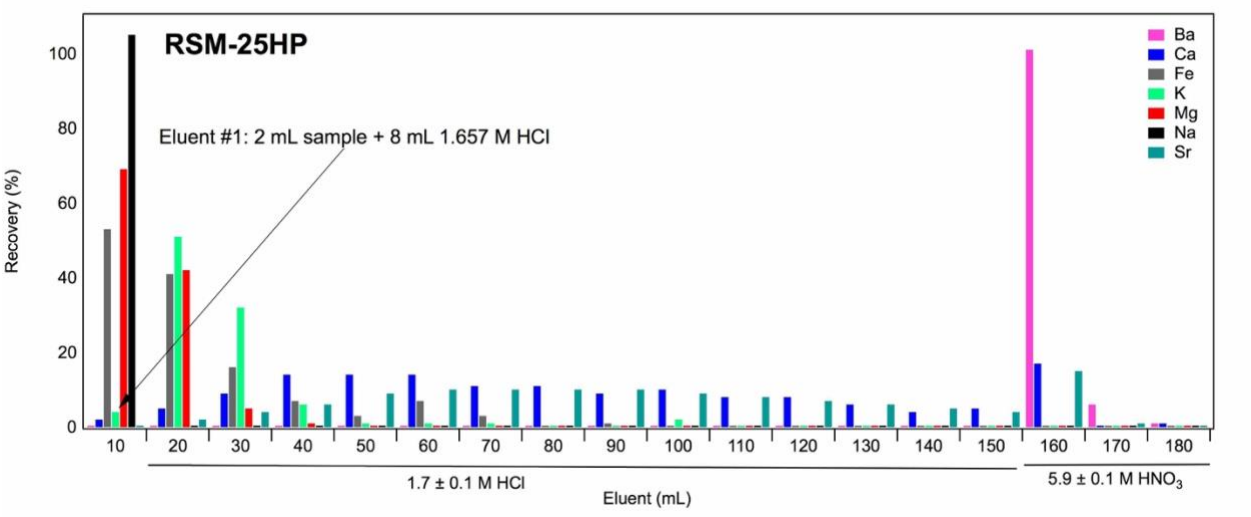

Figure 17: Elution profile of Sample 1F on RSM-25HP using 180 mL total wash volume.

^{226}Ra was added to the samples to determine if competition occurs between the ions. The procedure was the same, and the total wash volume was increased to 180 mL due to better separation. The elution profile of Sample 1 with ^{226}Ra for both resins are shown below.

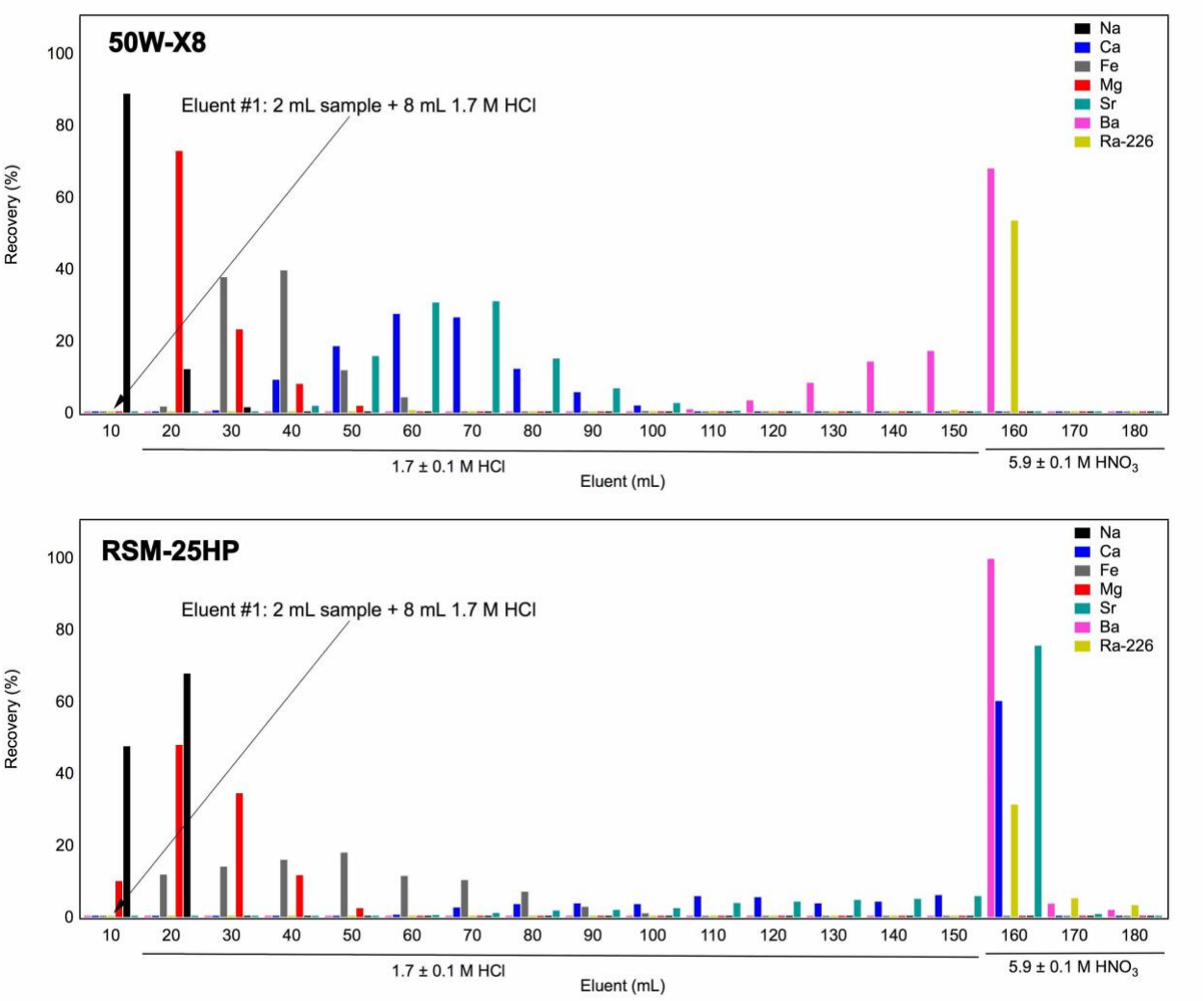

Figure 18: Elution profile of Sample 1F with ^{226}Ra on 50W-X8 (top) and RSM-25HP (bottom) using 180 mL total wash volume.

When ^{226}Ra is added to the sample, the ions compete for adsorption sites on the resin. The most notable change is in the 50W-X8 where 68% of the barium eluted out upon the introduction of 6 M HNO_3, meanwhile the barium elution in the RSM-25HP remained the same. It is also

observed that the recovery percentage of ^{226}Ra was much lower in these samples. This is due to the interference from other ions like barium during the electrodeposition process.

5.5 Application to Oil and Gas Wastewater Samples

The method outlined in the previous section was used for the digested flowback wastewater samples. Overall, most cations were recovered close to 100%. Some cations, for example calcium and sodium, showed recovery of >100% due to their prevalence in the environment, contributing to higher background.

Recoveries of 84 ± 2% and 97 ± 10% for ^{226}Ra was observed for 50W- X8 and RSM-25HP, respectively[48]. The distribution of the ^{226}Ra in 50W-X8 spans multiple eluents, whereas for the RSM-25HP, ^{226}Ra can be collected in less than 30 mLs, which reduces the amount of liquid solution that need to be collected. In addition, for RSM-25HP, the addition of 6 M HNO_3 ensures the collection of all ^{226}Ra, whereas in the 50W-X8 resin, a waiting time for collection of ^{226}Ra needs to be established to ensure proper collection of ^{226}Ra during the 1.7 mL wash since ^{226}Ra elutes out later than barium.

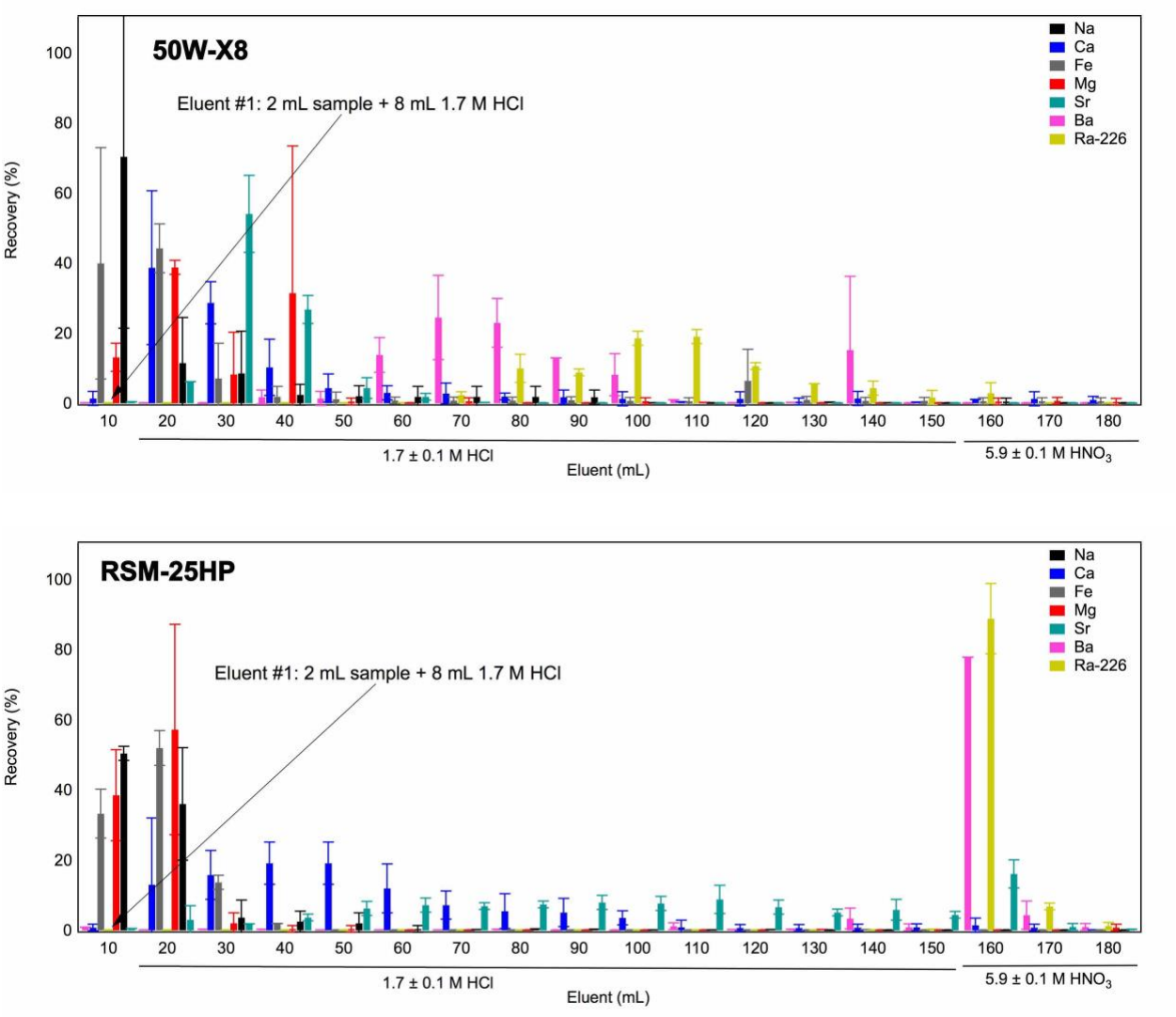

Figure 19: Elution profile of digested oil and gas flowback wastewater samples using 50W-X8 (top) and RSM-25HP (bottom) resin. All samples were washed with 150 mL of 1.7M HCl and 5.9 M HNO_3. Samples were analyzed in triplicate.

However, as stated in the previous section, interferences from ions such as barium can cause problems during the electrodeposition process. For samples containing only ^{226}Ra, a thin film was observed; however, for samples containing additional ions, the thickness of the film increased, leading to depression of detector signal because the alpha particles were unable to reach the detector. The figure below shows a comparison between a sample containing pure

^{226}Ra and the digested flowback sample, which contains 1.05 mg barium and other ions. The ^{226}Ra signal is significantly reduced, which is consistent with other literature findings[47,80]. As a result, it is imperative to reduce the amount of interfering ions prior to electrodeposition.

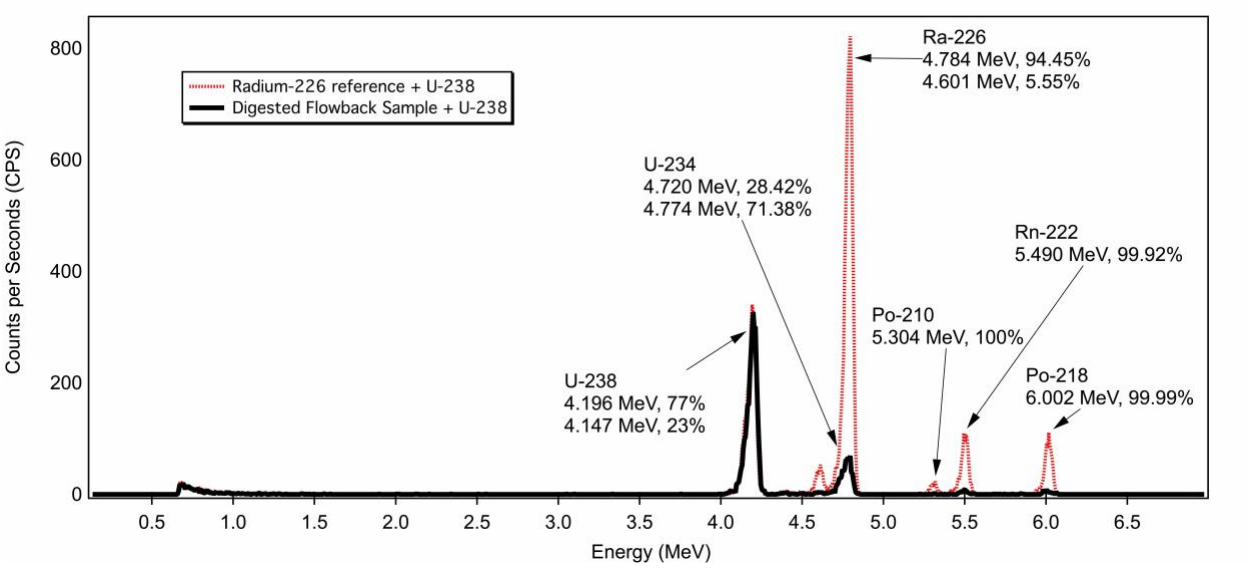

Figure 20: Alpha spectra of ^{238}U and ^{226}Ra and its daughters. The black solid line is the digested flowback sample and the red dotted line is the pure ^{226}Ra reference sample.

5.6 Summary

Batch resin uptake experiments were performed first to determine sorption with varying acid and acid concentrations as well as to study sorption kinetics. Results from the kinetics studies informed the experimental conditions needed to perform column experiments.

Column studies were performed on surrogate samples initially to assess the validity of the method followed by analysis of environmental samples, keeping the experimental conditions the same as much as possible. The 50W-X8 matched literature results well despite the type of environmental sample used. All elution profiles show that there are fractions in which barium, and in the case of the RSM-25HP resin, other cations (*Sr*, *Ca*), will elute out in the same

fractions that ^{226}Ra will elute out, as seen from elution profiles containing only ^{226}Ra. Previous experiments showed that the presence of strontium does not have the same effect on ^{226}Ra electrodeposition as barium does. The barium amounts in those fractions are greater than the critical value at which point the ^{226}Ra electrodeposition yields will start to decrease; therefore, it is essential to separate ^{226}Ra and barium from each other in order to attain accurate ^{226}Ra assays. Though the RSM-25HP resin requires an additional separation step, it is promising for ^{226}Ra separation from major cations in flowback water samples and concentrates the ^{226}Ra in a narrow band, reducing the eluent volume during collection.

Chapter 6: Separation of Radium from Barium Using Crown Ethers

6.1 Introduction

Previous studies illustrate how having barium in the same solution as ^{226}Ra can severely decrease the ^{226}Ra yield during electrodeposition[47,48]. In order to accurately assay ^{226}Ra via electrodeposition, it is important to have a pure ^{226}Ra compound, free of barium. This chapter focuses on the benefits of coupling crown ethers with separation techniques such as solvent extraction and solid-liquid extraction using RSM-25HP resin and solvent impregnated resins. Preliminary experiments will be done on radium and barium before moving on to actual environmental samples that were digested and run through the RSM-25HP resin, as described in Chapters 4 and 5.

6.2 Theory

6.2.1 Crown Ethers

"Crown ethers" are cyclic ethers containing several oxygen atoms, with a central cavity that is capable of accommodating a metal ion, especially alkali and alkaline earth metal ions. They are usually named using the total number of atoms in the ring and the number of oxygen atoms (e.g. 18-crown-6 is an 18-membered ring with 6 oxygen atoms).

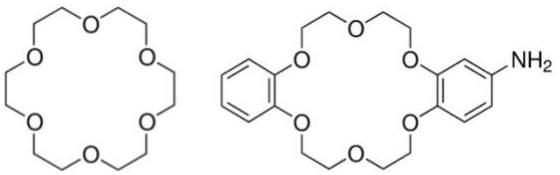

18-crown-6 4'amino-dibenzo-18-crown-6

Figure 21: Water-soluble (left) and water-insoluble (right) crown ethers. Both compounds have a cavity between 1.3 -1.6 Å.

Crown compounds are capable of both strong and selective metal complex formation and the stability of the complex formed is governed by the interactions with the lone pairs of electrons on the surrounding oxygen atoms as well as the ionic radii of the cation (see Table 2) and the polyether cavity (for 18-crown-6, the cavity size is between 1.3 – 1.6 Å)[81]. They are of interest in the field of analytical separations because they can act as extractants in solvent extraction processes or they can be loaded on resins to create an extraction chromatographic resin to separate or pre-concentrate metal ions[82]. A water-soluble crown ether and a water-insoluble crown ether (Figure 21) will be explored for their ability to separate barium and ^{226}Ra from each other.

6.2.2 Ion Exchange Experiments with Water Soluble Crown Ethers

There is a wide range of research done using crown ethers; however, very few researchers have focused on how crown ethers affect resin uptake using ion exchange resins. Delphin et al. (1978) showed that the presence of a water-soluble crown ether in the solution phase can prevent a strong cation-exchange resin from retaining an alkali metal ion because the addition of the crown ether will convert the free metal ion into the complexed form, preventing resin uptake[83]. For example, choosing a crown ether that is capable of forming a crown ether-metal complex with the ion of interest (e.g. Ra^{2+}) in the solution would inhibit the sorption of the free ion, meanwhile leaving the other interfering ions uncomplexed, allowing uptake by the resin. The opposite is also possible, where one can introduce a crown ether to complex with the interfering ion, allowing the ion of interest to be taken up by the resin[84].

Other studies, however, observed a different phenomenon, where the addition of crown ether caused an increase in the retention of radium by a strong cation resin, instead of seeing a

decrease, as reported by Delphin et al. (1978). Since crown ethers are neutral molecules, they are not rejected by the Donnan potential of the ion exchange resin; as a result, the crown ethers will distribute between the internal and external aqueous solutions, causing a synergistic interaction between the crown ether and the sulfonic acid group of the resin[84].

The ion exchange experiments done in this chapter focuses on how unsubstituted water-soluble crown ethers affect resin uptake on a newly developed strong acid cation resin (RSM-25HP) that exhibits higher affinity for both ^{226}Ra and barium compared to the well-researched 50W-X8 resin. Currently there is no data available on RSM-25HP resins with crown ethers; however, prior experiments in this project provides data on the behavior of the resin in the absence of crown ethers as a basis for comparison.

6.2.3 Solvent Extraction with Hydrophobic Crown Ethers

In addition to solid-liquid separations where ion exchange resins are used to obtain a pure fraction containing the radionuclide of interest, liquid-liquid extraction (LLE) or solvent extraction (SX) is another common method applied in separation of radionuclides. Analytes from an aqueous sample partition to a water-immiscible organic solvent phase, according to Figure 22. One disadvantage of solvent extraction is that it often requires handling and eventual disposal of hazardous organic solvents, which entails high production of organic waste [85].

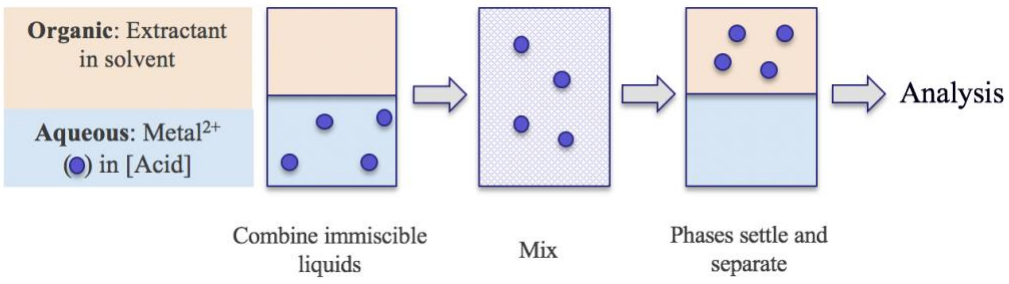

Figure 22: Idealized batch solvent extraction process

Two out of the few studies in the literature on solvent extraction of radium using crown ethers are one study done by Beklemlshev et al. (1994)[86] and one by Chiarizia et al. (1999)[87]. Beklemlshev et al. (1994) performed extractions from alkaline media into chloroform solutions of the proton ionizable crown ether with attached carboxylate groups. The extraction requires no specific counter anions and is reversible with respect to pH[86]. Chiarizia et al. (1999) performed extractions from aqueous hydrochloric acid solutions containing unsubstituted water-soluble crown ethers into xylene solutions containing a liquid ion exchanger (dinonylnaphthalenesulfonic acid, HDNNS). The goal was to mimic the sulfonic acid groups in strong cation resins but since the HDNNS is not bound to a polymer network, it may be able to interact more with the metal-crown ether complex. Their results show strong enhancement of ^{226}Ra, barium, and in some cases, strontium uptake, which aids in the development of extraction chromatographic resins that could be used for ^{226}Ra separation in the same way as ion exchange resins[87].

The solvent extraction experiments conducted in this chapter studies the potential separation between ^{226}Ra and barium using an aqueous HCl acid solution and hydrophobic crown ether (4'amino-dibenzo-18-crown-6) in toluene solution, which to our knowledge, has not been studied previously.

6.2.4 Solvent Impregnated Resin

The development of impregnated resins is considered a link between solvent extraction and ion exchange technologies and plays an important role in separation sciences[88]. The degree of retention of the extracting agent depends on the nature of the support, where the support should exhibit the following properties: chemically inert so that extractants do not react with it,

good mechanical stability, and should be easily produced, as well as allowing the extractant to attach to the support by adsorption[2]. Amberlite resins (XAD) satisfy these properties and are therefore the solid support of interest.

Currently, only one solvent impregnated resin experiments have been done on the removal of ^{226}Ra from aqueous sources[89]. The experimental conditions and materials Benzi et al. (1992) used differed from the materials used in this project. The solvent impregnated resins performed in this chapter used a XAD7 solid support impregnated with a water insoluble crown ether (4'amino-dibenzo-18-crown-6) dissolved in nitrobenzene. To our knowledge, these experiments have only been performed in the removal of arsenic from water[90].

6.3 Experimental Setup

6.3.1 Material

The water-soluble crown ether, 18-crown-6 (purum, ≥99.0%), and hydrophobic crown ether, 4'aminodibenzo-18-crown-6 (≥98%), were obtained from Sigma Aldrich and used without further purification.

Barium stock solutions were diluted to a final concentration of 10 ppm (mg/L) while in contact with resin. Standard calibration curves for barium were created to quantify the amount of barium using ICP-MS. Secondary stock solutions of ^{226}Ra were diluted to yield a final concentration of 8 Bq/mL while in contact with resin. For both barium and ^{226}Ra, aliquots were taken before and after resin contact. 100 µL aliquots were electroplated with ^{238}U for 4 hours. Following electrodeposition, the stainless-steel disks were counted for 24 hours on a previously calibrated alpha spectrometer. All experiments were done in triplicate.

6.3.2 Ion Exchange Studies with Water Soluble Crown Ethers

To determine the effect of the water-soluble crown ether, several experiments were performed in batch using RSM-25HP resin and aqueous solutions containing barium or ^{226}Ra. Competition studies were also conducted to assess the extraction contribution of the crown ether. The cation exchange resin (RSM-25HP), described previously, was used in the ion exchange studies with water-soluble crown ether.

The stock solutions were diluted to yield 8.63 Bq/mL ^{226}Ra solution and 10-ppm (mg/L) barium. For the acid dependence studies, the 18-crown-6 concentration was constant at 0.0001 M and the HCl concentrations varied from: 0.54 ± 0.04 M, 1.19 ± 0.02 M, 1.97 ± 0.02 M, 3.06 ± 0.02 M, 4.02 ± 0.01 M, 5.04 ± 0.01 M, and 6.28 ± 0.02 M. For the crown ether dependence studies, several experiments were conducted. The crown ether concentrations were varied from 0 M to 10^{-5} M while the HCl concentration was kept constant at 0.54 ± 0.04 M or 1.97 ± 0.02 M. Competition studies were also conducted where the aqueous phase contained both ^{226}Ra and barium. These studies are similar to the crown-ether dependence studies but using HCl concentrations of 0.54 ± 0.04 M, 3.06 ± 0.02 M, or 5.04 ± 0.01 M.

Aqueous solutions were added to 100 mg of RSM-25HP resin and were placed in a rotary wheel to mix at 30 rpm. After a 24-hour equilibration period, they were filtered and analyzed.

6.3.3 Solvent Extraction Studies with Hydrophobic Crown Ethers

The solvent extraction studies were carried out by first dissolving 4'amino-dibenzo-18-crown-6 ether in toluene (99.8%, anhydrous, Sigma Aldrich) to yield a 0.001 M solution. The crown ether-toluene mixture was pre-equilibrated with 15 mL of the desired acid (Acid = 0.0001 M, 0.01 M, 0.1M, and 1M HCl) for 24 hours. Following 24 hours, an equal amount of the pre-

equilibrated organic solution was added to an aqueous solution in the desired acid concentration. The experiments were conducted in triplicate with and without crown ether present in the toluene to determine if the crown ether had any effect in the extraction. The total solution of 6 mL (3 mL aqueous + 3 mL pre-equilibrated organic solution) was mixed for 24 hours. After 24 hours, the aqueous phase was removed, and an aliquot of the aqueous phase was taken for ion content analysis.

6.3.4 Solvent Impregnation of XAD7 Resin with Hydrophobic Crown Ethers

The Amberlite® XAD7-HP (20-60 mesh, acrylic matrix, 0.5 mL/g pore vol.) was purchased from Sigma Aldrich. The XAD7 resins were first washed with alcoholic hydrochloric acid (25% hydrochloric acid, 50% ethanol, 25% water) and then stirred. The resins were vacuum filtered and placed in a column. The resins were washed with ultrapure water (>18 MΩ/cm) to get rid of any HCl until the pH of the effluent reached neutral levels, and then dried in open air. A known amount of 4'-aminodibenzo-18-crown-6 was dissolved in nitrobenzene (>99.0%, ACS reagent, Sigma Aldrich) to yield a 2 mM and 4 mM concentration. Then, the XAD7 resin was added to the crown ether and nitrobenzene solution and mixed for 24 hours, after which the excess liquid was filtered gravitationally, and the resin loaded in the rotary evaporator for 48 hours at 50 °C. The figure below shows the final product of the resins in each phase: pure XAD7, XAD7 + nitrobenzene, XAD7 + nitrobenzene + 2 mM 4'amino-dibenzo-18-crown-6.

Figure 23: Pure XAD resin (left), XAD resin + nitrobenzene (middle), XAD resin + nitrobenzene + crown ether (right)

Once the resins were dried, an aliquot was taken and ground up for FTIR (Jasco 4700) analysis to determine if the crown ethers sorbed on the resins at all. These steps were done to XAD7 and nitrobenzene with and without crown ether in order to determine the effect of the crown ether addition.

Experiments follow the same procedures as ordinary ion exchange studies, where aqueous solutions were added to 100 mg of solvent impregnated resins and mixed using a rotary wheel at 30 rpm for 24 hours. Experiments were done on the resins with crown ether as well as resins with the nitrobenzene solvent to illustrate the extraction contribution of crown ether.

6.3.5 Application to Oil and Gas Wastewater Samples

The methods described above were applied to actual environmental samples. As seen in the earlier sections, wastewater from the Eagle Ford shale formation were digested in triplicate and 2 mL of this solution was evaporated and reconstituted in 2 mL 0.01 M HCl. This solution was introduced to a column filled with RSM-25HP and washed with 150 mL 1.7 M HCl solution to wash off the major Group II ions and 25 mL HNO_3 to elute out barium and ^{226}Ra, which was then collected. The total eluent collected was between 25 - 30 mL, which is assumed to contain

all the ^{226}Ra and barium. This sample was then evaporated and re-suspended in 10 mL 0.01 M HCl, to serve as the stock solution for the ion exchange and solvent extraction experiments coupled with crown ethers. An aliquot was taken before and after contact with resins/organic phase. Samples were analyzed for their barium content using ICP-MS and for the ^{226}Ra content, a 200 µL aliquot was taken and electrodeposited to give a final activity of 0.6 Bq.

For the ion exchange experiments, one set of experiments was conducted where the 18-crown-6 concentration was kept constant at 0.1 M while the HCl concentration was varied from 3 to 5 M and the other set kept the concentration constant at 5 M HCl while varying the 18-crown-6 concentration from 0.01 M to 0.1 M. For the solvent extraction experiments, the 4'amino-dibenzo-18-crown-6 concentration was kept constant at 0.001 M and the aqueous solutions were varied from 0.0001, 0.01, 0.1, and 1 M HCl. The organic solutions were first pre-equilibrated with acid concentrations not containing the digested sample. For the solvent impregnated resins, the environmental samples were dissolved in aqueous solutions with HCl concentrations: 0.001, 0.01, 0.1, 1, and 3 M HCl. These samples were then added to the solvent impregnated resins. All samples were contacted with resins/organic phase for 24 hours via rotary wheel or vigorous mixing.

6.3.6 Distribution Value

The distribution value (mL/g) for the ion exchange, and solvent impregnated resin studies is calculated as:

$$D = [(A_0 - A_f) / A_f] \; x \; (V / m)$$

where A_0 and A_f are the aqueous phase activity or concentration before and after equilibration, respectively; m is the weight of dry resin (g), and V is the volume of the solution (mL). All samples were analyzed in triplicate. This is similar to the resin uptake calculations,

$$\% \ Uptake = [(A_0 - A_f) \ / A_0] \ x \ 100\%$$

As for the solvent extraction studies, the distribution ratio (mL/g) was calculated as:

$$D = [M]_{org} / [M]_{aq} \ x \ V_{aq} / V_{org}$$

where V_{aq} and V_{org} is the amount (mL) of aqueous and organic phase added, respectively. Typically, equal amount of each phase is added for the experiment so that the ratio is equal to unity. $[M]_{aq}$ is the metal concentration in the aqueous phase and $[M]_{org}$ is defined as the metal concentration in the organic phase, which is defined as

$$[M]_{org} = [M]_{aq,\,i} - [M]_{aq,f}$$

where $[M]_{aq,i}$ is the metal concentration in the aqueous phase prior to contact and $[M]_{aq,f}$ is the metal concentration in the aqueous phase post-contact. By mass balance, it is assumed that the concentration in the organic phase is the difference in the aqueous phase concentration before and after contact.

6.3.7 Separation Factor

The separation factor, SF, is a measure of the efficiency of the separation process[91]. It is determined from the ratio of the distribution values of the two solutes. The radium/barium separation factor ($SF_{Ra/Ba}$) is defined as:

$$SF_{Ra/Ba} = D_{Ra} / D_{Ba}$$

6.4 Preliminary Results & Method Validation

6.4.1 Ion Exchange Studies with RSM-25HP Resin and Water-Soluble Crown Ethers

6.4.1.1 Crown Ether Dependence Studies

In order to study the effect of the water-soluble crown-ether, first resin uptake experiments using RSM-25HP resins were examined in the absence of the crown ether. The percent uptake of ions is reported in Figure 11.

Dietz et al. (1997) studied the uptake of calcium, strontium, barium and radium at 0.5 M HCl by the sulfonic acid resin as a function of crown ether concentration. They reported that the ions bring about some degree of uptake enhancement[84]. Similar experiments were conducted; however, RSM-25HP resin was used instead of 50W-X8 resin and only ^{226}Ra and barium were used.

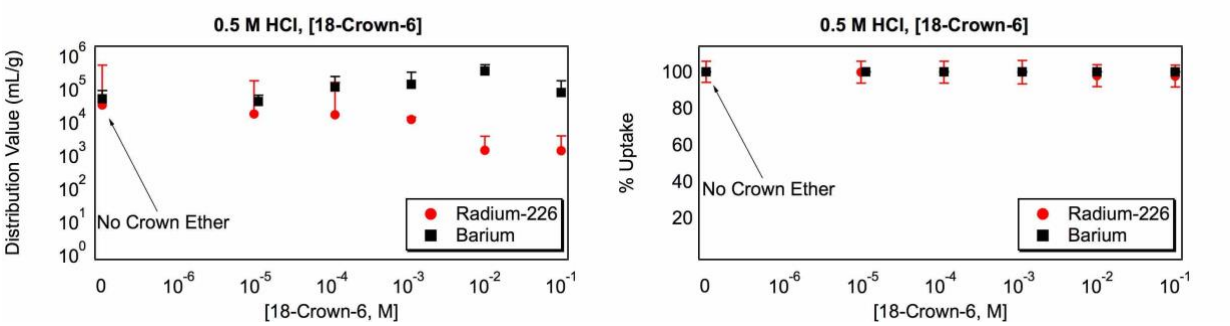

Figure 24: Ion exchange studies using RSM-25HP and varying [18-crown-6] in constant 0.5 M HCl solution. The left figure shows distribution value (D) and the right figure shows percent uptake of ^{226}Ra and Ba as a function of 18-crown-6 concentration.

For the 0.5M HCl, at first glance at the resin uptake experiments, there appears to be no effect on uptake when the crown ether concentration is varied (Figure 24, right). This is partly due to the high affinity of the resin for ^{226}Ra and barium ions, which is evident through the high distribution values. However, looking at the distribution values (Figure 24, left), it appears that increasing the 18-crown-16 concentration caused the ^{226}Ra distribution value to decrease relative

to the sample without crown ether and for barium, the distribution values increased. This suggests that ^{226}Ra formed a complex with the crown ether while the free barium ions were taken up by the resin at higher crown ether concentrations. This was also observed by Delphin et al.[83] Dietz et al.[87,92] showed that for ^{226}Ra mixed with varying concentration of 18-crown-6 in constant 0.5 M HCl, there is a synergistic effect between 18-crown-6 and the sulfonic acid in the Bio-Rad 50W-X8 resin; however, our results show no such effect in 0.5 M HCl. This is potentially due to the difference between the 50W-X8 resin and the RSM-25HP resin. From previous results in the batch and column studies, the RSM-25HP resin has higher affinity towards barium and ^{226}Ra compared to the 50W-X8 resin. RSM-25HP already has a high affinity to uptake the radium (up to 100%); therefore, adding crown ether would produce no additional effect, whereas, for 50W-X8, since the uptake is not 100%, there is a probability that synergism can occur to allow the 50W-X8 resin to take up 100% of the ^{226}Ra. As a result, in order to study any synergistic effect, it is necessary to study the dependence on 18-crown-6 with higher HCl concentrations so that the ^{226}Ra and barium will not experience near 100% uptake.

For this experiment, adding 0.01 M 18-crown-6 to the 0.5 M HCl solution resulted in a large separation factor between ^{226}Ra and barium ($SF_{Ba/Ra} \approx 240$). It is two orders of magnitude larger than what Chiarizia et al. (1999) reported ($SF_{Ba/Ra} \approx 1.3$) using 50W-X8 resin and the same aqueous condition and crown ether concentration[87]. This high separation factor shows promise for barium/radium separation.

6.4.1.2 Acid Dependence Studies

Since the uptake was near 100% using 0.5 M HCl, additional experiments were done to assess the degree of separation by keeping the 18-crown-6 concentration at 0.001 M and varying the HCl concentration in order to determine an optimum acid concentration.

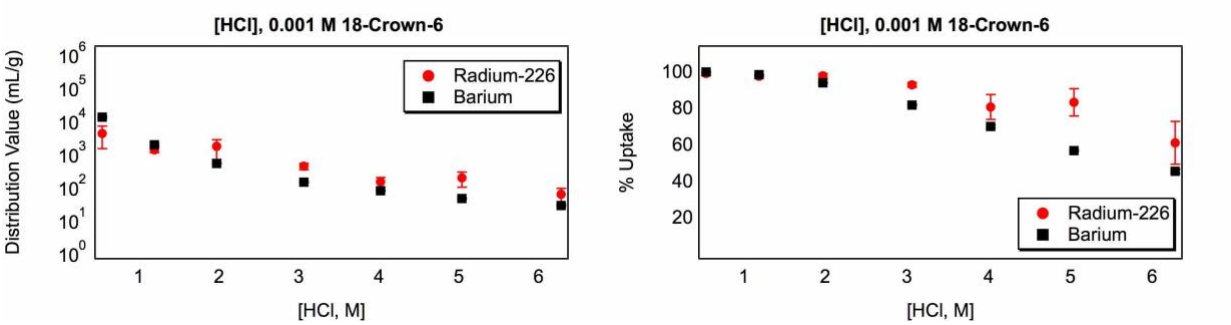

Figure 25: Ion exchange studies using RSM-25HP and varying HCl concentration and maintaining the 18-crown-6 concentration at 0.001 M. The left figure shows distribution value (D) and the right figure shows percent uptake of ^{226}Ra and Ba as a function of hydrochloric acid concentration.

As seen from the 0.5 M HCl experiments when the crown ether concentration was varied, the barium is preferred by the resin, which is seen at low HCl concentrations and constant crown ether concentration. However, at 2 M HCl, the resin begins to exhibit more preference for ^{226}Ra compared to barium. This is explained by the resin uptake experiments sans crown ether. In the resin uptake experiments (Figure 11), at >1 M HCl concentration, the RSM-25HP resin has slightly higher uptake percentage for ^{226}Ra (97%) compared to barium (93%). This implies that at higher HCl concentrations, the resin prefers ^{226}Ra to barium and the resin affinity for ^{226}Ra is much stronger than the radium-crown ether complex.

As the HCl concentration increases, it appears that the degree of separation between barium and ^{226}Ra is slightly increasing due to the resin's preference for radium at higher acid concentrations. Compared to the results seen with the low acid (0.5 M HCl) experiments, the

high acid (5 M HCl) experiments resulted in much lower separation factor ($SF_{Ra/Ba} \approx 4$) due to the protonation of the resin and crown ether. Since the likelihood of the resin taking up the metal ions or the metal ions complexing with the crown ether is low, both metal ions are likely going to stay in the aqueous phase, resulting in lower separation factors. Competition studies for adsorptions sites will be conducted using 3.06 ± 0.02 M and 5.04 ± 0.01 M HCl.

6.4.1.3 Competition Studies – Crown Ether Dependence

For the competition studies, the procedure was kept the same; however, both ^{226}Ra and barium were added in the aqueous solution. Here, the acid concentration is kept constant while the 18-crown-6 concentrations were varied.

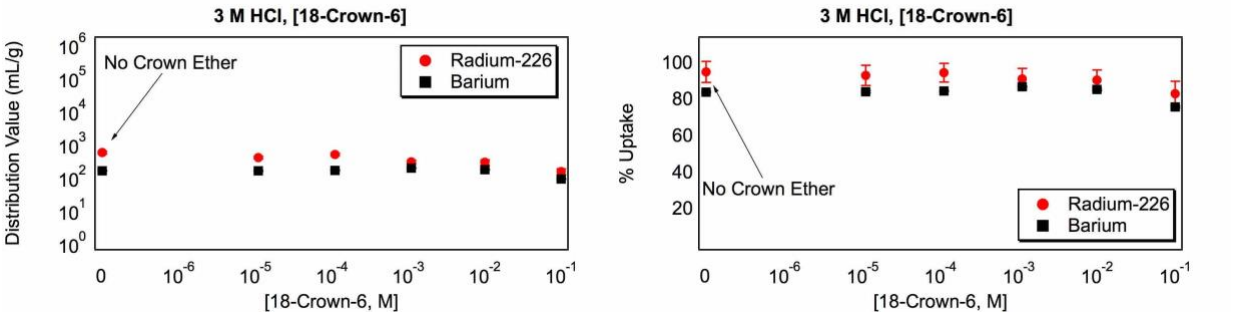

Figure 26: Ion exchange studies using RSM-25HP and varying 18-crown-6 concentrations in constant 3 M HCl solution. The aqueous solution contains both ^{226}Ra and barium. The left figure shows distribution value (D) and the right figure shows percent uptake of ^{226}Ra and Ba as a function of 18-crown-6 concentration.

In the graph above, the distribution values are what was expected. Increasing the HCl concentration lead to a decrease in distribution value as well as resin uptake. Increasing the 18-crown-6 concentration also led to a decrease in both ions' distribution value, meaning more ions stay in the solution. In addition, the degree of separation between ^{226}Ra and barium start to decrease as the 18-crown-6 concentration decreases; however, as seen from the acid dependence

study, the resin still exhibits a small preference for ^{226}Ra uptake compared to barium, except when the crown ether concentration is increased. Finally, studies using 5.04 ± 0.01 M HCl were conducted to determine the separation but also to assess if synergism is occurring at this acid concentration.

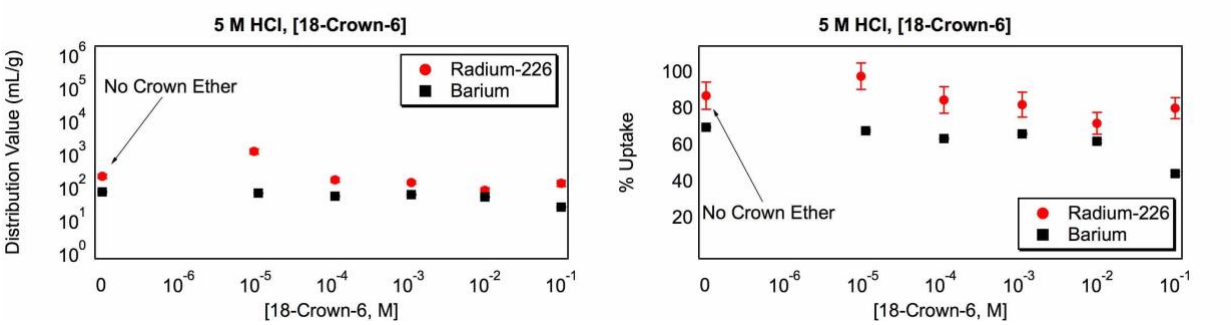

Figure 27: Ion exchange studies using RSM-25HP and varying 18-crown-6 concentrations in constant 5 M HCl solution. The aqueous solution contains both ^{226}Ra and barium. The left figure shows distribution value (D) and the right figure shows percent uptake of ^{226}Ra and Ba as a function of 18-crown-6 concentration.

For the 5.04 ± 0.01 M HCl, separation between radium and barium is more apparent. The synergism, as described by Dietz et al. (1999)[87] can be assessed because the resin no longer experiences 100% uptake. The increase in radium distribution coefficient at 10^{-5} M 18-crown-6 matches the results of Dietz et al. It appears that at that concentration, the distribution value of ^{226}Ra is higher relative to sample without crown ether, indicating possible synergism; however, for barium, it gradually decreases. This decrease may be resulting from the competition between ^{226}Ra and barium for adsorption sites on the resin. This possible phenomenon was explored further by comparing experiments where barium was by itself in the solution and where barium and ^{226}Ra were both in the solution.

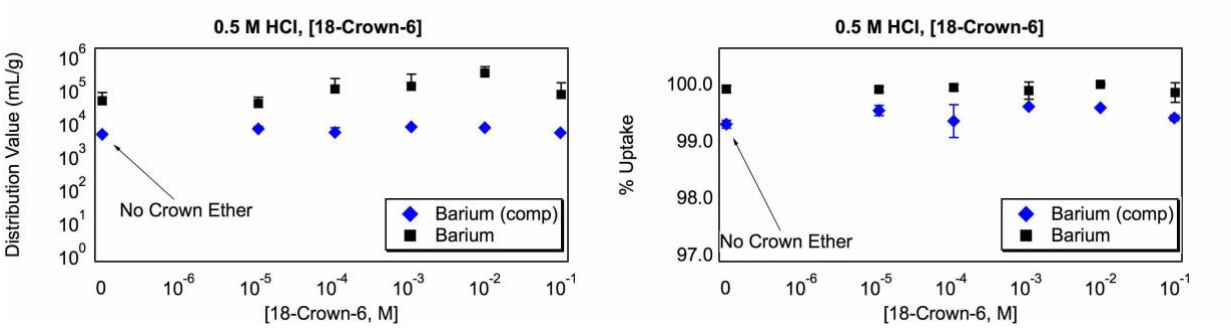

Figure 28: Ion exchange studies using RSM-25HP and varying 18-crown-6 concentrations in constant 0.5 M HCl solution. The left figure shows distribution value (D) and the right figure shows percent uptake of barium as a function of 18-crown-6 concentration. The behavior of barium when it is by itself in the solution (black square) is compared with its behavior when ^{226}Ra is present (blue diamond). Note the change in the y-axis for the percent uptake.

When comparing the barium distribution values from uptake experiments with barium by itself compared to barium and ^{226}Ra in the same solution, it was observed that the distribution value of the barium in competition experiments are much lower than the barium distribution value when barium is by itself in the solution. This points to the fact that there is competition occurring between barium and ^{226}Ra, where ^{226}Ra is preferentially taken up by the resin in the presence of barium. This phenomenon is observed in ordinary water treatment of low-saline samples; however, if the salinity of the solution increases, then ^{226}Ra will no longer be preferentially adsorbed[39].

6.4.2 Solvent Extraction Studies with Hydrophobic Crown Ethers

Hydrophobic crown ether (4'amino-dibenzo-18-crown-6) was dissolved in toluene to determine the extent of extraction of ^{226}Ra as compared to barium via crown ether. The results of the study are shown in the figure below.

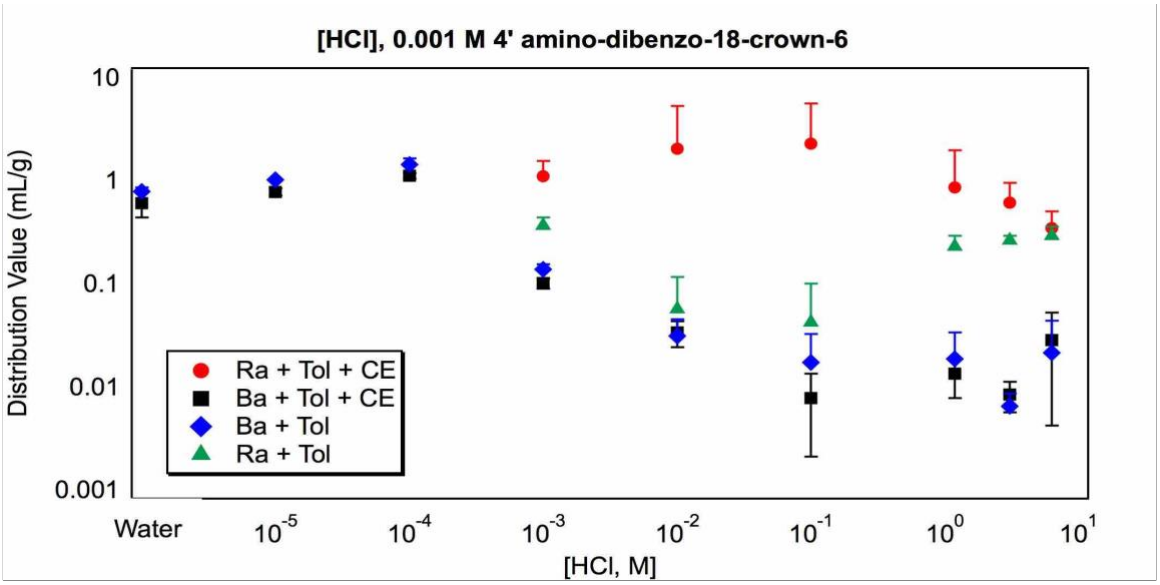

Figure 29: Solvent extraction studies using ^{226}Ra in aqueous HCl solution contacted with toluene containing 0.001 M 4' amino-dibenzo-18-crown-6.

From the figure, the distribution values are generally higher for ^{226}Ra with crown ether (CE) in the organic solvent compared to barium and as well as ^{226}Ra studies with just the organic solvent present. This shows that the hydrophobic crown ether is capable of not only extracting radium at 0.01, 0.1, and 1 M HCl but it is also capable of separating barium and radium from each other. The highest separation factor was observed for 0.1 M HCl ($SF_{Ra/Ba} \approx 290$), which is two orders of magnitude greater than solvent extraction experiments performed by Chiarizia et al. ($SF_{Ra/Ba} \approx 3$) (1999)[87].

^{226}Ra in <0.001 M HCl solution were also investigated; however, it was observed that electrodeposition of ^{226}Ra in a neutral solution was not possible due to ^{226}Ra adsorption on the walls of the electrodeposition cell.

6.4.3 Results from Ion Exchange Studies with Solvent Impregnated Resins

6.4.3.1 FTIR Results

The solvent impregnated resins were ground up into a powder for FTIR analysis. The spectra of pure 4'amino-dibenzo-18-crown-6 and normalized XAD and solvent impregnated XAD resins FTIR spectra are shown below.

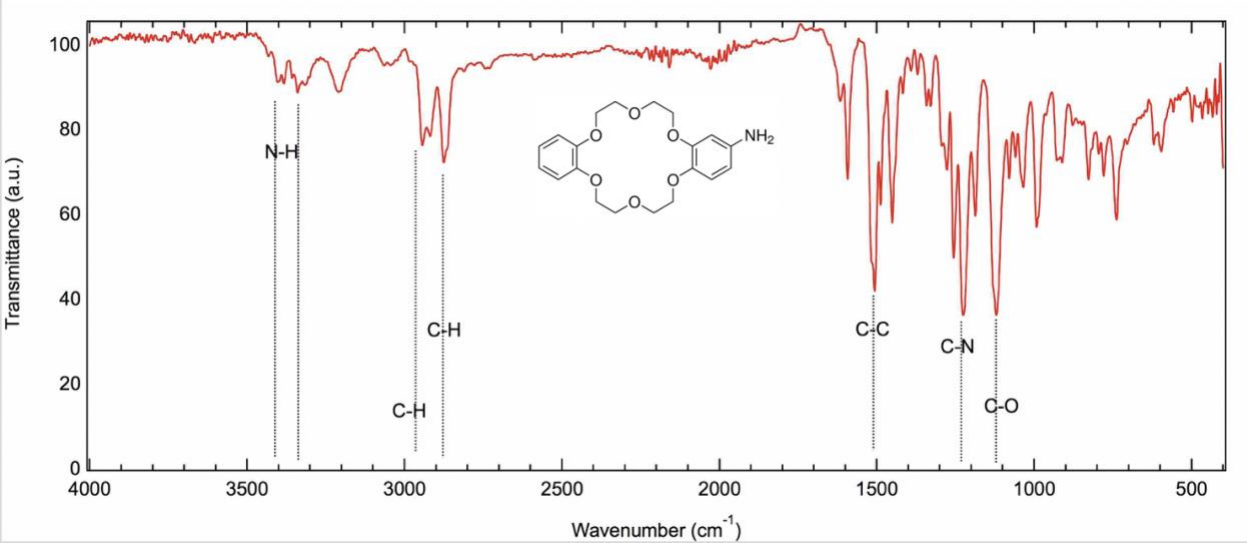

Figure 30: FTIR spectra of 4'amino-dibenzo-18-crown-6 with air as background

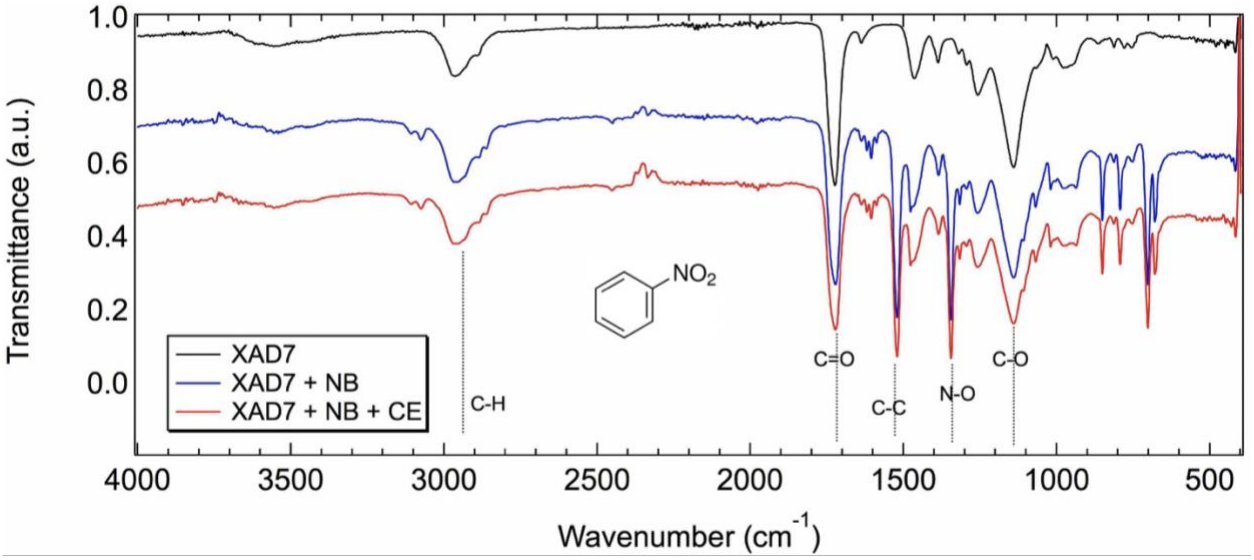

Figure 31: FTIR spectra of pure XAD7 resin (black), XAD7 + nitrobenzene (NB, blue), and XAD7 + NB + 4'amino-dibenzo-18-crown-6 (CE, red) with air as background

Figure 31 shows the FTIR spectra of pure XAD7 resin, XAD7 + NB (nitrobenzene), and XAD + NB + CE (crown ether). The normalized FTIR spectra of the resin with the crown ether (red) is no different from the XAD resin with just the nitrobenzene (blue). As a result, the FTIR spectra of the resins with crown ethers loaded on them were analyzed again with the XAD7 + nitrobenzene resin acting as the background to eliminate any signals caused by the XAD7 resin and the nitrobenzene solvent.

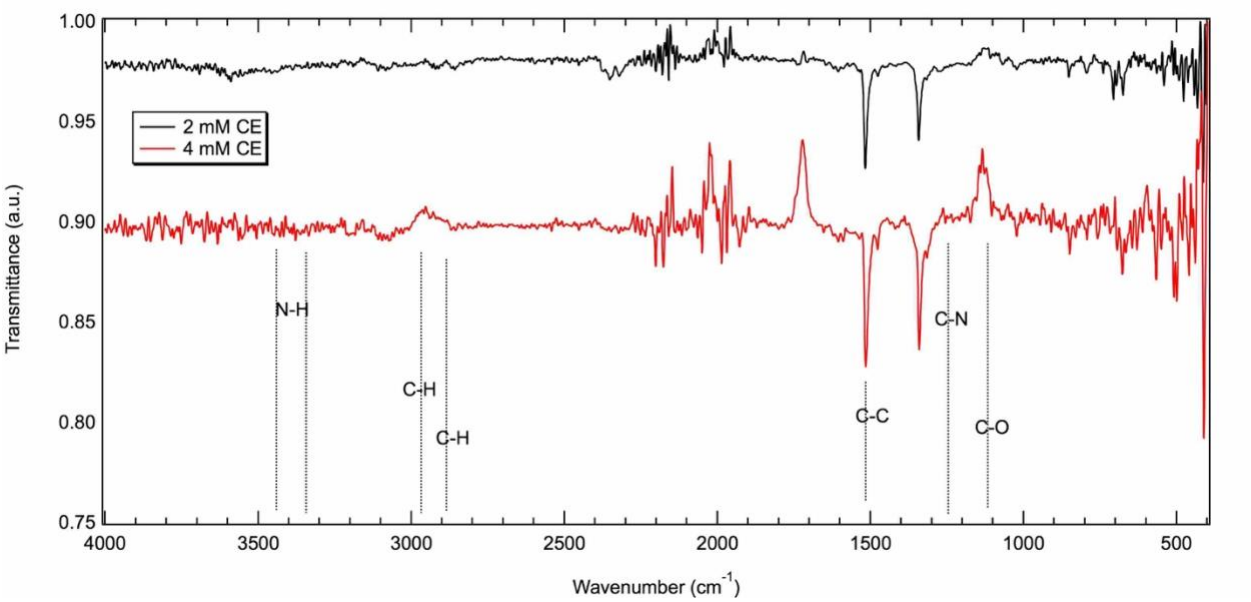

Figure 32: Normalized FTIR spectra of the XAD7 resins loaded with 2mM (black) and 4 mM (red) 4'amino-dibenzo-18-crown-6. The background, XAD7 resin + nitrobenzene, was subtracted from both spectra in order to remove any contributions due to the XAD7 resin and the nitrobenzene solvent.

Upon closer look and subtracting out the XAD and nitrobenzene signature contribution, the spectra only shows the C-C stretch from the aromatic ring at approximately 1500 cm^{-1}. The characteristic stretches from the pure 4'amino-dibenzo-18-crown-6 are the amino group (N-H stretch) and the C-N stretch in Figure 30 are not apparent; however, the stretches at 1500 cm^{-1} are in agreement with the increase of crown ether concentration. The stretch of the 4 mM crown ether spectra (red line) is twice that of the 2 mM spectra (black line). This, along with the physical differences of the dried resins (see Figure 23), suggests that there may be crown ether adsorbed on the surface of the resin; however, the concentration is too low for FTIR analysis. As a result, resins were used in batch experiments to determine if crown ether sorbed on the resin.

6.4.3.2 Batch Experiment Results

Batch ion exchange experiments were done to determine if the solvent impregnated resins were capable of extracting ^{226}Ra out of solution.

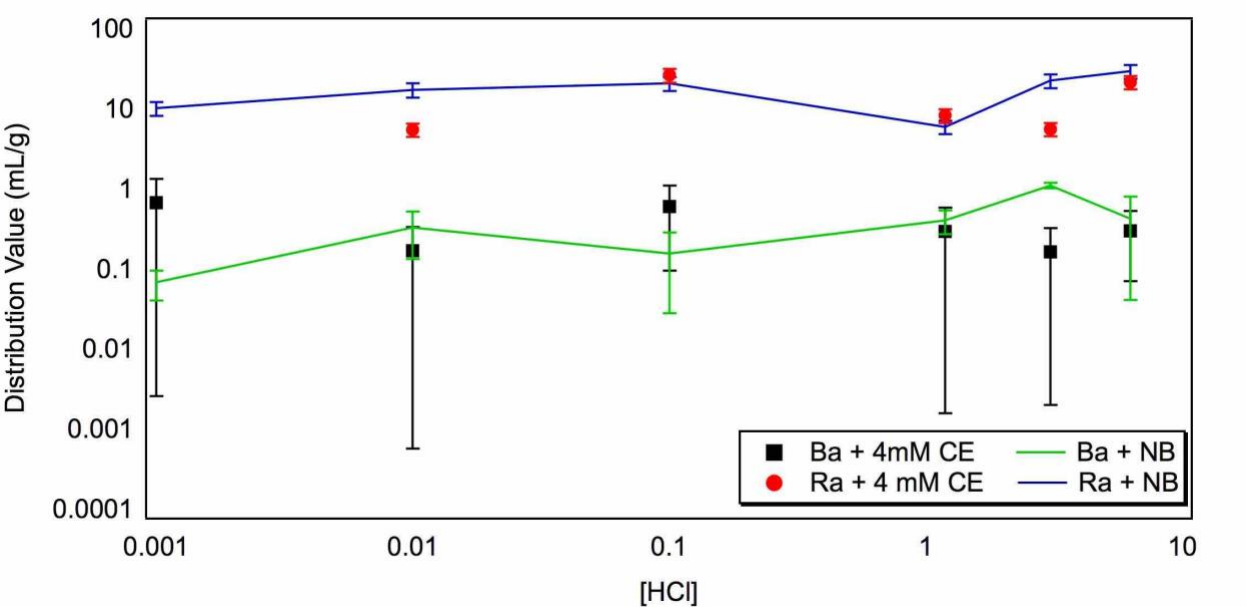

Figure 33: Ion exchange studies using ^{226}Ra or barium in varying HCl solutions and XAD7 resins impregnated with 4 mM 4'amino-dibenzo-18-crown-6 (CE) in nitrobenzene (NB).

In the results, the distribution values of resins impregnated with just nitrobenzene (blue and green line) and the resins with nitrobenzene and 4 mM 4'amino-dibenzo-18-crown-6 (red circle, black square) are relatively the same, indicating that extraction due to crown ether did not occur or the crown ether concentration was too low and did not sorb properly on the surface of the XAD7 resin. However, there is a significant difference between the distribution value of ^{226}Ra and barium, indicating that the XAD7 resin prefers to take up ^{226}Ra compared to barium. XAD7 is the most polar of all XAD resins and previous literature findings have indicated XAD resin uptake of ^{226}Ra. Benzi et al. (1992) demonstrated that the resins, XAD4 (non-polar) and XAD8 (weakly polar) were able to take up ^{226}Ra by 17.3% ± 2.2% and 12.2% ± 1.8%, respectively[89].

Therefore, exploiting the resin's (XAD7) ability to take up ^{226}Ra would be advantageous in future experiments.

6.5 Application to Oil & Gas Wastewater Samples

6.5.1 Ion Exchange Experiments with RSM-25HP and Water-Soluble Crown Ether

The results from the ion exchange studies are shown below. The first set includes varying the acid concentration and keeping the 18-crown-6 concentration constant at 0.1 M. It is also compared to the values with no 18-crown-6 present.

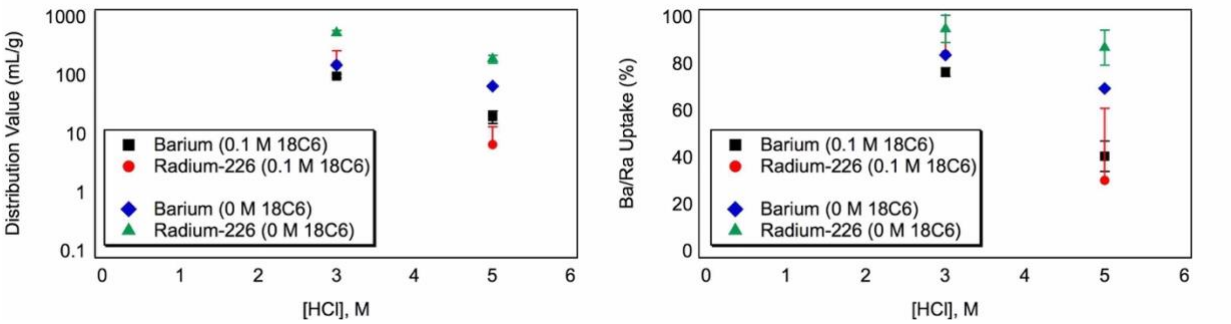

Figure 34: Ion exchange experiments using RSM-25HP and water-soluble crown ether as a function of HCl concentration on environmental samples. The left figure shows distribution value (D) and the right figure shows percent uptake of ^{226}Ra and Ba as a function of hydrochloric acid concentration.

In these results, high distribution values and percent uptake are observed when there is no 18-crown-6 present in both 3 M and 5 M HCl (blue and green markers). However, when 0.1 M 18-crown-6 is added (red and black markers), the values decrease, suggesting that the crown ether is holding back both ^{226}Ra and barium ions, which agrees with Delphin's findings in 1978[83] but not with Dietz observations (1997)[93]. For ^{226}Ra, it is also possible that the electrodeposition step was affected due to the presence of barium, since these results indicate very little separation occurring between the ions ($SF_{Ba/Ra} \approx 3$).

Additional studies were done to assess whether there is synergy occurring while analyzing the environmental samples. The acid concentration was kept constant at 5 M HCl while the 18-crown-6 concentrations were varied.

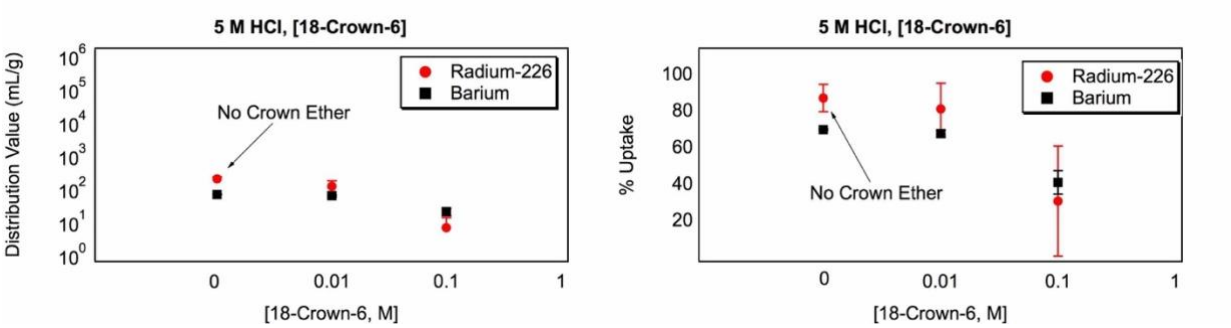

Figure 35: Ion exchange experiments using RSM-25HP and water-soluble crown ether as a function of 18-crown-6 concentration on environmental samples. The left figure shows distribution value (D) and the right figure shows percent uptake of ^{226}Ra and Ba as a function of 18-crown-6 concentration.

The results from this experiment is similar to what was seen in the method validation experiments. Increasing the 18-crown-6 concentration resulted in decrease of the distribution value. There is no synergism observed for 0.1 M and 0.01 M 18-crown-6 at 5 M HCl; however, the resin still exhibits preference for ^{226}Ra over barium.

6.5.2 Solvent Extraction Experiments with Water Insoluble Crown Ether

Solvent extraction experiments were performed on the environmental samples using the same parameters as outlined in the previous section.

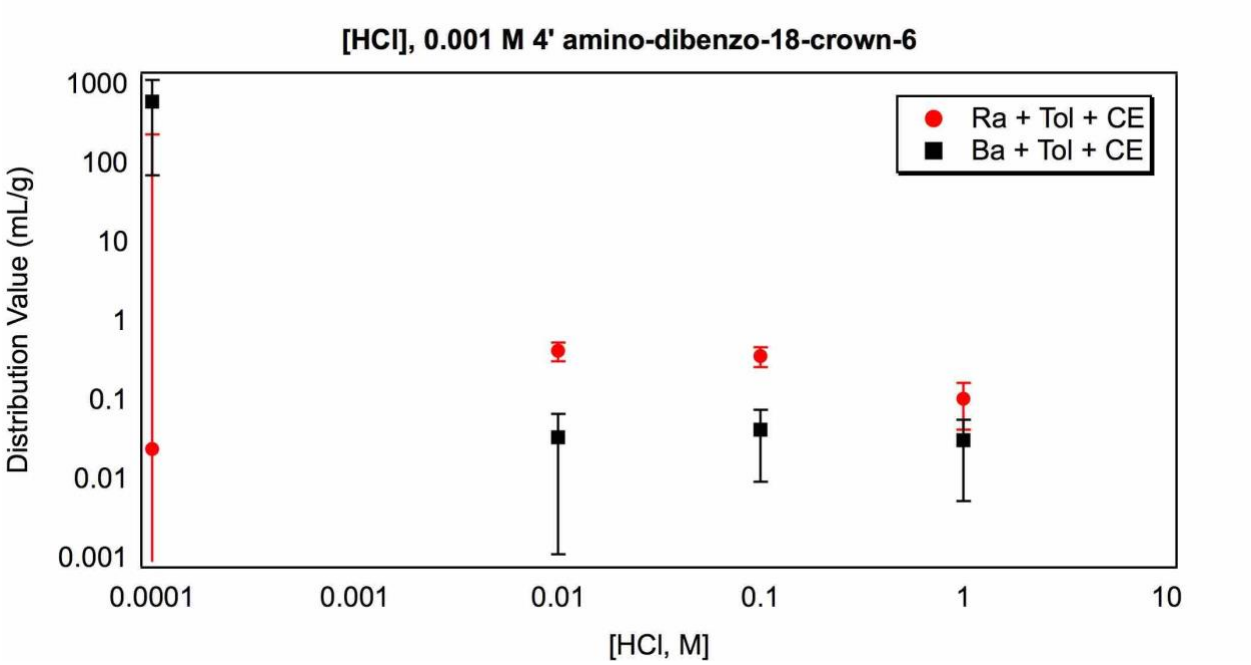

Figure 36: Solvent extraction experiments on environmental samples. The organic phase consists of 0.001 M 4'amino-dibenzo-18-crown-6 in toluene and was contacted for 24 hours with the aqueous phase, which contains the metal (^{226}Ra and Ba) in varying HCl concentrations.

The results from the solvent extraction study also give the same results as the method validation experiments, where ^{226}Ra is seen to be preferentially extracted to the organic phase as compared to barium. The separation factor using 0.1 M HCl in the method validation experiment was much higher ($SF_{Ra/Ba} \approx 290$) compared to the environmental samples ($SF_{Ra/Ba} \approx 8.5$), which could be due to the trace ions, like strontium, present in the collected eluents interfering with the separation process.

A high degree of extraction of barium is seen at 0.0001 M HCl. The likelihood of radium also experiencing high extraction is possible; however, this also shows the extent of the difficulty in electrodepositing ^{226}Ra at concentrations lower than 0.01 M, as seen from the high error values.

6.5.3 Ion Exchange Experiments with Solvent Impregnated Resins

Ion exchange experiments with resins impregnated with 4 mM 4'amino-dibenzo-18-crown-6 in nitrobenzene were studied.

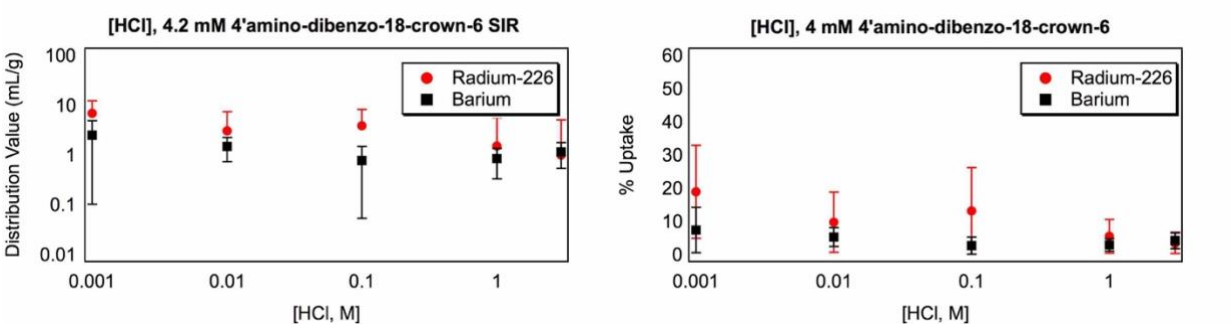

Figure 37: Ion exchange experiments with XAD7 resins impregnated with 4 mM 4'amino-dibenzo-18-crown-6 in nitrobenzene. 100 mg of solvent impregnated resins were contacted for 24 hours with metal (^{226}Ra and Ba) in varying HCl concentrations. The left figure shows distribution value (D) and the right figure shows percent uptake of ^{226}Ra and Ba as a function of 18-crown-6 concentration.

The results from this experiment matches the method validation experiments. Based on distribution values and percent uptake, the crown ether was not successfully adsorbed on the surface of the XAD7 resin, as evident by the high radium remaining in the solution, which contributed to low distribution values and low uptake. A 4 mM crown ether solution is not sufficient to promote adsorption; however, this technique was limited by the solubility of the 4'amino-dibenzo-18-crown-6 in nitrobenzene. Future experiments would require the identification of a solvent that would dissolve a higher crown ether amount.

6.6 Summary

When environmental samples are passed through the RSM-25HP resin, the ^{226}Ra and barium are efficiently separated away from group II ions; however, the presence of barium in the

eluent introduces challenges during ^{226}Ra assay. The presence of barium can significantly reduce ^{226}Ra electrodeposition yields by as much as 40% when 10 µg of barium is present in the sample; therefore, a secondary separation step is needed to accurately quantify ^{226}Ra via electrodeposition and alpha spectrometry.

The secondary separation step exploits the size selectivity of crown ethers to separate the chemically similar ions since ^{226}Ra has a slightly larger ionic radius than barium (see Table 2). The experiments conducted were: ion exchange studies using RSM-25HP and water soluble crown ethers; solvent extraction studies using water-insoluble crown ether (4'amino-dibenzo-18-crown-6) in toluene as the organic phase and varying HCl concentrations as the aqueous phase; and XAD7 resins impregnated with 2 mM and 4 mM 4'amino-dibenzo-18-crown-6 in nitrobenzene. A comparison of the separation factors in the method validation experiments and with the Eagle Ford shale wastewater samples are shown as well as a comparison with separation factors documented in the literature[87].

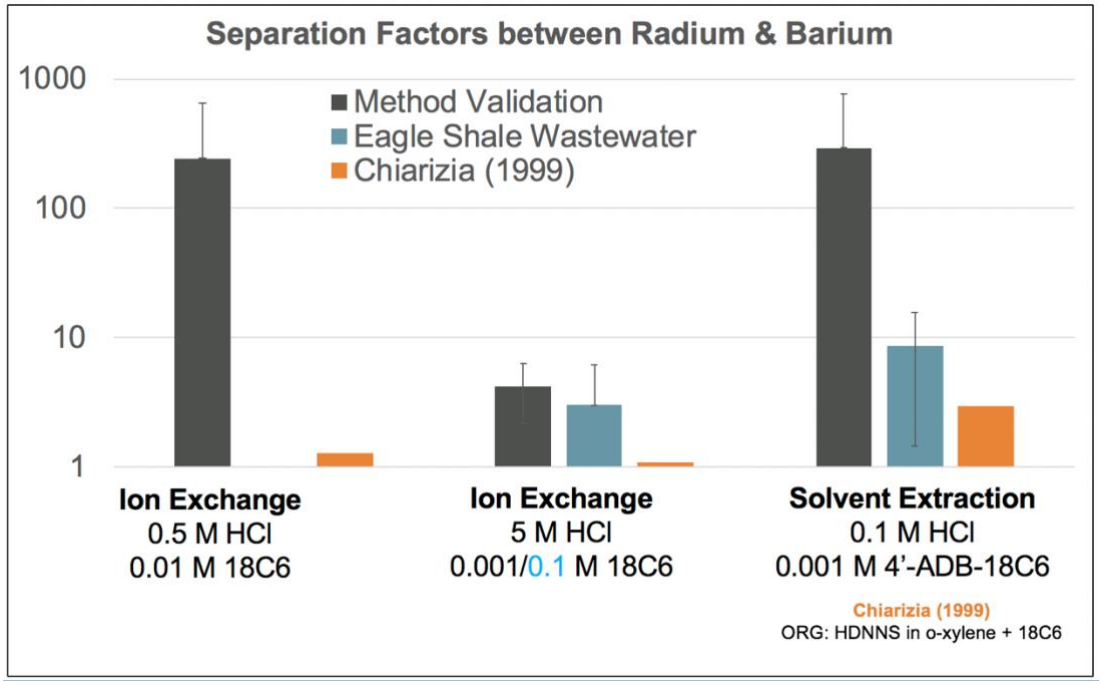

Figure 38: Summary of separation factors between radium and barium using ion exchange and solvent extraction experiments.

The ion exchange studies with water soluble crown ethers show very large separation factors especially at low acid concentrations (0.5 M HCl) but not for high acid concentrations (5M HCl) mostly due to the protonation of resin and crown ether. The solvent extraction studies are the most promising for ^{226}Ra and barium separation, with separation factors as high as 290; however, more extractant is needed in order to promote extraction and increase the distribution values.

Lastly, the ion exchange studies with the solvent impregnated resins is an attractive separation method to capitalize on the advantages of solid-liquid extraction and avoid the disadvantages of solvent extraction; however, the results here indicate no extraction of ^{226}Ra due to unsuccessful adsorption of the crown ether on the surface of the XAD resins. All of these experiments were also done to the environmental samples; however, the results were similar, and the only promising extraction was seen with solvent extraction.

CONCLUSION

The rise of unconventional production of natural gas (hydraulic fracturing coupled with horizontal drilling) has enabled access to previously unrecoverable natural gas in reservoirs worldwide. The increasing demand, mainly from power and industrial markets, will likely encourage the use of this technology to continually seek shale formations for energy productions. However, doing so will increase the amount of waste that needs to be managed.

Current wastewater management strategies have caused some concerns due to the composition of the water that flows from the shale formations up to the wells. This wastewater picks up radionuclides that exist naturally in soils and rocks, increasing the concentration in the surrounding environment. These radionuclides are also known as TENORM as they are enhanced by the advancements of oil and gas extraction technology. In the case of Marcellus shale wastewaters, the median value was 5,350 pCi/L of total radium[94], which is well above the U.S. EPA maximum contaminant level in drinking water (5 pCi/L)[95] and the U.S. NRC effluent discharge limit (60 pCi/L)[94]. Generally, these waters can be reused, disposed of in Class II injection wells, or temporarily stored in a pit.

The concerns primarily stem from radionuclide contamination of groundwater and soil as well as an increase in radiation dose to workers. ^{226}Ra is considered to be one of the most radiotoxic NORMs due to its long half-life, abundance of its parent, ^{238}U, and its short-lived daughter products that decay through alpha particle emissions. While alpha particles are generally not dangerous if it is outside the body, as soon as it enters the body, it could wreak havoc due to its ability to deposit all its energy in short distances, potentially causing double DNA strand breaks. Ingestion of ^{226}Ra can lead to bone cancer due to its tendency to accumulate in bones by following the same pathway as calcium. In addition, its daughter, radon-222, which

is a gas and decays via alpha particle emissions, can accumulate in poorly ventilated basements and due to its gaseous nature, it is easily inhaled and can cause lung cancer, making it the second leading cause of lung cancer.

There has been research done on potential treatment of these wastewaters in a brine treatment facility; however, results showed that stream sediments at the discharge point were ~200 times the background of the upstream sediments[22,96]. As a result, this project aims to chemically treat wastewaters from unconventional gas production as well as determine ways to assay radium.

Wastewaters from the Eagle Ford shale formation were obtained and though they did not have any ^{226}Ra, this wastewater was used as a platform for highly saline environmental samples. Samples were characterized by first determining where the radium goes if it is filtered as well as determining the total dissolved solids. Upon determination that radium will accumulate in the filters, the filters were digested in order to destroy any organics and allow for metal analysis. Two strong cation exchange resins were used, one with extensive literature data and another that is new and has few data, for batch and column ion exchange studies. Batch experiments were performed to get a general idea of their uptake behavior, which informed the parameters used in column experiments. Column experiments were performed in order to separate radium and barium from other metals, mainly, the group II metals. Results from this study showed that the new resin, RSM-25HP, provided higher degrees of separation of radium and barium from major group II cations as well as being economically favorable as it concentrated the ions to less volume. However, the challenge was the fact that radium and barium were eluted out at the same time, which complicates radium analysis via electrodeposition.

Electrodeposition studies of ^{226}Ra and ^{238}U showed that as little as 10 µg of barium could decrease the ^{226}Ra yield from 60-80% to 20% but maintain high recoveries for ^{238}U. This necessitates a secondary separation step in order to separate ^{226}Ra from barium. The secondary separation steps exploited the size selectivity of crown ethers since ^{226}Ra has a larger ionic radius than barium. Ion exchange studies with RSM-25HP and water-soluble crown ether, solvent extraction studies with water-insoluble crown ether, and impregnating resins with crown ethers were studied for surrogate samples as well as for the environmental samples. Of these experiments, solvent extraction studies are most promising for ^{226}Ra and barium separation, exhibiting large separation factors; however, it is necessary to explore other solvents in order to increase the concentration of the extractant and promote higher extraction.

The analytical, separation, and detection methods described in this dissertation illustrated a lab-scale cradle to grave process; however, more work is needed to maximize separation of ^{226}Ra and barium from each other. The analysis methods used here can be applied to other environmental samples such as wastes from the phosphate fertilizer industry[24] and uranium tailings. In addition, the recovery of pure ^{226}Ra can be used to produce ^{223}Ra, which is an FDA approved drug to treat castration-resistant prostate cancer. The methods used here can not only inform treatment methods of highly saline samples in order to prevent radionuclide contamination in the environment and additional radiation exposure to workers, but also serves as a source to produce a radioisotope that is capable of killing cancer cells.

APPENDIX I: ADDITIONAL EXPERIMENTS

AI.1 Direct Isotope Dilution Technique

A1.1.2 Introduction

The direct isotope dilution technique is an analytical tool to determine concentrations of the analyte of interest in unknown samples. This technique is attractive for its ability to quantify an unknown analyte without 100% recovery of the analyte by spiking a natural sample with an enriched isotope of the analyte. However, disadvantages include not being able to determine monoisotopic elements and the limitation imposed due to the half-life of the spike solution. Once the isotope spike has decayed substantially, the detection of the isotope becomes very difficult.

A1.1.1 Theory

This technique required the addition of known amounts of isotopically enriched substance to the sample of interest, effectively diluting the isotopic enrichment of the standard[97]. The isotopically enriched substance is ^{139}Ba, which is added to a sample with an unknown amount of natural barium. ^{139}Ba is formed by the neutron capture of natural barium:

$$^{138}_{56}Ba + ^{1}_{0}n \rightarrow ^{139}_{56}Ba + \gamma$$

which can also be written as ^{138}Ba (n,γ)^{139}Ba. The ^{139}Ba nuclide, with a 1.4-hour half-life, can be analyzed using an HPGe detector by counting the number of gamma decays at 165.9 keV. This solution was the "spike" stock solution with a specific activity, *A'*, calculated from the equation,

$$A' = \left(\frac{R'}{m'}\right)$$

where *R'* is the number of counts at the 165.9 keV gamma energy and *m'* is the amount of barium nitrate in the stock solution prior to irradiation. A known amount of the "spike" stock

solution was mixed with a known amount of unknown solution. A solution known to encourage precipitation of the target analyte was added, bringing the target analyte out of solution, effectively separating barium from other materials that do not readily form precipitates with the solution. The specific activity of the recovered mass (precipitates), *S*, can be calculated by,

$$\frac{S'}{S} = \frac{R'}{m' + m} = \frac{R_r}{m_r}$$

where R_r is the number of counts of the recovered solid sample at the 165.9 keV gamma energy and m_r is the final mass of the recovered sample. To determine the unknown mass, the ratio of the specific activities of the spike and the recovered sample was taken, according to the equation,

$$\frac{S'}{S} = \frac{R'/_{m'}}{R'/_{(m' + m)}} = \frac{m' + m}{m'} = 1 + \frac{m}{m'}$$

Rearranging gives an equation to solve for the unknown mass,

$$m = m'\left(\frac{S'}{S} - 1\right)$$

A1.1.2 Experimental Setup

A solution of 100-ppm barium nitrate was irradiated at the UCI Reactor Facility to activate some of the ^{138}Ba atoms to radioactive ^{139}Ba. The sample was irradiated with a neutron flux of 8 x 10^{11} neutrons cm^{-2} s^{-1} for one hour. A known amount (1 mL) of the radioactive 100-ppm barium nitrate solution was added to a 10 mL weighed glass centrifuge vial containing an unknown solution. A 1.8 M H_2SO_4 solution was added to the mixture to encourage precipitation. Once achieved, the supernatant was pipetted out of the solution (careful of not removing solid precipitate) to a waste container. The sample was then washed with 5 mL of water to dissolve any water-soluble sulfate compounds. Precipitates were again allowed to settle then water was

pipetted out and placed in the designated waste container. Samples were placed in an oven (182 ± 2 °C) for 30 minutes, cooled, weighed, and counted using the HPGe.

A1.1.3 Results

The constituents of samples S0F, S1F, and S3F were previously mentioned in Table 3. Figure 39 shows the calculated mass from this technique compared to the actual weight of the sample.

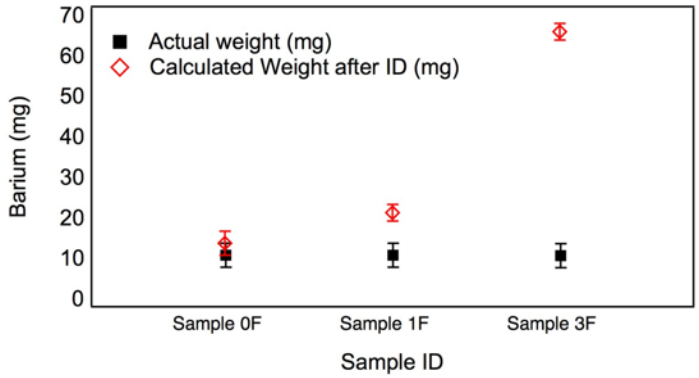

Figure 39: Results from the isotope dilution (ID) technique. Error values represent error in the weighing scale as well as random errors.

This method works for samples with pure barium or do not have other ions that will precipitate upon addition of sulfuric acid. The "unknown" mass of barium for S1F and S3F was calculated to be 49.5% and 83.9% more than the actual weighted mass, respectively. This increase in mass is due to other ions precipitating out with the addition of sulfuric acid. The water wash following the precipitation was included to dissolve any sulfate compounds; however, this step only applied to the dissolution of calcium sulfates. Table 8 provides an explanation of the phenomena that was observed in Figure 39 using the solubility, equilibrium constant[98], and reaction quotients of the ions that were present in Sample 3F.

Table 9: Sample 3F constituents' ion solubility information

S3F	Solubility in 100 mL water (20 – 25 °C)	Solubility Product (K_{sp})[98]	Reaction Quotient, Q	Precipitate?
$BaSO_4$	0.31 mg	1.08×10^{-10}	7.00×10^{-3}	Q > K, Precipitate
$SrSO_4$	13.5 mg	3.44×10^{-7}	2.59×10^{-2}	Q > K, Precipitate
$CaSO_4$	0.21 g	4.93×10^{-5}	5.67×10^{-2}	Q > K, Precipitate
$MgSO_4$, $Na_2(SO_4)$, $Fe_2(SO_4)_3$, $K_2(SO_4)$ are all soluble in water				

The general precipitation reaction is

$$AB(s) \overset{\Delta}{\leftrightarrow} A^-(aq) + B^+(aq)$$

where the left side represents the precipitate and the right side represents the ions dissolved in solution. The reaction quotient, *Q*, of the reaction above can be calculated using the equation:

$$Q = [A^-][B^+]$$

For *$BaSO_4$*, *$SrSO_4$*, and *$CaSO_4$*, *Q* is larger than the equilibrium constant, *K*, implying that the equilibrium shifts to the solid state (left); therefore, causing the precipitation to occur. This explains why the unknown mass calculated from this method was much higher than the actual weighted mass.

A1.1.4 Conclusions

With a highly saline matrix, containing calcium and strontium ions, such as the current environmental samples, this analytical method cannot be used to quantify the ions of interest, barium, which is used as a chemical analog for ^{226}Ra. A separation step would be necessary to isolate ^{226}Ra ions from calcium, strontium, and barium prior to using this technique.

REFERENCES

1. U.S. Energy Information Administration. *Annual Energy Outlook 2019 with Projections to 2050*. (2019).
2. Lutz, B. D., Lewis, A. N. & Doyle, M. W. Generation, transport, and disposal of wastewater associated with Marcellus Shale gas development. *Water Resour. Res.* **49**, 647–656 (2013).
3. Veil, J. A. *Water Management Technologies Used by Marcellus Shale Gas Producers*. (2010).
4. Stringfellow, W. T., Domen, J. K., Camarillo, M. K., Sandelin, W. L. & Borglin, S. Physical, chemical, and biological characteristics of compounds used in hydraulic fracturing. *J. Hazard. Mater.* **275**, 37–54 (2014).
5. Britt, L. Fracture stimulation fundamentals. *J. Nat. Gas Sci. Eng.* **8**, 34–51 (2012).
6. Various. Lower 48 states shale plays. *Energy* 1 (2011). Available at: www.eia.gov. (Accessed: 26th October 2017)
7. Gregory, K. B., Dzombak, D. A., Gregory, K. B., Vidic, R. D. & Dzombak, D. A. Water Management Challenges Associated with the Production of Shale Gas by Hydraulic Fracturing. *Elements* **7**, 181–186 (2010).
8. Arthur, A. J. D., Bohm, B., Layne, M. & ALL Consulting. Hydraulic Fracturing Considerations for Natural Gas Wells of the Marcellus Shale. in *The Ground Water Protection Council* (2008).
9. Tollefson, J. Secrets of fracking fluids pave way for cleaner recipe. *Nature* **501**, 146–147 (2013).
10. Xu, X. *et al.* A systematic assessment of carcinogenicity of chemicals in hydraulic-fracturing fluids and flowback water. *Environ. Pollut.* (2019). doi:10.1016/J.ENVPOL.2019.04.016
11. Nabhani, K. AL, Khan, F. & Yang, M. Technologically Enhanced Naturally Occurring Radioactive Materials in oil and gas production: A silent killer. *Process Saf. Environ. Prot.* **99**, 237–247 (2016).
12. Nelson, A. W. *et al.* Understanding the Radioactive Ingrowth and Decay of Naturally Occurring Radioactive Materials in the Environment: An Analysis of Produced Fluids from the Marcellus Shale. *Environ. Health Perspect.* **123**, 689–696 (2015).
13. Bank, T. *Trace Metal Geochemistry and Mobility in the Marcellus Shale*.
14. Rowan, E. L., Engle, M. a., Kirby, C. S. & Kraemer, T. F. *Radium Content of Oil- and Gas-Field Produced Waters in the Northern Appalachian Basin (USA): Summary and Discussion of Data*. *USGS Scientific Investigations Report 2011-5135* (2011).
15. Environmental Protection Agency. National Primary Drinking Water Regulations; Radionuclides; Final Rule 40 CRFR Parts 9. 141, 142. *Fed. Regist.* **65**, 1–47 (2000).
16. NRC. *NRC: 10 CFR 20.1201 Occupational dose limits for adults.* (2015).
17. Terrill, J. G., Ingraham, S. C. & Moeller, D. W. Radiation Exposure in the United States Radium in the Healing Arts and in Industry. *Public Heal. Rep.* **69**, 255–262 (1954).
18. National Research Council. *Health Risks of Radon and Other Internally Deposited Alpha-*

Emitters. (National Academy Press, 1988).

19. National Cancer Institute. Radon and Cancer. (2011). Available at: https://www.cancer.gov/about-cancer/causes-prevention/risk/substances/radon/radon-fact-sheet. (Accessed: 29th October 2017)
20. Ellsworth, W. L. Injection-Induced Earthquakes. *Science (80-.).* **341**, 1–8 (2013).
21. Nelson, A. W. *et al.* Matrix Complications in the Determination of Radium Levels in Hydraulic Fracturing Flowback Water from Marcellus Shale. *Environ. Sci. Technol. Lett.* **1**, 204–208 (2014).
22. Warner, N. R., Christie, C. A., Jackson, R. B. & Vengosh, A. Impacts of shale gas wastewater disposal on water quality in Western Pennsylvania. *Environmental Science and Technology* **47**, 11849–11857 (2013).
23. Weeks, M. E. The Discovery of the Elements. XIX. The Radioactive Elements. *J. Chem. Educ.* 79–89 (1933).
24. Sahu, S. K., Ajmal, P. Y., Bhangare, R. C., Tiwari, M. & Pandit, G. G. Natural radioactivity assessment of a phosphate fertilizer plant area. *J. Radiat. Res. Appl. Sci.* **7**, 123–128 (2014).
25. Parker, C. *et al.* Alpha Emitter Radium-223 and Survival in Metastatic Prostate Cancer. *N. Engl. J. Med.* **369**, 213–223 (2013).
26. Abou, D. S., Pickett, J., Mattson, J. E. & Thorek, D. L. J. A Radium-223 microgenerator from cyclotron-produced trace Actinium-227. *Appl. Radiat. Isot.* **119**, 36–42 (2017).
27. Deshayes, E. *et al.* Radium 223 dichloride for prostate cancer treatment. *Drug Des. Devel. Ther.* **11**, 2643–2651 (2017).
28. Kirby, H. W. & L., S. M. *The Radiochemistry of Radium*. (National Academy of Sciences - National Research Council, 1964).
29. Shannon, R. D. Revised Effective Ionic Radii and Systematic Studies of Interatomic Distances in Halides and Chalcogenides. *Acta Cryst.* 751–767 (1976).
30. Sill, C. W. & Olson, D. G. Sources and Prevention of Recoil Contamination of Solid-State Alpha Detectors. *Anal. Chem.* **42**, 1596–1607 (1970).
31. Hayes, T. *Sampling and Analysis of Water Streams Associated with the Development of Marcellus Shale Gas*. *Final Report for Marcellus Shale Coalition* (2009).
32. Lester, Y. *et al.* Characterization of hydraulic fracturing flowback water in Colorado: Implications for water treatment. *Sci. Total Environ.* **512**–**513**, 637–644 (2015).
33. Schultz, M. K. & Nelson, A. W. *Unconventional Drilling/Hydraulic Fracturing and Natural Radioactivity*. (2014).
34. Zhang, T., Bain, D., Hammack, R. & Vidic, R. D. Analysis of Radium-226 in High Salinity Wastewater from Unconventional Gas Extraction by Inductively Coupled Plasma-Mass Spectrometry. *Environ. Sci. Technol.* **49**, 2969–2976 (2015).
35. De Soete, D., Hoste, J. & Gijbels, R. *Neutron Activation Analysis*. (Wiley-Interscience).
36. Oram, B. Sources of Total Dissolved Solids (Minerals) in Drinking Water. *Water Research Watershed Center* (2014). Available at: http://www.water-research.net/index.php/water-treatment/tools/total-dissolved-solids. (Accessed: 9th

November 2017)

37. Haluszczak, L. O., Rose, A. W. & Kump, L. R. Geochemical evaluation of flowback brine from Marcellus gas wells in Pennsylvania, USA. *Appl. Geochemistry* **28**, 55–61 (2013).
38. Engle, M. A. & Rowan, E. L. Geochemical evolution of produced waters from hydraulic fracturing of the Marcellus Shale, northern Appalachian Basin: A multivariate compositional data analysis approach. *Int. J. Coal Geol.* **126**, 45–56 (2014).
39. Environmental Protection Agency. *Hydraulic Fracturing for Oil and Gas: Impacts from the Hydraulic Fracturing Water Cycle on Drinking Water Resources in the United States (Final Report)*. (2016).
40. Brannon H. Wilder, Harold S. Costa, Christine M. Kosmowski, W. E. P. SM 2540 Solids. *Phys. Aggreg. Prop.* **2**, 55–61 (2000).
41. Howard, C. S. Determination of Total Dissolved Solids in Water Analysis. *Ind. Eng. Chem. Anal. Ed.* **5**, 4–6 (2003).
42. Godsey, W. E. *Fresh, Brackish, or Saline Water for Hydraulic Fracs: What are the Options*. (1904).
43. Kotz, L, Kaiser, G, Tschopel, P and Tolg, G. Theory of Sample Preparation Using Acid Digestion , Pressure Digestion and Microwave Digestion (Microwave Decomposition). *Anal. Chem.* **260**, 207–209 (1972).
44. US.EPA. *Acid Digestion of Sediments, Sludges and Soils: Method 3050-B*. (1996).
45. Erickson, M. D. *The Procedures Manual of the Environmental Measurements Laboratory*. (U.S. Department of Energy, 1997).
46. Crespo, M. T. A review of electrodeposition methods for the preparation of alpha-radiation sources. *Appl. Radiat. Isot.* **70**, 210–215 (2012).
47. Jurado Vargas, M., Fernandez De Soto, F. Influence of Barium on the Electrodeposition of Ra-226. *J. Radioanal. Nucl. Chem.* **198**, 143–150 (1995).
48. Pier, R., Gaspar-Vargas, B., Romero, A. & Nilsson, M. Comparative study using ion exchange resins to separate and reduce NORM from oil and gas flowback wastewater. *J. Radioanal. Nucl. Chem.* **318**, 497–503 (2018).
49. Roman, D. Electrodeposition of radium on stainless steel from aqueous solutions. *Int. J. Appl. Radiat. Isot.* **35**, 990–992 (1984).
50. García-Tenorio, R. & García-León, M. Electrodeposition of Ra from a HCl + CH3-COONH4 aqueous solution. *Int. J. Radiat. Appl. Instrumentation. Part* **37**, 441–442 (1986).
51. Short, S. A. Measurement of All Radium Isotopes at Environmental Levels on a Single Electrodeposited Source. *Nucl. Instruments Methods Phys. Res.* **B17**, 540–544 (1986).
52. Orlandini, K., Gaffney, J. & Marley, N. An Improved Technique for the Rapid Assay of Radium Isotopes in Water. *Radiochim. Acta* **55**, 205–208 (1991).
53. Alvarado, J. S., Orlandini, M. D. & Erickson, M. D. Rapid Determination of radium isotopes by Alpha Spectrometry. *J. Radioanal. Nucl. Chem.* **194**, 163–172 (1995).
54. Mitchell, R. F. Electrodeposition of Actinide Elements at Tracer Concentrations. *Anal. Chem.* **32**, 326–328 (1960).

55. Lee, S. C., Choi, J. G. & Hodge, V. F. Electrodeposition of selected alpha-emitting nuclides from ammonium acetate electrolyte. *J. Alloys Compd.* **213**–**214**, 465–466 (1994).

56. Hallstadius, L. A Method for the Electrodeposition of Actinidies. *Nucl. Instruments Methods Phys. Res.* **223**, 266–267 (1984).

57. Talvitie, N. A. Electrodeposition of Actinides for Alpha Spectrometric Determination. *Anal. Chem.* **44**, 280 (1972).

58. Torrico, M. N., Boll, R. A. & Matos, M. *Electrodeposition of Actinide Compounds from an Aqueous Ammonium Acetate Matrix: Experimental Development and Optimization*. (2015).

59. Beesley, A. M. *et al.* Evolution of chemical species during electrodeposition of uranium for alpha spectrometry by the Hallstadius method. *Appl. Radiat. Isot.* **67**, 1559–1569 (2009).

60. Méndez, C. G. *et al.* Nanoscopic study of chemical species during uranium electrodeposition for alpha spectrometry sources. *J. Mater. Sci.* **45**, 5061–5070 (2010).

61. Weber, R., Vater, P., Esterlund, R. . & Patzelt, P. On the energy resolution of α-sources prepared by electrodeposition of uranium. *Nucl. Instruments Methods Phys. Res. Sect. A Accel. Spectrometers, Detect. Assoc. Equip.* **423**, 468–471 (1999).

62. Hansen, P. G. The Conditions for Electrodeposition of Insoluble Hydroxides at a Cathode Surface: A Theoreitical Investigations. *J. Inorg. Nucl. Chem* **12**, 30–37 (1959).

63. Glover, K M, Lally, A. E. Source Preparation in Alpha Spectrometry. in *Nuclear Instruments and Methods in Physics Research* **223**, 259–265 (1984).

64. Freeman, W. H. Standard Reduction Potentials. in AP20–AP27 (W.H. Freeman, 2010).

65. Nørskov, J. K. *et al.* Trends in the Exchange Current for Hydrogen Evolution. *J. Electrochem. Soc.* **152**, J23 (2005).

66. Hamilton, T.F., McRae, V.M., Smith, J. D. Radium Isotope Determination by Alpha-Spectrometry After Electrodeposition From Solution with Added Platinum. *J. Radioanal. Nucl. Chem.* **177**, 365–371 (1994).

67. Crespo, M. T. & Jiménez, A. S. On the determination of radium by alpha-spectrometry. *J. Radioanal. Nucl. Chem.* **221**, 149–152 (1990).

68. Vijh, A. K. & Conway, B. E. Electrode Kinetics Aspects of the Kolbe Reaction. *Chem. Rev.* **67**, 623–664 (1967).

69. Eberson, L. Studies on the Kolbe Electrolytic Synthesis: A Theoretical Investigation of the Mechanism by Standard Potential Calculations. *Acta Chem. Scand.* **17**, 2014–2018 (1963).

70. Donnan, M. Y. & Dukes, E. K. Carrier Technique for Quantitative Electrodeposition of Actinides. *Anal. Chem.* **36**, 392–394 (1964).

71. Short, S. A. Natural Radionuclides: Measurement of all radium isotopes at environmental levels on a single electrodeposited source. *Nucl. Instruments Methods Phys. Res.* **B17**, 540–544 (1986).

72. *Ion Exchange Technology I: Theory And Materials*. (Springer, 2012).

73. The Dow Chemical Company. *DOWEX: Ion Exchange*. (1964).

74. Largitte, L. & Pasquier, R. A review of the kinetics adsorption models and their

application to the adsorption of lead by an activated carbon. *Chem. Eng. Res. Des.* **109**, 495–504 (2016).

75. Kammerer, J., Carle, R. & Kammerer, D. R. Adsorption and ion exchange: Basic principles and their application in food processing. *J. Agric. Food Chem.* **59**, 22–42 (2011).
76. Lagergren, S. Y. Zur Theorie der sogenannten Adsorption gelöster Stoffe. *Handlingar* **24**, 1–39 (1898).
77. Ho, Y.S. and McKay, G. Pseudo-Second Order Model for Sorption Processes. *Process Biochem.* **34**, 451–465 (1999).
78. Hafizi, M., Abolghasemi, H., Moradi, M. & Milani, S. A. Strontium adsorption from sulfuric acid solution by dowex 50W-X8 resins. *Chinese J. Chem. Eng.* **19**, 267–272 (2011).
79. Nomngongo, P. N., Ngila, J. C., Msagati, T. A. M. & Moodley, B. Kinetics and Equilibrium Studies for the Removal of Cobalt, Manganese, and Silver in Ethanol using Dowex 50W-X8 Cation Exchange Resin. *Sep. Sci. Technol.* **49**, 1848–1859 (2014).
80. Martin, P. & Hancock, G. J. Samples of Ra in Environmental Samples by Alpha-Spectrometry. **42**, 63–69 (1991).
81. Pedersen, C. J. Cyclic polyethers and their complexes with metal salts. *J. Am. Chem. Soc.* **89**, 7017–7036 (1967).
82. Alfassi, Z. B. & Wai, C. M. *Preconcentration techniques for trace elements*. (Boca Raton, FL (United States); CRC Press Inc., 1991).
83. Delphin, W. H. & Horwitz, E. P. Effects of Crown Ethers on Ion Exchange Behavior of Alkali Metals. *Anal. Chem.* **50**, 843–848 (1978).
84. Dietz, M. L., Chiarizia, R., Philip Horwitz, E., Bartsch, R. A. & Talanov, V. Effect of Crown Ethers on the Ion-Exchange Behavior of Alkaline Earth Metals. Toward Improved Ion Exchange Methods for the Separation and Preconcentration of Radium. *Anal. Chem.* **69**, 3028–3037 (1997).
85. Hellé, G., Mariet, C. & Cote, G. Liquid-liquid extraction of uranium(VI) with Aliquat® 336 from HCl media in microfluidic devices: Combination of micro-unit operations and online ICP-MS determination. *Talanta* **139**, 123–131 (2015).
86. Beklemlshev, M. K., Elshani, S. & Wai, C. M. *Solvent Extraction of Radium with Crown Ether Carboxylic Acids*. *Analytical Chemistry* **66**, (1994).
87. Chiarizia, R., Dietz, M. L., Horwitz, E. P., Burnett, W. C. & Cable, P. H. Radium Separation Through Complexation By Aqueous Crown Ethers and Ion Exchange or Solvent Extraction*. *Sep. Sci. Technol.* **34**, 931–950 (1999).
88. Braun, T. & Ghersini, G. *Extraction chromatography*. (Elsevier Scientific Pub. Co, 1975).
89. Benzi, P., Righetti, R. & Volpe, P. Radium Removal from Aqueous Solutions By Variously Supported Ligands. *J. Radioanal. Nucl. Chem. Lett.* **164**, 211–220 (1992).
90. Ciopec, M. *et al.* Amberlite XAD7 resin functionalized with crown ether and Fe(III) used for arsenic removal from water. in *17th Polymers and Organic Chemistry (POC-2018)* (IUPAC & De Gruyter, 2018). doi:10.1515/pac-2018-0607
91. Jansen, J. C. Ideal Separation Factor. in *Encyclopedia of Membranes* (eds. Drioli, E. &

Giorno, L.) (Springer, Berlin, Heidelberg, 2016).

92. Dietz, M. L., Chiarizia, R., Horwitz, E. P., Bartsch, R. A. & Talanov, V. Effect of Crown Ethers on the Ion-Exchange Behavior of Alkaline Earth Metals. Toward Improved Ion-Exchange Methods for the Separation and Preconcentration of Radium. *Anal. Chem.* **69**, 3028–3037 (1997).

93. Dietz, M. L., Chiarizia, R., Horwitz, E. P., Bartsch, R. A. & Talanov, V. Effect of Crown Ethers on the Ion-Exchange Behavior of Alkaline Earth Metals. Toward Improved Ion-Exchange Methods for the Separation and Preconcentration of Radium. *Anal. Chem.* **69**, 3028–3037 (1997).

94. Rowan, E. L., Engle, M. A., Kirby, C. S. & Kraemer, T. F. Radium Content of Oil-and Gas-Field Produced Waters in the Northern Appalachian Basin (USA): Summary and Discussion of Data.

95. Booth, R. L. *E.P.A Methods for Chemical Analysis of Water and Wastes*. (1983).

96. Volz, Conrad, D. *et al.* Contaminant Characterization of Effluent from Pennyslvania Brine Treatment Inc., Josephine Facility: Implications for Disposal of Oil and Gas Flowback Fluids from Brine Treatment Plants. in *EPA Hydraulic Fracturing Study Technical Workshop 3, Fate and Transport* (2011).

97. The Living Textbook of Nuclear Chemistry. Isotope Dilution Techniques. Available at: http://livingtextbook.oregonstate.edu/chemlab/media/expt10.pdf. (Accessed: 9th November 2017)

98. Solubility Product Constants. *Chemically Bonded Phosphate Ceramics* 383–386 (2016). doi:10.1016/B978-0-08-100380-0.09995-4